ASSESSMENT OF THE TREATMENT OF DYE CONTAINING COMPOUND USING NANOCOMPOSITE PARTICLES

Assessment of the treatment of dye containing compound using nanocomposite particles

A Thesis submitted in the partial fulfillment of the requirements for the degree of

Master of Engineering

In

Chemical Engineering

By

MOUMITA SHARMA

Roll No – 001410302001

Registration No – 128877 of 14-15

Exam Roll No – M2CHE1501

Under the guidance and supervision of

Dr. Siddhartha Datta and Dr. Papita Das (Saha)

Department of Chemical Engineering

Jadavpur University

Kolkata – 700032

CERTIFICATE

*This is to certify that the thesis entitled "**Assessment of the treatment of dye containing compound using nanocomposite particles**"is submitted by **Moumita Sharma** student of Chemical Engineering Department of registration year 2014-2015 to this institute in partial fulfillment of the requirement for the award of the degree of Master of Engineering by Research.*

*This report is a bona-fide record of the work carried out by her under my supervision and guidance at the **Department of Chemical Engineering**, JADAVPUR UNIVERSITY, Kolkata-700032. It is further certified that no part of this thesis is submitted for the award of any degree.*

Dr. Siddhartha Datta

Department of Chemical Engineering

Jadavpur University

Dr. Papita Das (Saha)

Department of Chemical Engineering

Jadavpur University

APPROVAL

The following thesis is hereby approved as a credible study of an Engineering subject and presented in a manner satisfactory to warrant its acceptance as a perquisite to the degree for which it has been submitted. It is to be understood that by this approval, the undersigned do not necessarily endorse or approve any statement made, opinion expressed or conclusion drawn there in, but approve the thesis only for the purpose for which it has been submitted.

Department of Chemical Engineering

Jadavpur University

HOD (Department of Chemical Engineering)

.....

Dean (FET)

.....

Committee of final examination for evaluation of thesis

.....

.....

.....

ACKNOWLEDGEMENT

*I am grateful to **Chemical Engineering Department, Jadavpur University, Kolkata** for providing an opportunity to undertake this Project Work.*

While doing this project, I have come across many erudite personalities who had helped me a lot in doing and finishing this project simultaneously. It is their kind help and untiring effort that has resulted in completion of this project.

*I would like to express my heartful gratitude to **Prof. Dr. Siddhartha Datta and Associate Prof. Dr. Papita Das (Saha)** of Chemical Engineering Department of Jadavpur University, Kolkata for allowing me to complete this work under their elegant supervision and guidance. Their encouragement throughout the times of difficulties was something that cannot be expressed with mere words. I am deeply indebted to them.*

*I am very grateful to **Prof. Dr. Chandan Guha** (Head of the Department), Chemical Engineering Department, Jadavpur University and all other faculty members for their help and cooperation.*

I would like to extend my thanks to our Lab assistant who has helped me a lot all throughout my work. My sincere appreciation also extends to all my colleagues and others who have provided assistance at various occasions; it is not possible to list all of them in this limited space.

I am grateful to my mother, uncle and aunt who encouraged and supported me all through and helped me in all respect and my father who is missed every single day.

MOUMITA SHARMA

ABSTRACT

Toxicity caused by dye containing effluents has become an global issue that requires immediate action. Various process are utilized for the removal of dye containing effluents. Recently plant mediated synthesis of nanoparticles has gained importance due to its efficiency and simple operation. So an initiative is taken in the project for the removal of toxic dyes by using leaf extract mediated synthesis of Silver nanocomposites.

In this project few comparative studies were performed by Green synthesis of silver nanocomposites using Basil leaf extract (*Ocimum sanctum*) and Neem leaf extract (*Azadirachtaindica*) and soil. The first experiment involves a comparative study for the degradation of Gentian Violet dye using the three adsorbents. The second experiment involves a comparative study for the removal of two dyes Methylene Blue and Malachite Green. The third experiment consists of a study of binary solution of two dyes. The fourth experiment involves the comparative study between two binary solutions having different ratios of composition and in the fifth experiment a model (Polyacrylate column) is used to check whether dye degradation can be done using the adsorbents. The nanocomposites were characterized by color change, UV-VIS Spectroscopy, Scanning Electron Microscopy (SEM), Transmission Electon Microscopy (TEM), X-Ray Diffraction Analysis (XRD) and Fourier Transform Infrared Spectroscopy (FTIR). The color change to dark brown corresponds to the Plasmon absorbance of the silver nanocomposites. The SEM, TEM and FTIR studies also confirmed the formation of silver nanoparticles. Various experiments were carried out varying the properties like adsorbent dose, time, temperature, shaker speed, pH and concentration. Adsorption isotherms, thermodynamics and kinetics were also evaluated. Among the three adsorbents the silver nanocomposite made of *Ocimum sanctum* leaf extract is providing the maximum adsorption in different experiments about 98% which is appreciable.

Keywords:

Silver nanoparticles (AgNP), Silver nanocomposites (AgNP- Soil), Gentian Violet dye (GV), Malachite Green Dye (MG), Methylene Blue dye (MB), Basil leaf (*Ocimum sanctum*), Neem leaf (*Azadirachtaindica*), Percentage sorption, Isotherm, Kinetics.

CONTENTS **Page no**

INTRODUCTION

1.0 INTRODUCTION

1.1 DYES:

1.1.1 Definition

A dye is generally a natural or synthetic substance which is used to add color or change the color of a substance that has an attraction or affinity towards the substrate to which it is being employed. The dye is generally applied in an aqueous solution which can absorb wavelengths of light. Dyes are either natural or manmade or synthetic [Dyes, General Survey by Gerald Booth (2000), Ullmann's encyclopedia of industrial chemistry and Wikipedia].

1.1.2 Types of dyes:

Dyes are generally classified into two types

- Natural dyes.
- Synthetic dyes

Most of the natural dyes are obtained from plant sources like leaves, roots, barks, berries, fungi, lichens and woods. Examples of those natural dyes are woad, saffron, indigo, madder, tyrian purple etc. The discovery of man-made synthetic dyes has ended the large-scale market for natural dyes.

Synthetic dyes are nothing but man-made dyes that are prepared from petroleum by-products and earth minerals which are classified according to their solubility and chemical properties:

- Basic dyes are also water soluble cationic dyes like Acid dyes which are mainly used in acrylic fibers, wool and silk. For the proper settling of the dye on the fiber, acetic acid is added to the dye bath. They are mainly used in coloring of paper.
- Acid dyes are anionic dyes that are mainly used in silk, nylon, wool and acrylic fibres. They are soluble in water. Most of the synthetic food colors are acid dyes.
- Direct or substantive dyes are generally used on paper, leather, cotton, wool, nylon and silk. They are also used as pH indicators and biological stains. The dyeing is done in an alkaline dye bath with application of salts of sodium like sodium carbonate (Na_2CO_3), sodium chloride (NaCl) or sodium sulfate (Na_2SO_4).

- Mordant dyes demand the need of a mordant which improves the dye against water, perspiration and light. Example of mordant is potassium dichromate. Most of the natural dyes are of this type. Synthetic mordant dyes are used in wool especially for black and navy shades.
- Vat dyes are insoluble in water and cannot be used directly. So they should be reduced in alkaline solution for dyeing textile fibers. They are used in dyeing denims.
- Reactive dyes forms covalent bonds with natural fibers and thus considered best choice for cotton and cellulose fibers. They use a chromophore that is bonded with the substituent that reacts directly with the fiber material. Examples of reacting fibers are Procion MX, Cibacron F, Drimarene K etc.
- Disperse dyes are generally used in dyeing polyester, nylon, cellulose triacetate and acrylic fibers. They are water insoluble and requires a dispersing agent. They are generally sold as paste or in powder form.
- Azo dyes are prepared by treating the fiber with diazoic and coupling components. These dyes are insoluble in water and are produced directly onto the fibers. Most of these dyes are lacking importance due to their toxic and hazardous nature.
- Sulfur dyes are mainly used in dyeing cottons with dark colors. First the fabric is heated in a organic compound solution along with a nitrophenol derivative and sulfide or polysulfide which reacts to form a dark color that sticks to the fabric. Example is Sulfur Black 1.

According to statistics Azo dyes are the largest group of pigments that constitutes about 60-70% of all organic dyes produced in the world [Impact of Dye industries on the Environment, Slideshare.in (2014)].

1.1.3 Industrial applications of dyes:

They find their major application in textile, food and cosmetics industries but also are used in paper, ink, pharmaceutical, paints and leather industries.

1.1.3.1 Textile industries: One of the largest field of application of dyes is the textile industry. In the textile industries, the dyes used are generally synthetic obtained from coal tar and

petroleum based intermediates. In the dyeing section around 1000 litres of water are regularly used for 1000 kg of clothes processed. About 2-20% of these textile dyes are discharged as effluents in different water source which are toxic, carcinogenic as well as mutagenic due to presence of carcinogens like benzidine, naphthalene and other aromatic compounds [Problems caused by textile dyes, Textile learner.blogspot.in].

1.1.3.2 Food industries: Now a days use of food colorants have increased a lot in preparation of different food items – bakery products, cereals, desert powders, beverages, confectioneries, dairy and icecreams, meats and savouries. The dyes used are generally synthetic in nature because of wide hue range and competitive prices. As per Center for Science in the Public Interest (CSPI) few of the commonly used food dyes may be connected to numerous types of cancer, behavioral changes and hyperactivity among the kids. Some of the common food dyes are Brilliant blue, Indigo carmine, Citrus red, Fast red, Erythrosine, Tartrazine, Sunset yellow etc [Are you and your family eating toxic food dyes?, Mercola.com (2011)].

1.1.3.3 Cosmetics industries: Dyes had achieved a wide application in the cosmetic industry be it the hair dyes, lipsticks, nail polish, shampoo etc everywhere there is a massive application of dyes. Usually amino acids are used in the dye chemicals like m-Aminophenol, 4-amino-2-hydroxytoluene etc. Pigments of metal oxides like titanium dioxide, iron oxide, chromium dioxides, ultramarines, manganese violets, Iron blue, mica etc are also added. Allergies are the most common reaction of cosmetic dyes. Apart from that heavy metal present in dyes lead to metal poisoning, butylene glycol leads to skin irritation, Allure red and Tartrazine can lead to anxiety, migraines, cancer etc [Living in colors: the potential dangers of Artificial Dyes, Rachel Hennessey, Forbes.com].

1.1.3.4 Paper and Ink industries: Dyes also find their application in paper and ink industries mainly for coloring different grads of papers. The dyes which are used are generally sulfur and cationic direct dyes in paper industries. The ink industries generally uses metal oxide pigments like oxides of titanium, molybdenum, iron chromate etc. They get leeched in the ground causing serious health issues to human as well as wildlife. The finely ground metal powders can also cause different disease on inhalation.

1.1.3.5 Pharmaceutical industries: There is an increased usage of dyes in medicine. They are used in oral medicines like capsules, tablets, syrups also in detecting abnormalities like circulation problems, swelling, leaking of blood vessels etc. The dyes used are both synthetic as well as natural. Some of the common dyes used in oral pills are sunset yellow, indigo carmine and erythrosine which cause various health hazards.

1.1.3.6 Leather industries: The usage of dye in leather industries and tanneries has increased over the generation. Generally spirit or alcohol based dyes are used in leather industries where the alcohol gets absorbed into moistened leather. Leather dyeing consists of a pigment, a casein or nitrocellulose resin and a solvent. Apart from that acid, basic, metalized and direct dyes are also used. These tannery effluents are discharges into different water sources which consist of various heavy metal oxides, carcinogenic aromatic dyes and other hazardous chemicals which is highly dangerous for aquatic species and also humans.

1.1.4 Hazardous Effects of Dyes

Different hazardous effects of dyes are briefly described below:

- Air Pollution: The operation performed in the different industries leads to various gaseous emissions which is polluting the atmosphere badly.
- Water pollution: The effluents from the textile, ink, food, pharmaceutical industries and tanneries are evacuated in water sources without proper treatment. This water sources ultimately merge with rivers or ponds or other larger water bodies causing serious health hazards in animals and humans.
- In water the presence of dyes reduces the light penetration capacity thus inhibiting and retarding the photosynthetic activity of algaes and other aquatic plants that seriously affects the food chain and destructs the aquatic environment.
- Textile and tannery dyes can cause allergies like contact dermatitis and respiratory diseases, allergies to eye, skin irritation, allergy of mucous membrane and upper respiratory tract.
- The highly toxic dyes in water also cause the oxygen deficiency that limits the beneficial uses like irrigation, drinking water and recreation.

- Azo dyes have toxic effects especially carcinogenic and mutagenic. If they are somehow ingested they are metabolized by intestinal microorganisms causing severe DNA damage.
- Inhalation of metal pigments may cause lung cancer and other chronic respiratory diseases and also cause triple primary cancer in kidney, liver and urinary bladder.

1.1.5 Legal laws governing dye industries:

In countries like India, Pakistan and Malaysia the Environmental laws are recommended but not mandatory [Evaluation of Central Pollution Control Board, IIM Lucknow, 2010]. Some of the laws that regulates the dye industries constituted by Central Pollution Control Board (CPCB) are

- The Air (Prevention and Control of Pollution) Act, 1981 – For providing prevention and restraint of air pollution
- The Environment protection Act, 1986 – For providing protection and improvement of environment.
- The Public Liability Insurance Act, 1991 – For providing public liability insurance for the purpose of providing instant solace to persons affected by accidents happening while handling any menacing substances and for materials associated therewith or incidental occurings.
- The National Environment Tribunal Act, 1995 – For providing strict liability for damages and destructions emerging out of any accident happening while handling any perilous substances and for the establishment of National Environmental Tribunal for efficient and rapid disposal of cases arising from such accident.

In the experiments done in this project three dyes were used which are Gentian Violet (GV), Methylene Blue (MB) and Malachite Green (MG).

1.1.6 Gentian Violet (GV) dye:

Crystal violet or gentian violet (hexamethyl pararosaniline chloride) is a triarylmethane dye. It is mainly used as a histological stain and in Gram's method of classifying bacteria. Gentian Violet (GV) dye have molecular weight 408, molecular formula $C_{25}H_{30}N_3Cl$ and maximum absorption peak λ_{max} 578nm [Triarylmethane and diarylmethane dyes, Gessner and Mayer (2000),

Ullmann's encyclopedia of industrial chemistry and Wikipedia]. The chemical structure is given below

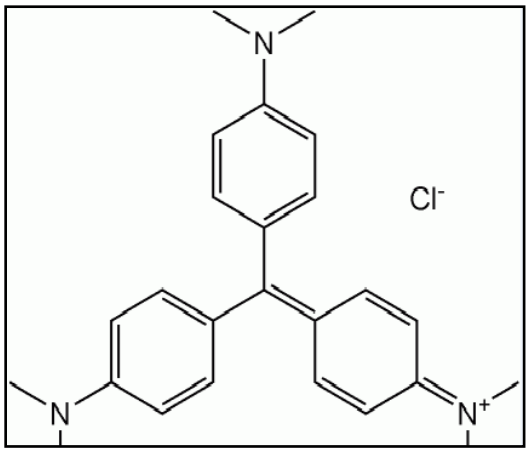

Figure 1.1

Chemical Structure

of Gentian Violet dye

1.1.6.1 Uses of Gentian Violet:

- Gentian violet has antibacterial, antifungal, and antihelmintic properties and was formerly important as an antiseptic for topical use.
- Crystal violet is not used as a textile dye. Instead, it is used to dye paper and as a component of navy blue and black inks for printing, ball-point pens, and ink-jet printers.
- It is also used to colorize diverse products such as fertilizers, antifreezes, detergents, and leather and in forensics, gentian violet is used to develop fingerprints.
- When conducting DNA gel electrophoresis, crystal violet can be used as a nontoxic DNA stain as an alternative to fluorescent, intercalating dyes such as ethidium bromide.

1.1.6.2 Disadvantages:

Though it has many uses it has various disadvantages too.

- Oral administration can cause gastrointestinal irritation and intravenous injection can cause depression in the white blood cell count.
- Causes serious eye damage if somehow gets inside the eyes.
- It is considered as a carcinogen suspected of causing cancer.
- It is very toxic to aquatic life with long lasting effects.

1.1.7 Methylene blue dye

Methylene blue also known as methylthioninium chloride is a heterocyclic aromatic chemical compound with the chemical formula $C_{16}H_{18}N_3SCl$. It can be used as a stain and as a medication [Methylene Blue, The American Society of Health-System Pharmacists (2016) and wikipedia]. The chemical structure is given below

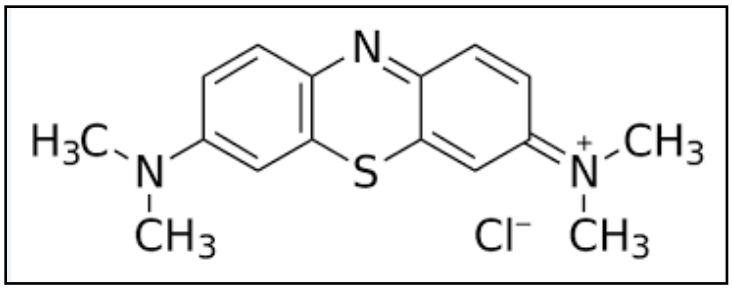

Figure 1.2

Chemical Structure

of Methylene Blue Dye

1.1.7.1 Uses of Methylene blue dye:

- Due to its high oxidizing property, Methylene blue are used as an antidote to potassium cyanide poisoning and also prescribed as urinary analgesic or antispasmodic.
- Methylene blue combined with light has been used to treat resistant plaque psoriasis.
- In surgeries such as sentinel lymph node dissections, methylene blue can be used to visually trace the lymphatic drainage of pertinent tissues.
- Methylene blue is added to bone cement in orthopedic operations to provide easy discrimination between native bone and cement. It also increases the hardening of the bone cement.

1.1.7.2 Demerits of Methylene Blue:

Various disadvantages of using the Methylene blue dye are as follows

- Inhalation of the dye can cause dizziness, fever, headache and mental confusion.
- If injected at a certain area can cause skin irritation and even necrosis.
- If consumed can cause nausea, vomiting, abdominal pain and bladder irritation.
- It can also cause hemolytic anemia if exposed for a long time.

1.1.8 Malachite green dye

Malachite green (MG) is an organic compound that is used as a dyestuff classified in the industry as a triarylmethane dye and also using in pigment industry. Formally, malachite green refers to the chloride salt $[C_6H_5C(C_6H_4N(CH_3)_2)_2]Cl$. The intense green color of the cation results from a strong absorption band at 621 nm [S. Srivastava, R. Sinha, D. Roy (2004), "Toxicological effects of malachite green", Aquatic Toxicology 66 (3): 319–29]. The chemical structure is given below.

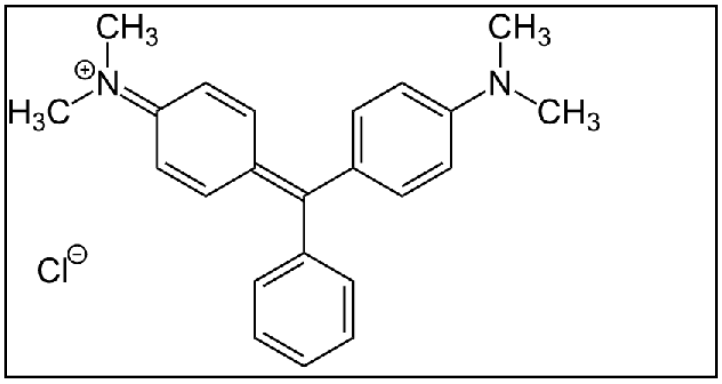

Figure 1.3

Chemical Structure

of Malachite Green dye

1.1.8.1 Uses of Malachite green:

- Malachite green is traditionally used as a dye for materials such as silk, leather, and paper and used as biological stain for microscopic analysis of cell and tissues.
- MG is used as parasiticide in agriculture and active against the oomycete *Saprolegnia*, which infects fish eggs in commercial aquaculture.
- MG has frequently been used to catch thieves and pilferers. The bait, usually money, is sprinkled with the anhydrous powder. Anyone handling the contaminated money will find that on upon washing the hands, a green stain on the skin that lasts for several days will result.

1.1.8.2 Harmful effects:

Various harmful effects of Malachite Green dye are as follows:

- It has been reported to cause carcinogenesis, mutagenesis, chromosomal fractures, teratogenecity, respiratory toxicity and developmental abnormalities.
- Histopathological effects of MG include multi-organ tissue injury.

1.2 REMOVAL TECHNIQUES AVAILABLE:

Since these dyes have destructive effect on humans, plants, wildlife as well as aquatic systems, the presence of this dyes in the industrial waste water is becoming an alarming threat that requires immediate measures. Since the dyes are mostly obtained in the industrial effluents, the industries should perform proper treatment of the effluents for the removal of these harmful dyes before dumping them in any water sources or landfills. These dyes cannot be removed from the effluents by simple techniques. There are several well known physical, chemical and biological treatments for the removal of dyes from waste water. They are:

1.2.1 Membrane filtration:

Membrane filtration has a variety of possible applications, in the dye industry. The largest of these is dye desalting, and concentration of the finished items, which is most commonly applied to reactive dyes, but can also be used on other substances such as sulfur dye and direct dyes. There are four basic membrane filtration processes. These are, in decreasing order of particle size:- reverse osmosis, nanofiltration, ultrafiltration and microfiltration.

Reverse osmosis is utilized to separate charged ions by applying a pressure, which exceeds the osmotic pressure of a solution, across a semi permeable membrane [Chen et al., (2004)]. This technique is often used to produce ultrapure water for laboratories and process. Nanofiltration is capable of distinguishing particles of a few nanometres in diameter. While large ions and organic molecules are kept, smaller ions can pass through. Once the pores in the membrane are large enough that the product may be considered to be porous, the methodology is referred to as Ultrafiltration which is generally used in industry for purification of process and concentration. The coarsest type of membrane filtration, which can manage particles of few microns in diameter, is known as Microfiltration. The main problem associated with this process is incomplete removal of contaminants, high energy requirement, and high cost of the membrane and longevity of the membrane. After long term use the membrane get clogged with the contaminants present in the waste water and is damaged due to extra pressure on the membrane.

1.2.1 Oxidation:

Oxidation is an important technique in removal of the dyes which is widely used in plants and industries. Various advanced oxidation processes such as Photocatalysis (UV/TiO_2 or ZnO),

Ozonation, Fenton reactive process and ultrasonic oxidation are used mostly in the treatment of industrial effluents.

1.2.1.1 Photocatalysis:

Mainly the photocatalytic degradation or the degradation of dyes from effluents have been carried out with sunlight and broad spectral radiation sources such as UV lamps and TiO_2 or ZnO as a photocatalyst. The traditional source of UV is a mercury vapor high-pressure lamp, which is a gas discharge source. Few problems are related with the use of UV lamps emitting over a broad spectral wavelength range which are the power instability for a long term due to excessive heating of lamps during the operation, longer exposure time, low photonic efficiency for complete mineralization of pollutants. But now a days various other UV radiation source like UV-LEDs, UV emitting diodes etc are used (Kumar et al.,2016).

1.2.1.2 Chemical Oxidation methods:

In Chemical oxidation processes like Fenton, Electrofenton, Photofenton etc the waste particles from the industrial effluents are degraded by the help of chemical oxidation by the use of hydrogen peroxide. There are many disadvantages associated with this process like the high cost of the chemicals, emission of various harmful by products, it creates hazardous constituent like secondary effluent problem along with the production of harmful gases (Babuponnusami et al., 2014).

1.2.1.3 Ozonation:

The ozonation processes are possibly one of the most effective methods for the treatment of wastewater containing organic substances from chemical and agrochemical industries, textile industry, paints, etc. The disadvantages associated with the process are high operating cost. The cost of the equipment is very high and also it requires high voltage and electricity for its operation [Gharbani, 2010].

1.2.2 Coagulation and Flocculation

In wastewater treatment, coagulation and flocculation techniques are mainly used for the removal of colloidal material, which adds the color and turbidity in water by bringing suspended particles for the purpose of settling and for the preparation of the water for filtration. There are three specific steps in this method which are Coagulation, Flocculation, and Sedimentation.

Coagulation is a simple, effective and inexpensive way to improve the quality of wastewater. It can improve the taste and odor, makes the water safer for chlorination, and makes the water easier to treat for domestic purposes. Some of the commonly used coagulants are alums, lime, iron salts and other organic polymers. Flocculants are polymers with high molecular weight consisting of various functional groups. They can be easily separated by sedimentation or floatation. However a major demerit of the technique is operational costs. A faint quantity of physico chemical sludge is also formed which has to be treated and processed externally.

1.2.3 Activated carbon sorption:

In water treatment activated carbons are generally used for absorption of variety of water pollutants for removing unwanted tastes and odors, including hazardous chlorine and various chemicals and dissolved gases, also in some cases it is effective against microorganisms. The use of carbon filtes have been certified for the removal of lead metal, dyes, asbestos, cysts, and coliform but some of the disadvantages of the methods are product recovery requires an expensive distillation or extraction. The carbon adsorption process is being extensively used for the degradation of dyes from synthetic dye effluents by various researchers. The safe and economical methods of preparing adsorbents include, tapioca peel activated carbon, sewage treatment plant sludges, neem leaf powder, soil, fly ash, rice bran based activated carbon etc (Jolly et al., 2013).

1.2.4 Biological treatments:

Biological degradation is one of the economical alternative when compared with other physical and chemical processes. Methods like adsorption by (dead or living) microbial biomass, fungal decolourization, bioremediation and microbial decolourization techniques are commonly used in the treatment of industrial effluents because many organisms such as bacteria, algae, fungi and yeast are capable of accumulating and degrading different dyes. Biological treatment requires large surface area and is cheaper than other methods. Depending on different oxygen demands, the method is classified into aerobic and anaerobic techniques. Aerobic biological treatment is the conventional treatment method because of high efficacy and varied application. Moreover, when it is compared to chemical methods, for biological process investment operating costs are 3-10 times less than chemical methods. But the disadvantage is it is a time consuming process and is very unpredictable depending on the nature of the microorganisms (Saha et al., 2011).

1.2.5 Adsorption

By definition, Adsorption is the adhesion of atoms, ions, or molecules from a gas, liquid, or dissolved solid to a surface by chemical or physical bonding. The method creates a film of the adsorbate on the surface of the adsorbent and is a surface phenomenon.

Among various procedures used one of the efficient treatment technique for the removal of dyes from water at minimal cost is adsorption. Adsorption has proven successful on lowering dye concentration from industrial effluents by using adsorbents viz. activated carbon, clay, peat, chitin, nanoparticles and others.

Among all this techniques used, adsorption process is used in the project because of its simplicity, treatment efficacy and economy.

1.2.6 Advantages of Adsorption:

The major advantages of this technique include

2 High efficacy in removing dyes and pigments from diluted effluent solutions.
3 Ease in handling and low operating cost.
4 Removal of the dye containing wastes from effluent irrespective of toxicity.
5 Short time of operation and with proper arrangements recovery is possible.

Because of these manifold advantages, adsorption of dyes is the most promising separation and purification method from industrial effluents.

1.3 NANO PARTICLES USED:

Recently, metal nanoparticles have focused the attraction of researchers due to their unique Physical, chemical, biological and antimicrobial properties. Different noble metals are used for the preparation of nanoparticles among which silver nanoparticles play an important role due to its immense application in everyday consumer life – pharmaceuticals, food storage containers, sterilizers, medical devices to reduce infections, bandages and a number of household items. Apart from that they are also used in microelectronics, sensors, cleaning agents, ink preparation, catalysis, nonlinear optics and information storage (Kumar et al., 2014 and Ahmed et al., 2015)

According to ancient Indian treatise Ayurveda, Silver nanoparticles was considered as a miracle medicine against all types of infectious diseases because of its antibacterial activity. The

silver nanoparticles have large surface area as a result they come in better contact with the micro organisms. Again as they enter inside an organism, they release silver ions that disrupts the cell membrane causing leakage of cell components, degrades the enzyme that prevent the nutrition supply and also prevents DNA replication ultimately leading to the death of the pathogen.

There are many ways of production of silver nanoparticles such as:

- Reduction in solution and Thermal decomposition
- Chemical and Photochemical reactions (Raghavendra et al., 2016 and Zhou et al., 2015)
- Electrochemical, Sonochemical reactions and Laser Technology
- Microwave techniques (Josheph et al., 2015)
- Biological routes (Saha et al., 2011 and Natarajan et al., 2010) and

1.4 Green synthesis of silver nanoparticles:

Among all the methods described above the recently developed green synthesis or synthesis using plant extracts is the most simple, economic and less time and energy consuming technique. The preparation of silver nanoparticles chemically involves reduction in solution in commercial cases using sodium borohydrate ($NaBH_4$) which increases the toxicity in the environment and capping agents like polyvinyl alcohol and gelatin were also used to prevent agglomeration.

The green synthesis can be done using many plant parts –

- Leaves, roots, tuber [Sadhegi et al.,2015], fruits [Moghaddam et al.,2014]
- Seeds [Dhand et al., 2016], barks [Ahmad, 2009], peel [Saeed et al., 2010], buds,
- Mesocarp [Mariselvam et al., 2014] and even flowers [Senthilkumaar et al., 2006].

Many scientists, researchers, universities and laboratories has worked on the green synthesis of various metal nanoparticles like silver (Ag), gold (Au) [Patra et al., 2015], copper (Cu), Nickel (Ni) , Chromium(Cr) [Hossain et al., 2005] etc from various plant extracts of *Croton sparsiflorus morong* leaf [Kathiravan et al., 2015], *Alternanthera dentata* leaf [Kumar et al., 2014], *Azadirachta indica* leaf [Satapathy et al., 2013], *Ocimum sanctcum* leaf , *Eucalyptus oleosa* [Pourmortazavi et al.,2015], *Artocarpus heterophyllus* (jackfruit) leaf [Saha et al., 2012], *Eucalyptus chapmaniana* leaf [Sulaiman et al., 2013], *Ulva lactuca*(seaweed) [Kumar et al., 2013] etc but comparative studies checking the effectiveness of a better adsorbent are very few.

In the comparative studies the leaf extracts of basil plant (*Ocimum sanctum*) and neem (*Azadirachtaindica*) are used for the preparation of the silver nanocomposites.

1.4.1 Basil leaves (*Ocimum sanctum*) and its uses:

Holy Basil (*Ocimum sanctum*) commonly known as tulasi is an aromatic plant, part of the family Lamiaceae which is native of India and widespread across the Southeast Asian tropics. Basil leaves are strongly fragranted and cultivated and used for medicinal and religious purposes, and also for its essential oil. It is widely known across the Indian subcontinent as a medicinal plant and also used in preparing herbal tea. According to Ayurveda, holy Basil has a valuable role within the tradition of Vaishnava people of Hinduism, in which devotees perform worship using holy basil plants or leaves.

1.4.2 Neem leaves (*Azadirachta indica*) and its uses:

Neem (*Azadirachta indica*) commonly known as Indian lilac is a tree belonging to family Meliaceae is a native of Indian subcontinent. Extraction of oil is done from the seeds and the fruits of the plant. As believed by Ayurveda and Unani practitioners the leaves are considered as antibacterial, antidiabetic, antifungal, sedative, contraceptive as well as antihelmintic. It is also used for detoxifying blood, maintaining sugar levels, treating skin diseases like psoriasis and eczema and improve liver functions.

Both the leaves contain chlorophylls, flavonoids, xanthophylls, alkaloids, free sugars, oligosachharides, traces of elements, lipids and terpenoids. It is supposed that the terpenoids and the flavonoids present in the leaf extracts are responsible for the reduction of the silver ions from the silver nitrate solution and the amino acids, polyol groups and free sugars are responsible for acting as stabilizing or capping agents.

Characterization of the composites were also done and the formed two silver nanocomposites and soil are then used for various experiments for the removal of the dyes Gentian Violet, Methylene Blue and Malachite Green in both single and binary solutions. The result obtained are then plotted in graphical forms and compared and conclusions were drawn.

AIMS AND OBJECTIVES

2.0 AIMS AND OBJECTIVES

Degradation of dye containing effluents has become a serious issue that threatens the life of humans as well as wildlife, aquatic organisms – in the whole it compromises the ecosystem. Since it has manifested its hazardous effect immediate measures should be taken in preventing further damage to the ecosystem of the environment. The green synthesis has proved its efficiency in degrading the dye as per the literature review so a small attempt is been taken in the degradation of few hazardous dyes by using adsorbents prepared by the Green synthesis of Basil and Neem leaves and a comparative study is done.

The aim and objective of the project done was

- Characterization of the two nanoadsorbents formed from Basil and Neem leaf extracts and also the soil used in the study.
- Investigate the removal mechanism of the dyes by using the adsorbents.
- Study the influence of different experimental batch parameters on removal rate of the dyes used in both singular and binary dye solutions.
- Perform a few comparative studies to check which adsorbent is providing the maximum percentage removal.
- Study the Adsorption isotherm, Kinetics and thermodynamics of both singular and binary dye solutions.
- A model experiment is also performed to check whether the degradation of dye effluents if dumped in a landfill causing ground water contamination can be prevented or not.
- Investigate whether use of the green synthesis is advantageous for the removal of dyes from the effluents or not.

LITERATURE REVIEW

3.0 LITERATURE REVIEW:

In this process adsorption process is considered because of its efficiency and easy technique. The definition and types of adsorption is provided below.

3.1 ADSORPTION:

3.1.1 Definition

Adsorption is a process in which a substance (adsorbate) in gas or liquid phase, assembles or accumulate on a solid surface. It is based on the capability of porous materials with large surfaces to selectively retain compounds on the surface of the solid (adsorbent). There are two types of adsorption; physical and chemical adsorptions [Unit operations of Chemical Engineering, Mcabe and Smith, 6th edition].

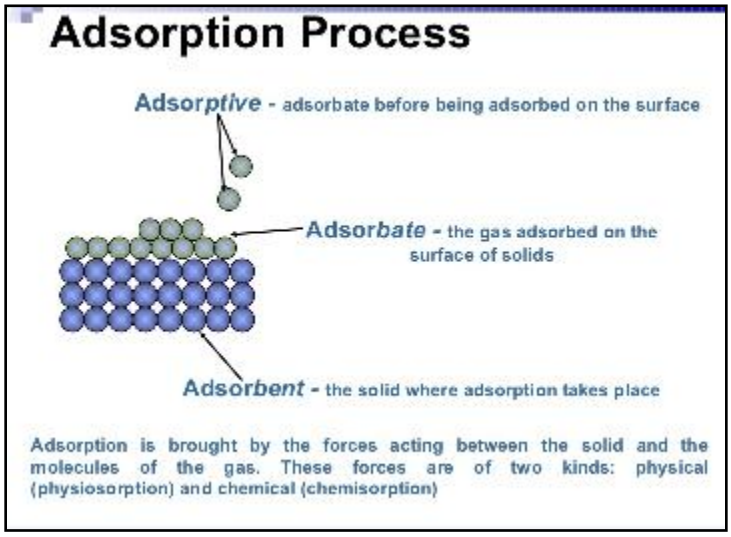

Figure 3.1

Adsorption process pictorial demonstration

3.1.2 Physical Adsorption and Chemical Adsorption

Physical adsorption or physisorption is achieved by Van der Waals forces, dipole interactions, and hydrogen bonding. There is no electron exchange between adsorbent and adsorbate. Because there is no activation energy required for physical adsorption, the time needed to reach equilibrium is very short. Physical adsorption is a non–specific and a reversible process.

Chemical adsorption or chemisorption results from the chemical link between adsorbent and adsorbate molecule, therefore it is specific as well as irreversible. Binding between adsorbent and adsorbate by covalent bond is called weak chemical adsorption, and that by ionic bonds is called strong chemical adsorption.

3.2 ADSORBENTS

The adsorbents used in this project are silver nanocomposites (AgNP-Soil) from Basil leaf extract (*Ocimum sanctum*), Neem leaf extract (*Azadirachta indica*) and only Soil which is considered as a great natural adsorbent. Nanotechnology has gained great height with potential application in many fields from electronics, medicine to cosmetics. It has open paths for many fast growing industries one of which is pollution control in waste water effluents [Pandian et al., 2015].

3.2.1 Silver nanoparticles

Silver nanopaticles (AgNP) is one of the novel method which has gained recognition for its wide range of applications like sensors, optics, electronics and even medicine (sterilizers, disinfectant, antimicrobials etc) [Prabhu et al., 2012]. There are many ways of production of silver nanoparticles among which green synthesis or synthesis using plant extracts is simple, economic and less time and energy consuming technique.

3.2.2 Characteristics of Silver nanoparticles (AgNP):

- Large surface area to volume ratio
- Bactericidal and fungicidal activities
- Unique optical, electrical and thermal properties.

3.2.3 Application of silver nanoparticles (AgNP):

- **Diagnostic Applications:** Silver nanoparticles are used in biosensors and numerous assays where the silver nanoparticle materials can be used as biological tags for quantitative detection.
- **Antibacterial Applications:** Silver nanoparticles are incorporated in apparel, footwear, paints, wound dressings, appliances, cosmetics, and plastics for their antibacterial properties.
- **Conductive Applications:** Silver nanoparticles are used in conductive inks and integrated into composites to enhance thermal and electrical conductivity.
- **Optical Applications:** Silver nanoparticles are used to efficiently harvest light and for enhanced optical spectroscopy including metal-enhanced fluorescence (MEF) and surface-enhanced Raman scattering (SERS).

To find about the efficiency of the adsorption process the study of Adorption isotherm, Kinetics, Thermodynamics are necessary a brief study of which is given below.

3.3 ADSORPTION ISOTHERMS

Adsorption isotherms, which are the presentations of the amount of the solute adsorbed per unit of the adsorbent as a function of equilibrium concentration in bulk solution at constant temperature .If a quantity q of adsorbate is adsorbed by a porous solid adsorbent at constant temperature and the steady state equilibrium concentration, then the function q describes the adsorption isotherm. The isotherm rises in the initial stages with higher slope at low C_e and q_e values. This indicates that initially there are numerous readily accessible sites. A variety of isotherm equations have been in use some of which have a theoretical foundation and some being of more empirical nature [Transport processes and unit operations, Christie Geankoplis, 3rd edition].

3.3.1 Langmuir Isotherm

A basic assumption of the Langmuir theory is that the sorption takes place at specific homogenous sites within the adsorbent. It is then assumed that once a ion or molecules occupies a site no further sorption can take place at that site. The rate of sorption to the surface should be proportional to a driving force multiplied by are. The driving force is the concentration in the solution and the area is the amount of bare surface [Langmuir, 1916].

$$\frac{C_e}{q_e} = \frac{C_e}{q_o} + 1/(K_L . q_o)$$

Where C_e is the equilibrium concentration, q_e is the amount of ions or molecules adsorbed (mg/g), q_0 ($mg.g^{-1}$) is the maximum adsorptive capacity and K_L ($L.mg^{-1}$) is the energy of adsorption. Another important parameter in the Langmuir is the separation factor R_L which indicates the nature of isotherm (R_L>1 is considered unfavorable, R_L=1 is considered linear, R_L=0 is irreversible and 0<R_L<1 is considered favorable) and is represented by the equation

$$R_L = 1/(1 + K_L . C_e)$$

3.3.2 Freundlich Isotherm

Freundlich Isotherm assumes that the uptake of ions occur on a heterogenous surface by

multilayer adsorption and that the amount of adsorbate adsorbed increases infinitely with an increase in concentration. It is the most popular model for a single solute system, based on the distribution of solute between the solid phase and aqueous phase at equilibrium [Freundlich, 1906]. Linear Equation of Freundlich Isotherm is

$$lnq_e = lnK_F + (1/n)lnC_e$$

Where C_e is the equilibrium concentration, q_e is the amount of ions or molecules adsorbed (mg/g), K_f and n are Freundlich constants related to the adsorption capacity and adsorption intensity respectively. A plot of log q_e versus log C_e gives a linear trace with a slope of 1/n and intercept of log K_f. When 1/n > 0, the change is adsorbed on concentration is greater than the change in ion concentration in solution. It is often found that the Freundlich equation is fitted well to the data at higher and intermediate concentrations, since the equation does not approach Henry's Law of ideal dilute solutions.

3.3.2 Temkin isotherm:

The temkin model is linearly represented as equation

$$q_e = (RT/b)\ln(AC_e)$$

Where A and B are temkin isotherm constant ($L.g^{-1}$) and heat of sorption ($J.mol^{-1}$) respectively. R is the gas constant ($J.mol^{-1}k^{-1}$), b is the temkin isotherm constant linked to energy parameter B. The derivation of the Temkin isotherm assumes that the fall in the heat of sorption is linear rather than logarithmic, as implied in the Freundlich equation.

3.4 ADSORPTION THERMODYNAMICS:

The thermodynamics of an adsorption process is obtained from a study of the influence of temperature on the process. The standard Gibb's Energy was

$$\Delta G° = -RT \ln K_c$$

The equilibrium constants K_c was evaluated at each temperature using the following relationship

$K_c = C_a/C_e$

Where K_c = distribution coefficient for adsorption.

C_a = equilibrium concentration on the adsorbent.

C_e = equilibrium concentration in solution.

Other thermodynamic parameters such as change in standard enthalpy Δ*H*° and standard entropy Δ*S* ° were determined using the following equations.

$$\Delta \mathbf{G°} = \Delta \mathbf{H°} - \mathbf{T}\Delta \mathbf{S}\ °$$

Δ*H*° and Δ*S* ° were obtained from the slope and intercept of the Vant Hoffs plot of ln k_{eq} versus 1/T, Negative value of Δ*H*° indicates that the adsorption process is exothermic. The negative values of Δ*G*° reflect the feasibility of the process and the values become more negative with increase in temperature. Standard entropy determines the disorderliness of the adsorption at solid-liquid interface. The positive value if Δ*S* ° shows that increasing randomness at the solid-liquid interface during the adsorption process.

3.5 ADSORPTION KINETICS:

The study of adsorption kinetics describes the adsorbate uptake rate and predicts the residence time of dyes at the solid-liquid interface. The Lagergren's pseudo-first-order and Ho–McKay's pseudo-second-order models [Ho and McKay, 1999] were applied to the experimental datas.

- **Pseudo-first-order:** $\ln(q_e - q_t) = lnq_e - K_1 t/2.303$

The values of pseudo-first-order rate constants, k_1 (min^{-1}) and qe (g. mg^{-1}) were calculated for the three adsorbents from the slopes and intercepts of the graphs between log (q_e - q_t) versus t .

- **Pseudo-second-order:** $\frac{t}{q_t} = \frac{1}{K_2 . q_e^2} + t/q_e$

where q_t and q_e are the amount of adsorption at equilibrium and at time t respectively and K_2 is the rate constant of the pseudo second order adsorption process.

The rate parameters K_2 and q_e can be directly obtained from the intercept and slope of the plot of t/qt versus t. The values of rate constant are obtained graphically for both adsorption models.

3.6 BRIEF DESCRIPTIONS OF FEW LITERATURE PAPERS:

Now a lists of experiments done by different researchers are been provided which has helped a lot in gaining ideas while completing the projects. The experiments performed and results concluded were briefly described.

- Satapathy et al., 2014 has experimented the development and characterization of a novel nano adsorbent from soil and leaf extract of *Azadirachta indica* which act as reducing as well as capping agents. Response Surface Methodology (RSM) is applied to investigate the effect of different operating parameters on uptake of crystal violet (CV) dye and a Two level Three factor (2^3) factorial Central Composite Design (CCD) is used for optimization of the process parameters. Multiple Response optimization was employed to the experimental data to discover the optimal condition for a set of response, simultaneously by using desiring function. The optimal removing efficiency of the nanocomposite is very high.
- In this paper silver nano particles were manufactured using *Cocos nucifera* (Red spicata dwarf) mesocarp extract and its ability to degrade azo dye Malachite Green by photocatalysis under solar irradiation is observed. The bioextract of Cocos nucifera fruit is known to consist phyto - components that proffer antioxidant, antihelmintic activity, antibacterial, anti-inflammatory and antiviral properties. The AgNPs synthesized using CN extract exhibit their potential in application for wastewater treatment by photocatalytic degradation of dyes and other complex organic compound under solar illumination. Solar catalytic degradation of organic pollutants using AgNPs synthesized using an agro waste provides dual fold advantages of waste utilization and energy efficient treatment of large quantities of dye containing effluents using solar energy (Babu et al., 2015).
- H. Hou et al., 2012 has studied the removal of Congo red (CR) dye from aqueous solution using Hydroxyapatite - Chitosan composite. A hydroxyapatite-Chitosan (HAP-CS) composite is developed via embedding of HAP into CS by co precipitation method. The possible adsorption mechanism of CR dye adsorption on HAP-CS composite includes electrostatic interactions, surface complexation, ion exchange and hydrogen bonding. As an effective and low cost adsorbent, HAP-CS composite is presumed to have a glorifying future for the dye polluted water purification.
- Ahmed et al., 2015 has experimented on the green synthesis of silver nanoparticles using the leaf extract of *Skimmia laureola* and its antibacterial property. The bioactive chemical constituents in the leaf extract of *S. laureola* such as triterpenoids, skimmidiol and coumarins are mainly involved for the synthesis of silver nanoparticles. This type of

phyto mediated synthesis appears to be cost effective, eco friendly and an alternative approach to conventional physical and chemical methods. These nanoparticles manifested potential bacteriostatic effects against Gram positive and Gram negative Human pathogen bacterias.

- This paper bring to light the preparation of silver nanopaticles in a greener way using tea leaf extract and evaluation of its stability and antibacterial property. The study of silver ion release from the tea extract synthesized AgNP showed a good stability in terms of time dependent release of the silver ions and it is compared to PVA (Poly vinyl alcohol) coated AgNPs, uncoated AgNPs and commercial AgNPs . In addition the antibacterial property was observed using the growth curve and Kurby-Bauer disc diffusion method. As a result of larger size and less silver ion release at a certain time limit, the biosynthesized AgNP showed faint antibacterial activity against E.coli (Q.Sun et al., 2014).
- Kumar et al., 2013 has experimented the photocatalytic degradation of methyl orange dye employing silver nanoparticles developed from *Ulva lactuca* (sea weed). The FTIR studies revealed the existence of bioactive functional groups such as phenolic compounds, amines and aromatic rings that act as the reducing and capping agents. Due to complexity in the marine environmental conditions, marine plant has become a rich source of biologically active substances as well as terrestrial plants. It is stated compared to other irradiation technique, solar light is found to be fastest in decolorizing the methyl orange dye in presence of metal catalyst. Altogether the photocatalytic activity of silver nanoparticles may be due to excitation of SPR (Surface Plasmon Resonance), which is nothing but swaying of charged density that can circulate in the interface between metal and dielectric medium.
- In this paper *Butea monosperma* leaf extract is used for the formulation of gold and silver nanopaticles. It is been characterized using various analytical techniques and its potential application in cancer therapeutics is detected. Both the nanocomposites are stable in biological buffers and compatible toward normal epithelial cells as well as cancer cell lines. Compared to pristine drugs, noteworthy inhibition in the cancer cell proliferation is observed by the administration of nanoparticle drug delivery system using FDA approved anticancer drug Doxorubicin (DOX). Thus it is considered that the biosynthesized

nanoparticles will be useful for the development of cancer therapy using nanomedicine approach in near future (Patra et al., 2015).

- This paper includes green synthesis of silver nanoparticles using *Coffea Arabica* seed extract and its antibacterial property. Silver nanoparticles are gaining importance in the medical fields antimicrobials, testing tools for diagnosing and detecting sensitive biomolecules and sterilizers. When the nanoparticles enter a pathogen it releases silver ions, thereby killing it. Due to this properties, nano silver act as a killing agent of broad spectrum of Gram positive and Gram negative bacteria including the antibiotic resistant strain. The key components responsible for the silver ion release are terpenoids, glycosides, alkaloids and phenolics (flavonoids, coumarins, tannins and ubiquinones) as obtained in IR Spectroscopic readings. The study concluded that the silver nanoparticles formed have strong and almost equal antimicrobial activity compared to the standard drug "ampicillin" (Dhand et al., 2016).
- Pandian et al., 2015 has studied the green synthesis of nickel nanoparticles using *Ocimum sanctum* leaf extract and its application in dye and pollutant removal is observed. In the study adsorption of the industrial dyes like crystal violet, eosin and orange II azo dye and anionic pollutants like nitate (NO_3^-) and sulphate (SO_4^{2-}) is observed. Monolayer adorption is eloquent in all the cases. The mean free energy aquired by Dubinin-Radushkevich isotherm showed physical adsorption of adsorbates on the nickel nanoparticle surface. Thus it is stated that nickel nanoparticles are effective in treating tannery and textile effluents.
- This study reveals use of *Alternanthera dentata* leaf extract at room temperature in the green synthesis of silver nanoparticles and their antimicrobial property. *A. dentata* is a small to medium perennial garden shrub with purple foliage commonly used for beautification of garden. The study revealed that the silver nanoparticle exhibit antibacterial action against familiar known species of bacterias like *E.coli, P. aeruginosa*, *E. faecalis* and *K. pneumonia* . The method used is very easy to perform, simple, inexpensive and eco friendly. The colloidal solution is very stable indicating that the extract can be used both as stabilizing agent and reducing agent for the preparation of Ag nanoparticles (Kumar et al., 2014).

- Mariselvan et al., 2014 has studied the green synthesis of silver nanoparticles from the extract of the inflorescence of *Cocos nucifera* for stipulated antibacterial property. Here silver nanoparticles are formulated using ethyl acetate and methanol in the ratio 40:60 from the extract of the mesocarp of the tree *Cocos nucifera*. The synthesized AgNP has shown great antimicrobial property against human bacterial pathogens like *Klebsiella pneumoniae*, *Pseudomonas aeruginosa*, *Bacillus subtilis* and *Salmonella paratyphi*. It is reported that when silver nanoparticles are attached to the surface of the silver membrane, the respiratory activities and penetrability of the bacterial cell becomes unstable. Other studies revealed that when bacterial cells are treated with silver ions the DNA of the bacteria loses its ability to replicate. However the exact mechanism needs further studies.
- This paper showed a study on the preparation of the silver nanoparticles using *Ziziphora tenuior* extract at room temperature. Biomolecules present in the plants extract can reduce the metal salt to metal ions in the nanoparticles in a single step green synthesis process. The involved reducing agents includes various soluble plant metabolites like alkaloids, terpenoids, phenolic compounds and coenzymes. The FTIR measurement showed strong evidence for proteins to form a coat over the silver nanoparticles to stabilize and prevent the agglomeration of the particles (Sadeghi et al., 2015).

The antimicrobial property is measured by MIC and MBC. The definition of MIC is the lowest concentration of the antimicrobial agent that prevent the visible growth of microorganisms and the word MBC is defined as the lowest concentration of the antimicrobial agent that prevent the growth of microorganisms onto nanocomposite free media after subculture.

- This paper includes the use of banana peel extract in the green synthesis of the silver nanoparticles and their antimicrobial property against representative microorganisms. The peel extract act as both stabilising and reducing agent. Silver nanoparticles manifested effective antibacterial activities against pathogens of yeast and bacteria. The minimum inhibitory concentration (MIC) and minimum bactericidal concentration (MBC) were deducted. The rigid structure of the cell wall of the gram positive bacteria are due to thick peptidoglycan layer that prevent the penetration of silver nanoparticles however the gram negative bacteria has a thin peptidoglycan layer. The synthesized

nanoparticles showed synergistic effect with levofloxacin antibiotic, the antimicrobial activity stipulated by 1.16-1.32 fold (Ibrahim, 2015).

- This paper includes the concoction of silver nanoparticles from marigold flower (*Tagetes erecta*) in a flower broth that act as reducing agent and its synergistic antimicrobial potential. The dried powder of the flower are made by cold percolation method followed by defattation by hexane and extraction in acetone. Synergistic antimicrobial prospect of silver nanoparticles are evaluated with various commercial antibiotics against fungal species (*Candida albicans*, *Candida glabrata* and *Cryptococcae neoformans*), Gram negative bacterial species (*E. coli* and *P. aureuginosa*) and Gram positive (*Bacillus cereus* and *Staphylococcus aureus*). As tested in the strains of fungus and bacteria (Gram negative), the antifungul effect of AgNPs along with antibiotics was better than antibiotics devoid nanoparticles, thus signification of the present study is in the production of biomedical products (Padalia et al., 2014).
- Babuponnusami et al., 2014 has done a review on Fenton process and its improvements for wastewater treatment. For the complete mineralization of the wastewater, the increase in the disposal of refractory organics asks for newer technologies. Advanced oxidation processes (AOPs) is a promising technology for the treatment of such wastewaters which presents a general review on methods developed to decolorize and degrade organic pollutants. Various methods such as Fenton, electro-Fenton, sono-electro-Fenton, sonophoto-Fenton, sono-Fenton, photo-Fenton and photo-electro-Fenton are discussed. The use of nano-zero valent iron in treating refractory compounds were also discussed.
- Kumar et al., 2015 studied the green synthesis of silver nanoparticles using Andean blackberry fruit extract which is a dark-red colored, juicy, and flavored berry (*Rubus glaucus Benth.*). It is consumed mainly in Ecuador, Peru and Colombia as frozen pulp, fresh jam, juice, and to a minor extent as wines. It is concluded from the study that flavonoids, ellagitannins and anthocyanins present in the berry is responsible for the green synthesis of AgNPs. The antioxidant efficacy of the AgNPs was also evaluated and found >78%. Thus the process could be a promising candidate for many biomedical applications as it is environment compatible too.
- Yahyaei et al., 2014 has worked on the rapid adsorption of binary dye pollutants onto the nanostructred mesoporous alumina. In this study ordered mesoporous alumina (OMA)

with pore size of about 5 nm has been used for removal of dye pollutants from binary systems including methyl orange+ bromothymol blue, methyl orange+ reactive yellow and methyl orange+ methyl violet. Derivative spectrophotometry was used for simultaneous determination of the dyes concentrations. The results show that OMA is a nice adsorbent for rapid removal of dyes (especially anionic ones) from aqueous solution. Though OMA cannot remove MV from the aqueous solution, the attractive interaction between the cationic MV and anionic MO may cause the removal of MV by OMA in the binary solution. As the rate of dye removal by the prepared OMA is elevated, this adsorbent can be suggested as a potential adsorbent for flow systems.

- Josheph et al has worked on a microwave-assisted green synthesis of silver nanoparticles and the study on catalytic activity in the degradation of dyes. Biogenic methods are supposed to be a safer alternative to normally used physical and chemical methods of nano synthesis due to their environment friendly nature and cost effectiveness. One major demerit of biological methods is their slow nature. In this study, a novel microwave-assisted green method for the rapid synthesis of silver nanoparticles is reported. By microwave irradiation using the leaf extract of *Biophytum sensitivum*, synthesis of silver nanoparticles is done that act as as both the reducing and stabilizing agent. *B. sensitivum* is a small annual herb part of the family Oxalidaceae. The herb is very useful since flowers of the plant are significant for its medicinal, cultural and traditional values. The catalytic activity of the silver nanoparticles prepared using *B. sensitivum* leaf extract was detected by using them in the degradation reactions of dyes like methyl orange and methylene blue by $NaBH_4$.
- Baghizadeh et al., 2015 has experimented the green synthesis of silver nanoparticles using seed extract of *Calendula officinalis* in liquid phase. Marigold having the botanical name *Calendula officinalis*, is an annual herb and a member of composite family. It is used in common medicine, especially for wound healing, blood purification, jaundice and used as an antispasmodic. Various chemical researches have enforced the presence of different types of compounds, the main being triterpenoids, coumarines, flavonoids, quinones, carotenoids, volatile oil and amino acids. The elevated phenolic content of the hot water extract of *C. officinalis* own strong anti-oxidant properties, that assist in the reduction of Ag cations to Ag/NPs.

- Velusamy et al., 2015 has experimented a greener approach for synthesis of antibacterial silver nanoparticles using aqueous solution of neem gum (*Azadirachta indica L*.) Neem gum is a naturally occurring water soluble, complex polysaccharides procured from the bark of *Azadirachta indica* (part of family Meliaceae). The neem gum is clear, bright and brown colored which was utilized in many industries such as paper, cosmetics, textile, varnish and pharmaceuticals. The hydroxyl and carboxyl groups present in the gum smoothens the formation of silver nanoparticles during autoclaving as evident from the FTIR analysis. The synthesized silver nanoparticles exhibited antibacterial activity against clinical isolates of *Salmonella enteritidis* and *Bacillus cereus*. Also, the antibacterial activity of the silver nanoparticles was further affirmed by degradation of test bacterial DNA. The results advocates that the gum mediated synthesized silver nanoparticles could be used as a potent antibacterial agent against clinical pathogens.
- Mahmoodi et al., 2011 has studied the binary system dye removal from colored textile wastewater using activated carbon and obtained Kinetic and isotherm studies. This paper investigates the ability of activated carbon (AC) to adsorb two anionic dyes Direct Blue 78 (DB78) and Direct Red 31 (DR31) from colored wastewater in single and binary systems. Surface features of AC were detected using fourier transform infrared (FTIR) and scanning electron microscopy (SEM). Effects of AC dosage, salt on dye removal and initial dye concentration were investigated at 25 °C and the isotherm and kinetics of dye adsorption were studied. Adsorption kinetic of dyes was studied in single and binary systems and rate of adsorption was found to follow pseudo — second order kinetic model. The isotherm data of dyes in single and binary systems followed Langmuir isotherm. Results indicated that AC could be used as an adsorbent to remove the anionic dyes from single and binary pollutants systems.
- An et al., 2015 has worked on the enhancement removal of crystal violet dye using magnetic calcium ferrite nanoparticle in single- and binary-solute systems. Novel adsorbent of $CaFe_2O_4$ magnetic nanoparticles (MNPs) was prepared as an effective adsorbent to degrade dye pollutants, acid dye (congo red, CR) and cationic dye (crystal violet, CV) were investigated in single and binary systems. The adsorption tests showed that $CaFe_2O_4$MNPs presented an excellent high affinity to CR (efficiency of CR removal, 96.1%) due to H-bonding interactions as well as dipole–dipole between adsorbent and

acid dye molecules, while CV was hardly adsorbed in single system. The stipulated adsorption was attributed to the symbiotic effect due to the electronic attraction between CV and CR, which promoted CV co-adsorption on $CaFe_2O_4$. Because of the excellent regeneration capacity the $CaFe_2O_4$MNPs are considered to be innovative materials for the uptake of, for instance, toxic dyes from wastewater.

- Atarod et al., 2016 has studied green synthesis of Ag/TiO2 nanocomposite using *Euphorbia heterophylla* leaf extract and detection of its excellent catalytic activity for removal of variety of dyes in water. In this study a facile synthesis of TiO2/Ag nanocomposite by extract of leaves of *Euphorbia heterophylla* is reported without any stabilizer or surfactant. At room temperature, the Ag/TiO2 nanocomposite was found to be effective catalyst for reduction of various dyes, such as Methyl orange (MO), 4-nitrophenol (4-NP), Congo red (CR) and Methylene blue (MB) in the presence of $NaBH_4$ in solution. Catalysis reactions were monitored by employing UV–vis spectroscopy which followed pseudo-first order rate equation. Catalyst used in the process can be recovered and reused several times without significant loss of its catalytic activity.
- Raghavendra et al., 2016 has studied the step-reduced synthesis of starch-silver nanoparticles. Silver nanoparticles were directly formulated in a single step by microwave irradiation of a mixture of starch, deionized water and silver nitrate. This is different from the commonly used procedure for starch-silver nanoparticle synthesis in which silver nanoparticles are obtained by preparing a starch solution as a reaction medium first. Thus, the additional step related to the preparation of the starch solution was removed. In addition, no extra reducing agent was utilized. The adopted method was straight forward and facile, formulating spherical silver nanoparticles with diameter below 10 nm that showed good antibacterial activity. Additionally, influence of starch on the size of the silver nanoparticles was observed.
- Oh et al., 2016 has demonstrated the use of analogous reducibility of phytochemicals for the synthesis of silver nanoparticles. Two phytochemicals were used, gallic acid and protocatechuic acid, that have similar chemical structures but acute differences in their chemical potentials. The keen difference in their potential difference improves the control over the minimization of silver precursors such that their composition and concentration are optimized for both the growth steps and nucleation of NP synthesis. Both steps were

carefully monitored using spectrophotometry and electron microscopy. To calculate the chemical reducibility of the phytochemicals to Ag^+ ions by cyclic voltammetry, the surface interaction of the phytochemicals on the nanoparticles was characterized using computational simulation, and electrochemical analysis and a plausible mechanism of size control was suggested. This novel and valuable method to control the size and the size distribution of silver nanoparticles enables new applications in, biomedical science, materials science and chemical sensor development.

- Fruit extract of *Sterculia acuminate* was used in the formation of biogenic silver nanoparticles (AgNPs) which was further characterized by, FTIR, UV–vis spectroscopy, XRD, Zeta potential and TEMPSA studies. Formation of AgNPs was confirmed initially by spectroscopic studies with the characteristic peak at 426 nm. XRD and TEM reports revealed that AgNPs are highly crystalline and spherical in structure with average particle size of 10 nm. Again catalytic efficiency synthesized AgNPs was detected for the removal of various organic dyes such as 4- nitrophenol (4-NP), methylene blue (MB), methyl orange (MO), direct blue 24 (DB24) and phenol red (PR). It was found that removal of MB and DB24 was rapid than that of other dyes. It is the first report on reduction of organic dyes PR and DB24 using $NaBH_4$ as reducing agent in the existence of catalytic amount of AgNPs. Hence this synthesis process may be the best substitute of both chemical and other physical methods used in industry for large scale production of NPs (Bogireddy et al., 2016).
- By appending silver nitrate as a source of silver ions, Silver nanoparticles (AgNPs) were synthesized in low cost skim natural rubber latex. Ammonia that was left over in latex was believed to form a complex with silver ions before reacting with the reducing agents (glucose and other organic compounds). Moreover, protein in latex could also control the growth of the particles by acting as a capping agent. Factors, which include D-glucose content, ammonia content and protein content, were studied to conclude their effects in the production. TEM images confirmed that the size of AgNPs in the sample was 6–26 nm and the synthesized AgNPs could inhibit the growth of *Staphylococcus aureus* and *Escherichia coli.* (Suwatthanarak et al., 2016).

MATERIALS AND METHODOLOGY

4.0 MATERIALS AND METHODOLOGY

4.1 MATERIALS:

The leaves of neem (*Azadirachta indica*) and Basil/ tulsi (*Ocimum sanctcum*) were collected from the Sonarpur area of Kolkata, West Bengal. This two particular leaves are considered because of their high bactericidal and fungicidal activities and both of them are well considered as ayurvedic herbs which act as tonic, astringent and antiseptics. Moreover these two leaves are easily available in tropical countries like ours. The soil required for the synthesis of nanocomposite is also collected from the same area. The chemicals used in the experiment like Silver nitrate ($AgNO_3$) and the dyes Gentian Violet (GV), Methylene Blue (MB) and Malachite Green (MG) were bought from Merck Company (Germany).

Figure 4.1 Leaves of Neem (*Azadirachta indica*) and Basil (*Ocimum sanctum*)

4.2 METHODOLOGY:

The methodology is briefly described in four steps. They are

- Collection of the leaves and preparation of the leaf extracts.
- Leaf extract mediated synthesis of the silver nanoparticles.
- Preparation of silver nanocomposite and
- Preparation of dye stock solution.

4.2.1 Collection of the leaves and Preparation of leaf extracts:

a. The fresh and healthy leaves of neem (*A. indica*) and basil/tulsi (*O. sanctum*) are collected separately from Sonarpur area.
b. Then they are washed thoroughly thrice using double distilled water to remove the impurities present in the leaves shown in figure below.
c. After that the washed leaves are chopped into fine pieces using a sterilized knife and then taken separately in two 250 ml beaker and 100 ml of double distilled water is added to both of them and it is boiled for 15- 20 minutes.
d. Thus we get two separate leaf extracts – the extract obtained from neem leaf is pale green in colour whereas the Basil leaf extract is a little darker in hue.
e. The two green color solution obtained is allowed to cool for around 2 to 3 hours and filtered using filter paper.
f. These pale green solutions are the required leaf extracts which will act as the reducing, stabilizing as well as capping agent.
g. The solution is sealed tightly in air sealed bottles and placed in 4 degree Celsius for further use.

Figure 4.2 shows the washed Basil leaves and the filtered extract.

4.2.2 Synthesis of the silver nanoparticles using leaf extract:

a. 1 mM of silver nitate solution is prepared. Then 95ml of silver nitrate solution is taken in two 250ml Erlenmeyer flasks and 5 ml of the leaf extracts of neem and basil are added in a dropwise manner to both the flasks separately.

b. Now for the complete bioreduction of the solutions the flasks were placed in a microwave oven at 300W for 10 to 15 minutes.
c. Now a color change is observed from pale green to pale red and at then to dark reddish brown.
d. The absorption maxima of the solutions are measured in a UV-VIS Spectrophotometer.
e. Then the colloidal mixtures obtained are cooled and kept for future use.

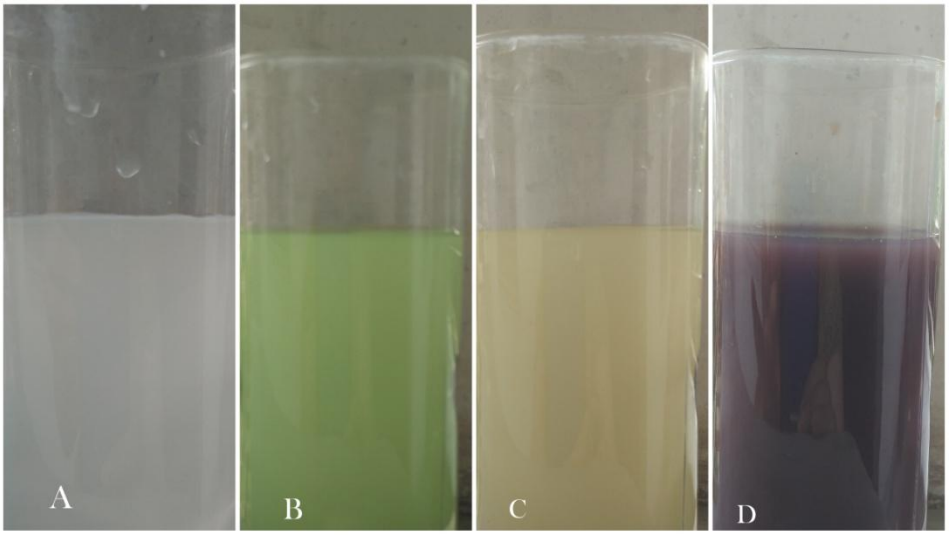

Figure 4.3 The change in the color of the leaf extract containing silver nitrate solution

4.2.3 Preparation of silver nanocomposites:

a. Soil needed for the preparation of the silver nanocomposites is first collected, dried and churned into fine particles.
b. After that the impurities and uneven particles present in it is removed by sieving the soil.
c. Now the silver nanoparticles containing colloidal mixture of both the leaves are added to the soil separately in two beakers and mixed properly using a hand stirrer.
d. The solution mixtures are placed in an incubator shaker overnight for thorough mixing.
e. After the completion of about 12 hours the mixtures are taken out and allowed to settle for another 12 hours.
f. The supernatant obtained is therefore removed and the settled composites are separated then dried, churned into fine particles and sieved which act as the required adsorbents.

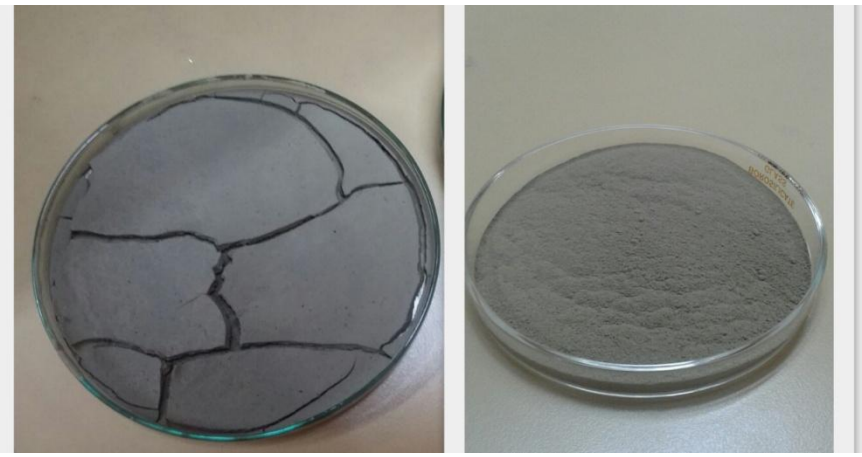

Figure 4.4 the formation of nanocomposite

4.2.4 Preparation of dye stock solution:

a. Three dyes were used in the experimental procedure - Gentian Violet (GV), Methylene Blue (MB) and Malachite Green (MG).
b. Gentian Violet (GV) dye have molecular weight 408, molecular formula $C_{25}H_{30}N_3Cl$ and maximum absorption peak λ_{max} 578nm.
c. Methylene Blue (MB) dye have molecular weight 319.85, molecular formula $C_{16}H_{18}ClN_3S$ and maximum absorption peak λ_{max} 667nm.
d. Malachite Green (MG) dye have molecular weight 364.911, molecular formula $C_{23}H_{25}N_2Cl$ and maximum absorption peak λ_{max} 618nm.
e. The solid dyes were added to double distilled water to get the required stock solution.
f. Now different concentrations were obtained by diluting the stock solution.

Figure 4.4 The dye solutions used

4.3 CHARACTERIZATION OF THE NANOCOMPOSITES FORMED:

The comparative studies are performed using the adsorbents made of neem, basil leaf and only soil. The 3 composites are characterized by UV-VIS Spectroscopy, Scanning Electron Microscopy (SEM), Transmission Electron microscopy (TEM), Fourier Transform Infrared Spectroscopy (FTIR) and X-Ray Diffraction (XRD) Analysis.

4.3.1 UV-VIS Spectroscopy Analysis:

During the synthesis of silver nanoparticles from the leaf extract and silver nitrate solution, a change in color is obtained from pale green to pale red and at last dark reddish brown. The surface Plasmon resonance of the nanoparticles formed in the colloidal mixture is measured using a UV-visible spectrophotometer (Lambda 25 Perkin Elmer) in a range of 400-700nm. Furthermore the batch studies are also conducted using the UV-visible spectrophotometer. UV/Vis spectrophotometer calculates the intensity of light which is passing through a sample (I), and tallies it to the intensity of light before it passes through the sample (I_0). Ratio I/I_0 is called the transmittance, which is related to Absorbance. The main parts of a spectrophotometer are a light source, a diffraction grating in a monochromator or a prism, a detector and a holder for the sample. The radiation source is mostly a Tungsten filament or a deuterium arc lamp, that is continuous over the ultraviolet and visible region (190-800 nm).

4.3.2 Scanning Electron Microscopy:

The size and the morphological characterization of the silver nanoparticles formed in the composites are determined using SEM. A thin layer of metal (gold) using a sputter coater is used to coat the samples for providing a better image, to arrest the electrical charge accumulation, and microscopic analysis were performed using Scanning electron Microscope (Model Hitachi S-3000N) with an electron acceleration voltage of 20 kV for excitation of the samples. The SEM scans consists of a narrow, tapered electron beam back and forth over the specimen (here nanocomposites). When the beam collides a particular area, surface atoms ejects a tiny shower of electrons, and these are trapped by a special detector.

4.3.3 Transmission Electron Microscopy:

The morphology of the nanocomposites formed were also measured by Transmission electron

microscope. TEM is a commonly a microscopy technique in which a beam of electrons is transmitted through an ultra-thin component, reacting with the component as it passes through it. The image was formed due to the interaction of the electrons that are transmitted through the nanocomposites. A TEM is made of several components, which include a phosphor screen, vacuum system in which the electrons travel, a series of electromagnetic lenses, an electron emission source for generation of the electron stream, as well as electrostatic plates.

4.3.4 Fourier Transform Infrared Spectroscopy (FTIR) Analysis:

The presence of different functional groups in the three composites can be measured by using the FTIR Analysis since each group has a specific energy absorption band. So the analysis for three components were done in a FTIR Spectrophotometer (Perkin-Elmer Spectrum version 10.4.4 model) in a wavelength range of 4000-400 cm^{-1}. The spectrometer consists of a source of infrared light, emitting radiation throughout the whole frequency range of the instrument. Light from the source is split into two beams of equal intensity. One beam is made to pass through the sample while the other is a reference beam. At the wavelength where the sample has absorbed, the detector receives a weak beam from the sample while the reference beam will return full intensity. The frequencies where the sample does not absorb, both the beams will have equal intensities.

4.3.5 X-Ray Diffraction (XRD) Analysis:

Analysis of X-ray diffraction of the nanocomposite adsorbent was carried out using X-ray diffractometer equipment with a Cu Kα radiation source and Braggs angle ranging from 20 -80 degrees for the three adsorbents to find out the crystalline nature of the three composites. Generally crystals are regular arrays of atoms, and X-rays is considered waves of electromagnetic radiation. The atoms scatter X-ray waves, primarily through the atoms' electrons, as a result an X-ray striking an electron generates secondary spherical waves ejected by the electron. A regular range of scatterers produces a regular array of spherical waves which eliminate each another out by destructive interference and also add constructively in a few specific directions, determined by Bragg's law.

$$2dsin\theta = n\lambda$$

Here θ is the incident angle, and λ is the wavelength of the beam.

4.4 Batch Studies:

Batch studies were carried out in 250-mL Erlenmeyer flasks with 100 mL of dye solution. A certain weighed amount of two nanocomposites and soil were added separately to the dye solution in separate flasks. The flasks were agitated at a speed of 140 rpm in an incubator shaker at 308 K. The influence of pH (2.0– 10.0), initial dye concentration (100–500 mg L^{-1}), nanocomposite dosage (0.025–0.2 g/L) and temperature (298, 303, 310, 313, 318 K) were evaluated. At regular time intervals samples were collected and centrifuged for analysing the residual dye concentration in the solutions. The residual amount of dye in each flask was investigated using UV/VIS spectrophotometer (Lambda 25 Perkin Elmer). The amount of dye adsorbed per unit of nanocomposite for all three of the adsorbents were determined according to a mass balance equation:

$$q_e = \frac{(c_i - c_e)V}{m}$$

where C_i is the initial dye concentration (mg L^{-1}), C_e is the equilibrium dye concentration in solution (mg L-1), V is the volume of the solution (L), and m is the mass of the nanocomposite in g.

The percent removal (%) of dye was calculated using the following equation:

$$\left\{\frac{c_i - c_e}{c_i}\right\} * 100$$

The result obtained in terms of the effects of parameters are compared for the three adsorbent used and plotted in form of graphs.

4.5 EXPERIMENTAL PROCEDURE:

Green Synthesis of metallic nanoparticles has gained worldwide recognition for the removal of harmful dyes from waste water. Though the process has gained recognition in laboratories and research facilities but it is still not used in industries in effective removal of the dyes from effluents. Various plant part extracts are used in preparation of the metallic nanoparticles. In our study silver nanoparticles are prepared from the leaf extracts of neem leaf (*Azadirachta indica*) and Basil leaf (*Ocimum sanctum*). These two nanoparticles are then mixed with soil to produce nanocomposites and comparative studies were performed using various dyes to study about the

effectiveness of the nanocomposites prepared. A few comparative studies were performed in this project. They are:

- In the first experiment a comparative study is performed for the removal of Gentian Violet dye using three composites - silver nanocomposite made of neem leaf (*Azadirachta indica*) extract, silver nanocomposite made of Basil leaf (*Ocimum sanctum*) extract and only soil. Batch studies are carried out varying parameters like Adsorbent dose, Temperature, Time, Dye concentration, Agitation speed, pH etc. Then the adsorption isotherm, thermodynamics and kinetics were measured and conclusions were gained.
- In the second experiment a comparative study between two dyes were performed using three nanocomposites – silver nanocomposite made of neem leaf (*Azadirachta indica*) extract, silver nanocomposite made of Basil leaf (*Ocimum sanctum*) extract and only soil. The two dye solutions of Methylene blue and Malachite green were prepared separately of same concentration 10 ppm. Keeping all the parameters constant like adsorbent dose, temperature, time, dye concentrations, pH etc experiments were done to see in which dye we are getting the maximum adsorption or in which dye the maximum percentage removal is obtained and conclusions are obtained from it.
- In the third experiment a binary dye solution is prepared using Methylene Blue and Malachite Green dye of same concentration 10ppm in the ratio 1:1. After that previously used three adsorbents are used for the removal of the dyes from the binary dye solution. Batch studies were performed varying various parameters, adsorption isotherm, thermodynamics and kinetics were measured and they are correlated.
- In the fourth experiment again a comparative study is performed where two binary solutions are prepared using Methylene Blue and Malachite Green dyes in different ratios 3:7 and 7:3 respectively. Now three adsorbents - silver nanocomposite made of Basil leaf, silver nanocomposite made of Neem leaf and soil were used for the removal of the dyes from the binary solutions. Batch studies, Adsorption isotherm, thermodynamics and kinetics were performed, compared and conclusions were drawn from it.
- In the fifth experiment a model experiment is done to check the efficiency of *Ocimum sanctum* nanocomposite in removing dye effluents if dumped in a landfill like structure to prevent groundwater contamination. This experiment is done in form of a model since a

large area to create a landfill was not present since it can be hazardous and also can be time consuming. In the experiment a column is prepared using poly acrylic sheet such that in the middle there is a semi permeable membrane that prevent the direct flow of dye containing solution through water. The length and diameter of the column is 19cm and 6 cm respectively. At first, the column is filled with silver nanocomposite made of *Ocimum sanctum* leaf extract for around 4 cm height above that the Methylene Blue solution of concentration 50ppm is added upto a height of 12 cm. Therefore in the total height of 19 cm, the bottom 4 cm is nanocomposite and the above 12 cm is dye solution of concentration 50ppm and pH 2, since optimum pH obtained is 2 from the previous batch experiments. The whole setup was kept at room temperature. Now the experiment was performed for 15 days. Each day the adsorbed solution was taken out of the bottom and the optical density was measured in a spectro photometer and a graph is plotted between time (in days) and the percentage removal. Similar experiment is done using only soil as adsorbent.

The results of the experiments are given in different segments in Result and Discussion.

RESULTS AND DISCUSSION

5.0 RESULTS AND DISCUSSION

5.1 CHARACTERIZATION RESULTS:

5.1.1 UV-VIS Spectroscopy:

The synthesis of silver nanoparticles in aqueous extracts were identified by collecting the samples and measuring using UV–VIS spectrophotometer. For the nanocomposite made of basil leaf the maximum absorption peak is obtained at 422 nm and for the nanocomposite made of neem leaf the maximum absorption peak is obtained at 435 nm shown in figure 5.1 and 5.2.

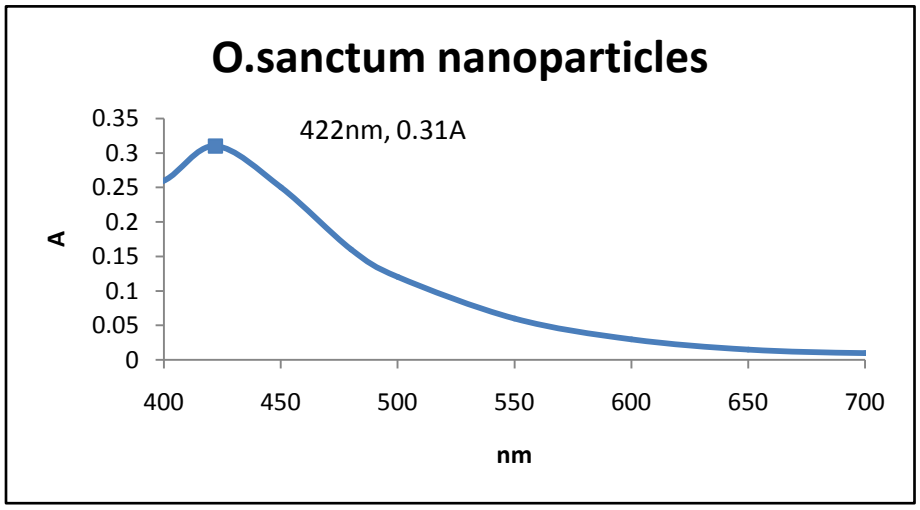

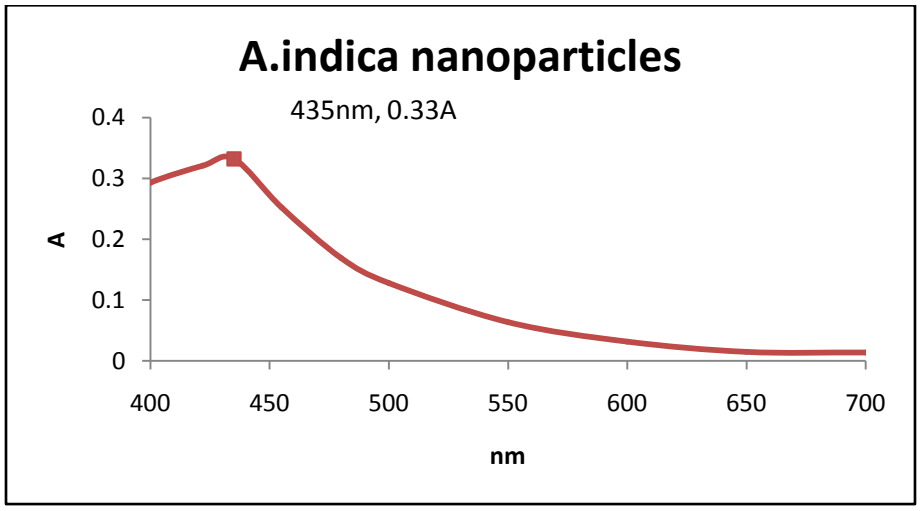

Figure 5.1 and 5.2 represents the UV-VIS Spectroscopic result of *O.sanctum* and *A.indica* nanoparticles

5.1.2 SEM Analysis:

The SEM images of the three adsorbents are shown in the figure 5.3, 5.4 and 5.5. The figure indicated that the soil showed a crystalline mass form and the shape of silver nanoparticles were

spherical, oval and irregular polygonal for both the adsorbents made of neem and basil leaf extracts and the average size obtained was around 38.7nm which was a good agreement with earlier reports.

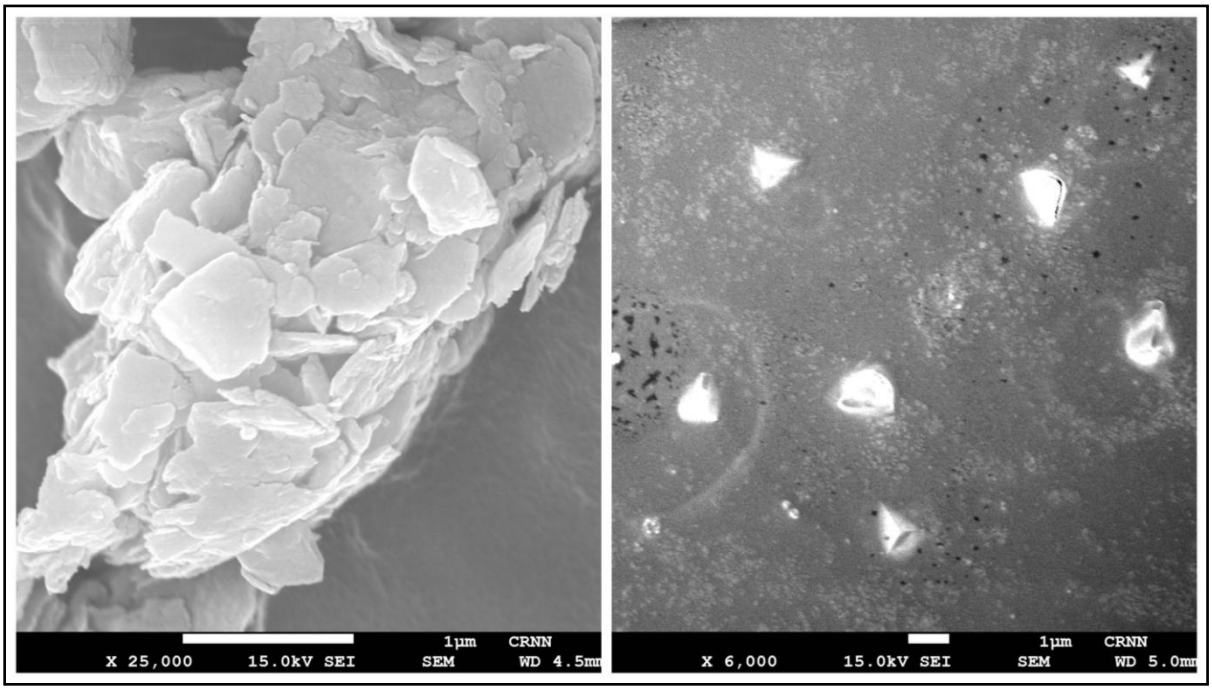

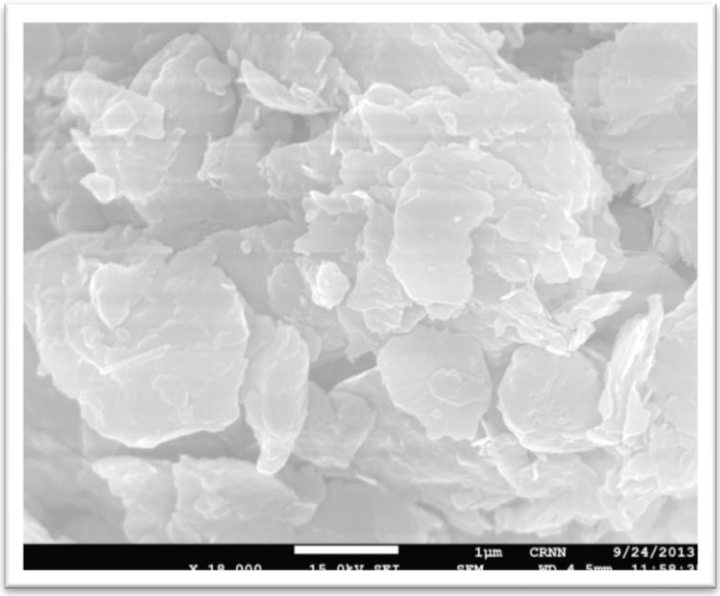

Figure 5.3, 5.4 and 5.5 represents the SEM image of Silver Nanocomposite made of *O.sanctum, A.indica* and only Soil adsorbent.

The soil sample used in the experiment had a pH of 7.4, moisture content of 27% and amount of clay present 28 %, silt 66 % and sand 5 %.

5.1.3 TEM Analysis:

The TEM image of the soil-AgNP from *O. sanctum* and *A. azadirachta* were also provided in figure 5.6 and 5.7. The morphology of the silver nanoparticles formed were quite spherical and the size ranges from 36.4 to 40.2 nm, the average of which was nearly 38.5nm which was quite a match to the SEM results obtained earlier.

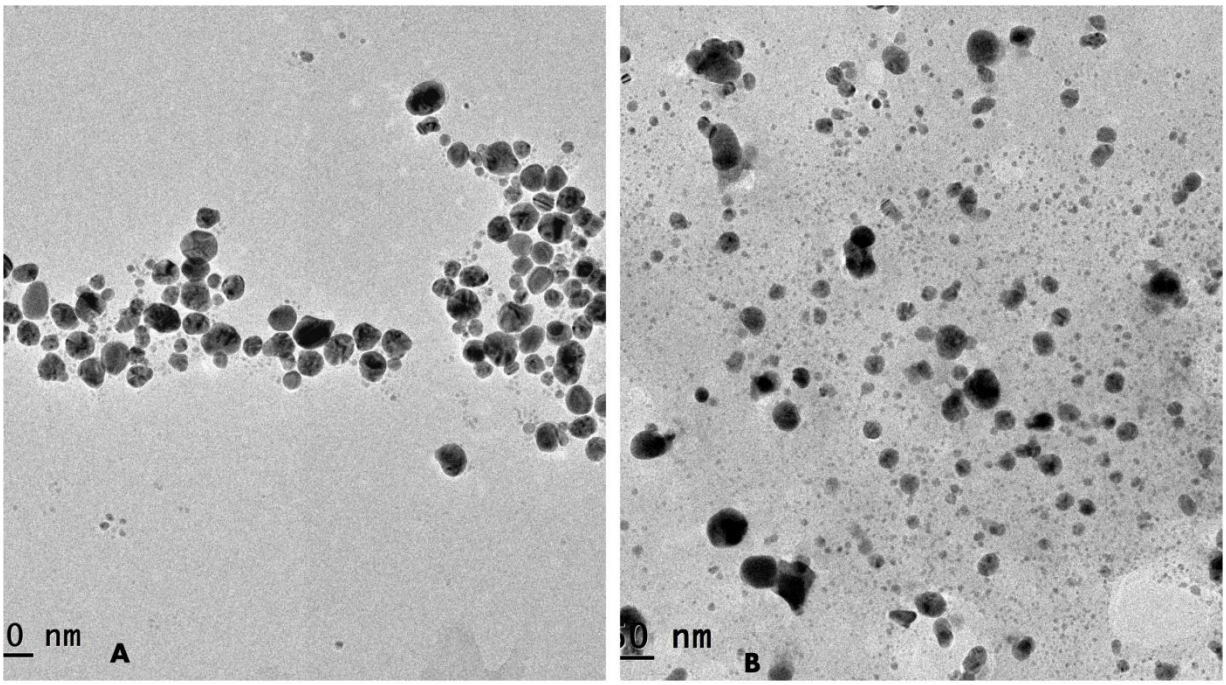

Figure 5.6 and 5.7 represents the TEM images of Basil leaf nanocomposite and Neem leaf nanocomposite respectively.

5.1.4 FTIR Analysis:

Fourier Transform Infrared spectral analysis was carried for the three adsorbents, showed range of absorbance bands in 400–4,000 cm^{-1} is shown in the figure 5.8. The peaks of the absorption bands for adsorbent made of basil leaf were at 3960, 2929.4, 2120.4, 1659.5, 1465.4, 1316.6, 1075.2, 776.5, and 693.4 cm^{-1} which is due to the presence of phenolic group, ketones, triple bond C-C and C-N groups, protein amide I, Carbonyl group C=O, esters, carboxyl groups,

aromatic C-H benging patterns, alkenes respectively. The peaks of the absorption bands for adsorbent soil were at 693.41, 776.40 and 986.99 cm^{-1} which indicated the presence of alkene, alkyne and aromatic C-H bends and amines C-N group respectively. The peaks of the absorption bands for adsorbent made of neem leaf were at 721, 1,637.27, 2,364.3, 3,334.1 and 3,745.08 cm^{-1} suggesting alkenes, carbonyl groups, protein amide I, aromatic rings, Hydroxyl group, Triple bond C-N, alcohols and phenols [Sun et al., 2014]. A trace amount of chloride, carboxyl group,disulfide, tertiary ammonium ions and hydrogen bonds were also observed [Pandian et al., 2015]. A table showing the functional groups and their corresponding absorbance is also provided.

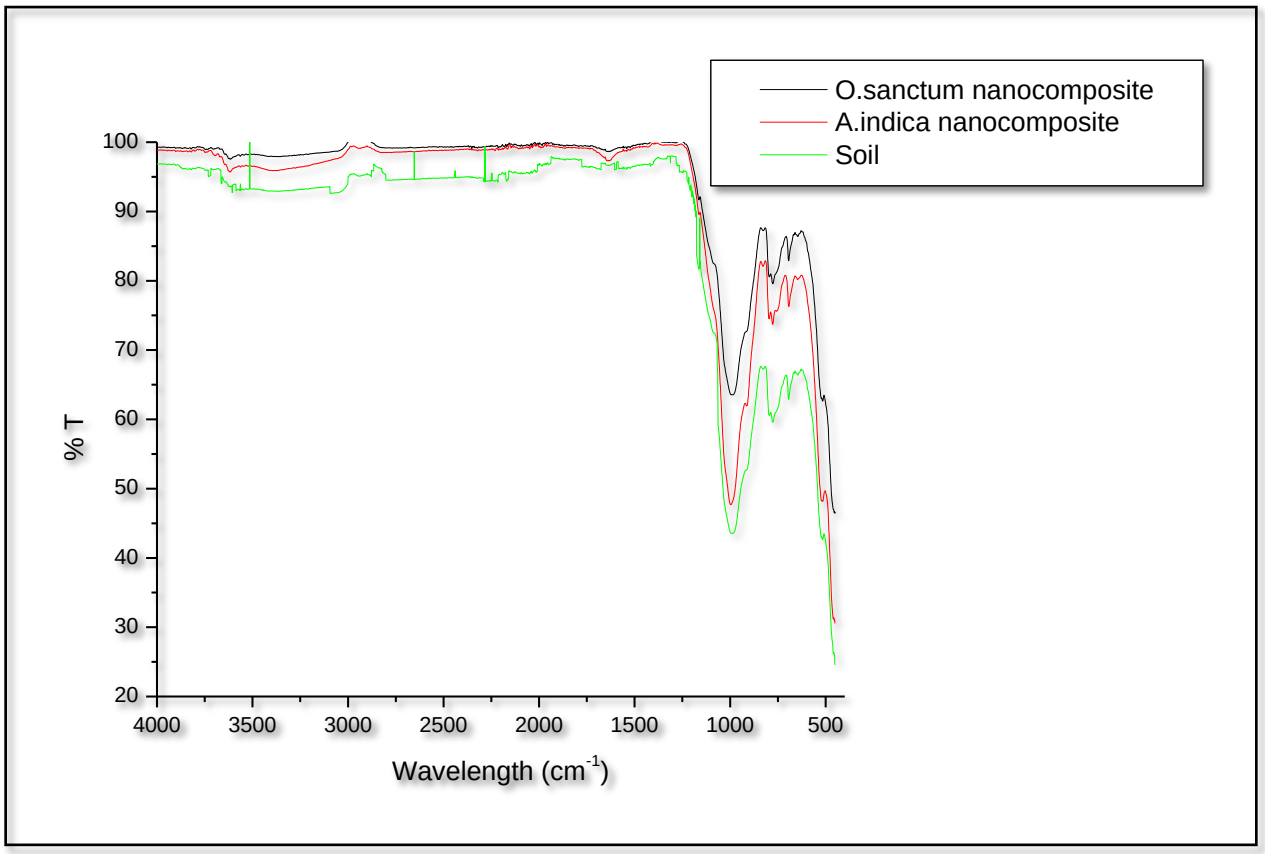

Figure 5.8: FTIR spectroscopic image of the three adsorbents

5.1.5 XRD Analysis:

XRD analysis of Ag-nanocomposite form *A. indica* and *O. sanctum* leaf extracts and only Soil demonstrated the crystalline nature of the adsorbents shown in figure 5.9. The maximum peaks

for the silver nanocomposite from *O.sanctum* were observed at 27.8, 32.3, 38.1, 46.3, 54.9, 67.5^0 and 76.7^0 respectively which index to (1 1 0), (1 1 1), (2 0 0), (2 1 1), (2 2 0), (1 0 3) and (0 0 4) respectively for face centered cubic silver as well as silver oxide. And maximum peaks for the silver nanocomposite from *O.sanctum* were observed at 27.9, 38.3, 44.3, 64.3 and 77.5 and the corresponding values of lattice plane are indexed at (1 1 1), (2 0 0), (2 2 0) and (3 1 1) of face-centered cubic (fcc) silver [Dhand e tal., 2016]. The major components present in nanocomposites were Silver(Ag), quartz, feldspar, mica, amphibole, kaolinite and calcite due to the presence of soil in the composite. The crystalline size of the silver nanocomposites were found using the Scherrer formula given below.

$$D = 0.94\lambda/\beta \cos\theta$$

D is the average crystalline size, λ is the X Ray wavelength, β is the full width half maximum (FWHM) and θ is the diffraction angle. The crystalline size of both the composites is around 32 to 38nm which is agreeable with the SEM and TEM results.

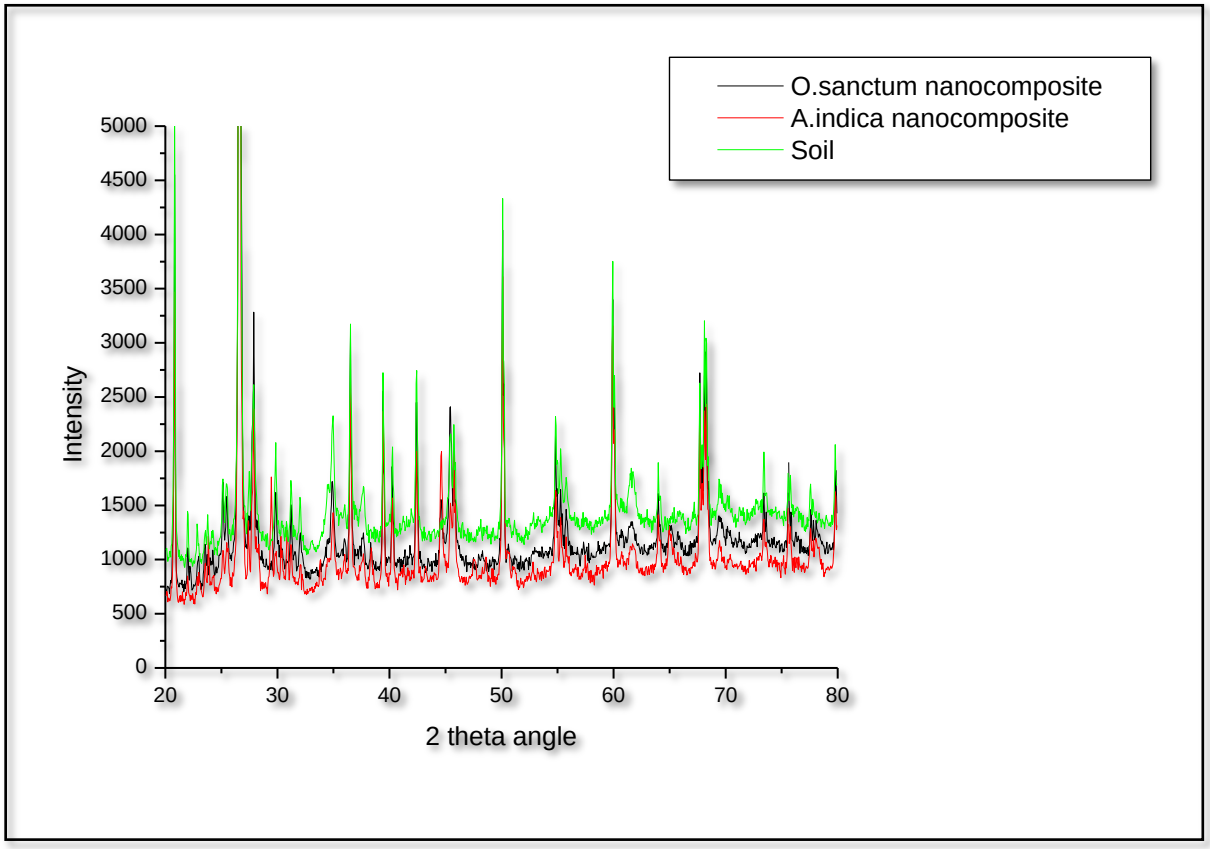

Figure 5.9: XRD image of three adsorbents

5.2 BATCH EXPERIMENTS

5.2.1 EXPERIMENT 1 : Comparative study between three adsorbents for the removal of Gentian Violet dye.

In this experiment silver nanocomposites is made of *Ocimum sanctum* and *Azadirachta indica* leaf extract and soil. A comparative study has been done using the two nanocomposites and simple soil for the removal of Gentian violet dye. It is observed out of the three adsorbents used the silver nanocomposite made of *Ocimum sanctum* leaf extract is providing the maximum adsorption of about 98.99%. Now during the batch experiments the effects of different parameters are illustrated below.

5.2.1.1 Effect of mass of adsorbents:

100 ml of gentian violet dye of concentration 200 mg/L were taken in five conical flasks and in them 25mg, 50mg, 75mg, 100 mg and 200 mg of nanocomposite made of *O. sanctum* were added and placed in a shaker incubator at speed 120 rpm. The temperature was maintained at 308K throughout the process. The same process was carried out for composites made of *A. indica* and only soil adsorbents and percentage removal was obtained.

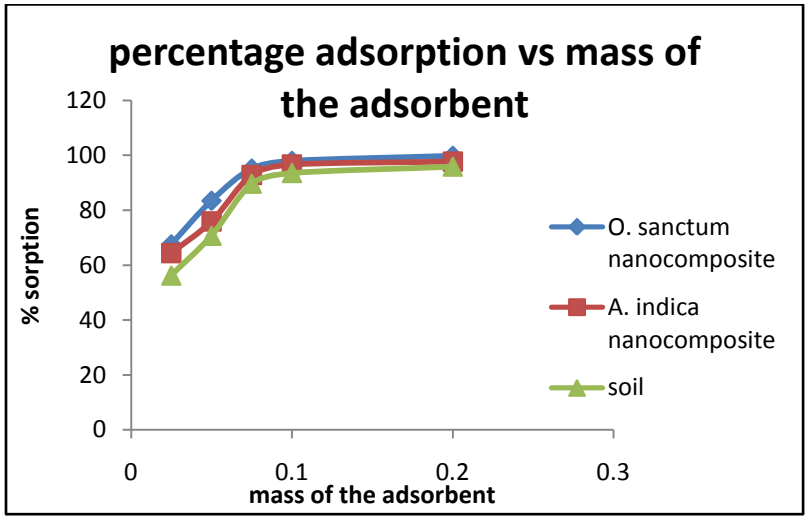

Figure 6.1 Percentage adsorption vs the mass of the adsorbent

It was observed from figure 6.1 that with the increase in the adsorbent dosage from 25mg to 200 mg there was a gradual increase in percentage removal for all the three adsorbents. The reason of this behavior may be due to increased surface area of adsorption and availability of more binding sites.

5.2.1.2 Effect of Temperature:

The effect of temperature was obtained for the temperatures 298K, 303K, 308K, 313K and 318K respectively for all the three adsorbents at shaker speed 120 rpm. In all the three adsorbents, with the increase in temperature there was an increase in the percentage removal shown in figure 6.2. The increasing temperature may be explained by the increased attraction of binding sites with the dye molecules at higher temperature or an increase in motion of the dye molecules which may result in rapid adsorption.

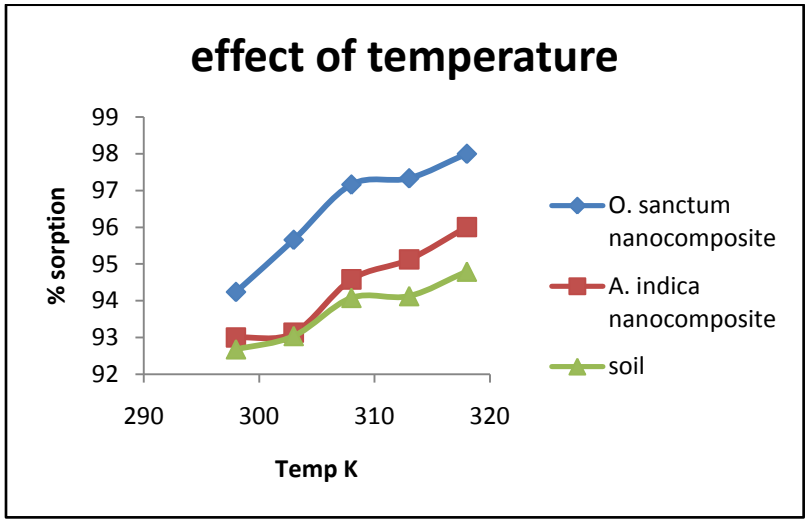

Figure 6.2 Percentage adsorption vs temperature

5.1.2.3 Effect of pH:

pH stability of the nanocomposites were done in a range of pH 2 to 10 having constant temperature 308K and shaker speed 120 rpm shown in figure 6.3. UV- VIS spectrophotometer reading showed that maximum removal of dyes were obtained at pH 2 for all the three adsorbents from the solutions at λ_{max} value 580 nm.

The GV dye solution had an optimum pH of 7.2 and the soil-AgNP from *O.sanctum*, *A. indica* and soil had pH 7.6, 7.8 and 7.4 respectively. In the comparative study the maximum adsorption was showed by the soil-AgNP from *O.sanctum* which was 98.49 %.

At lower pH the adsorbents and the cationic dyes shows strong columbic repulsion which may be a reason for increased percentage removal.

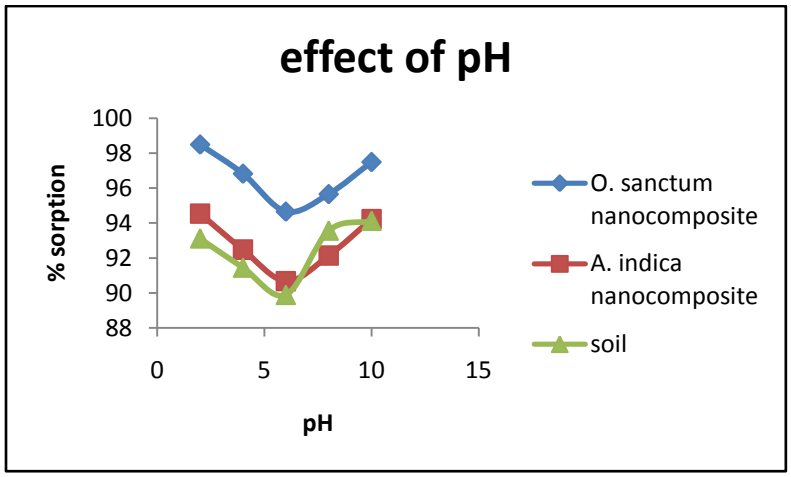

Figure 6.3
Percentage adsorption vs pH

5.2.1.4 Effect of dye concentration:

The effect of the dye concentration in a range of 100 to 500 mg L^{-1} for three adsorbents at 308K and pH 2 were shown in the figure 6.4. The adsorption process was highly influenced by the initial concentration of the dye (adsorbate). It was observed that until a certain point, the amount of dye adsorbed does not change with increase in the dye concentration as shown in figure 6.4, after which there was a gradual decrease.

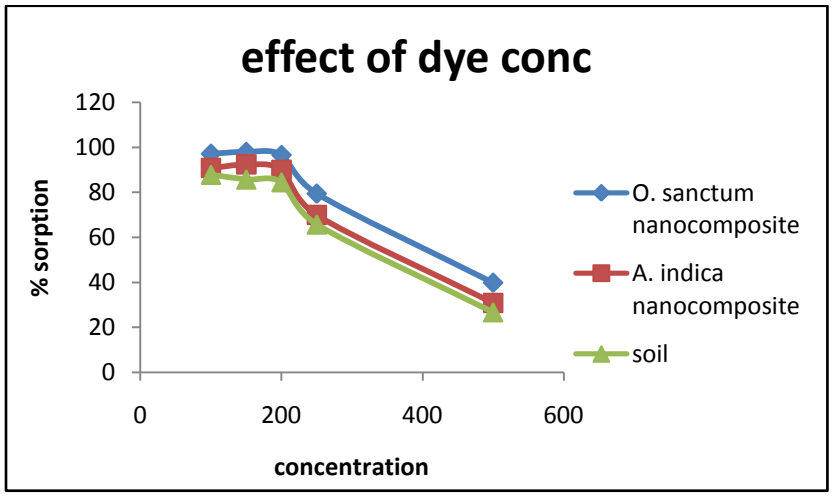

Figure 6.4
Percentage adsorption vs dye concentration

In the figure it is observed that with increase in dye concentration from 100 to 200 mg L^{-1} for all the three composites there was increase in percentage removal but from concentration 200 to 500 mg L^{-1} there was a decrease. If the concentration of GV in solution is higher, the active sites of

the nanocomposites may have been surrounded by a lot of GV ions which results to a more efficient adsorption phenomenon. Above the equilibrium concentration, the adsorption site in AgNP composites were saturated as a result excess dyes remains in the solution and decreases the percentage of adsorption.

5.2.1.5 Effect of contact time and agitation speed:

The experiment of contact time was performed for time - 2mins, 5mins, 8mins, 12mins, 15mins, 30mins, 60mins, 90mins and 120mins for pH 2, temperature 308K and 120 rpm. The experiment was performed for soil, soil-AgNP for *O.sanctum* and soil-AgNP for *A.indica*.

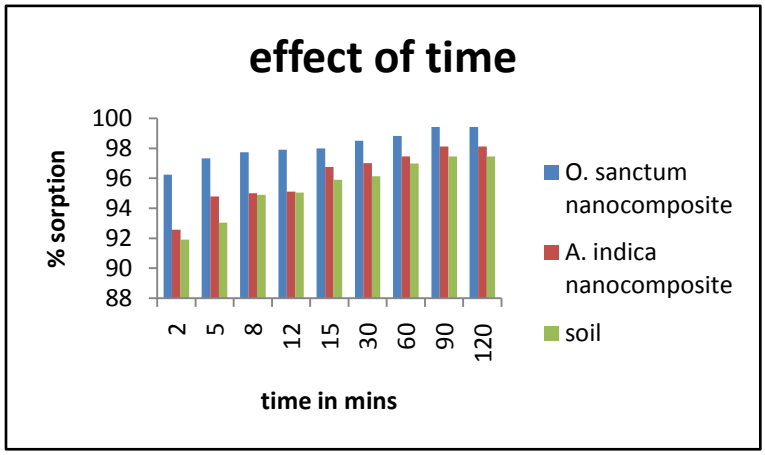

It was observed that the percentage removal keeps on increasing with increase in contact time but after certain time when it reaches equilibrium there was no further change in the removal. It may be due to the fact that contact time increases the availability of active sites while further increase causes immobilization of the cationic dyes on the silver nanoparticles. Similar trend was observed in agitation speed experiment.

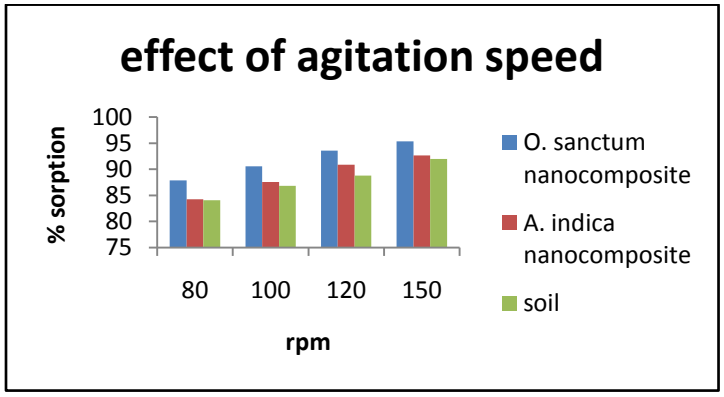

Figure 6.5 and 6.6 Percentage adsorption vs contact time and agitation speed

5.2.1.6 Adsorption isotherms:

- **Langmuir isotherm:**

The experimental data c_e/q_e was plotted against c_e for the three nanocomposites at temperature 308Kand is shown in figure 6.7. Value of q_m and K_L were determined from the plot. Parameters and correlations are obtained from the plots of Langmuir provided in the table 1.

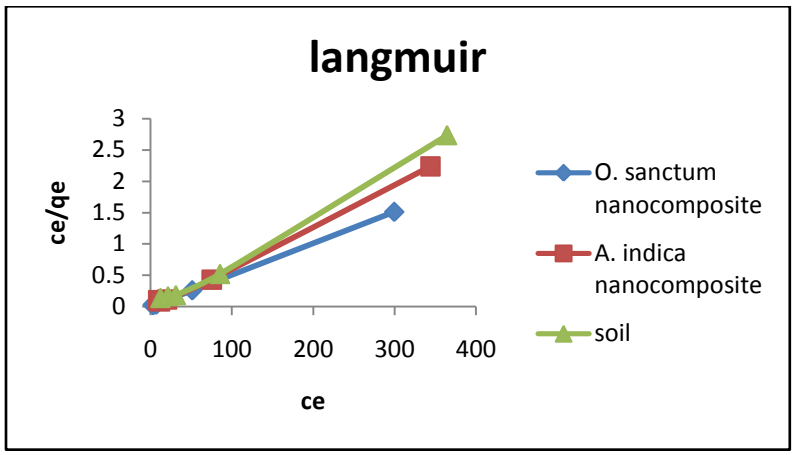

Figure 6.7 C_e/q_e vs C_e Langmuir Isotherm

The Langmuir model was well fitted with the value of R_L between 0 to 1 which indicates a favorable adsorption of adsorbates. Moreover higher correlation coefficient (R^2) indicated that the surface of silver nanoparticles and soil had accommodated a monolayer of adsorbate without any interaction between adsorbed species. Similar trend was reported by Pandian et al., 2015 and Satapathy et al., 2013 for dyes.

- **Freundlich isotherm:**

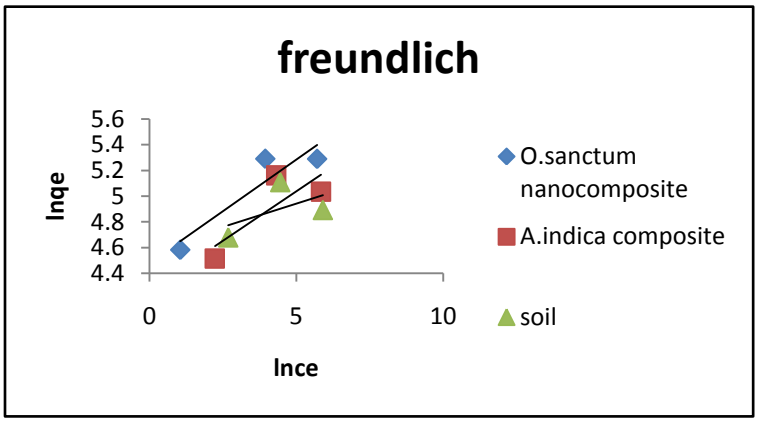

Figure 6.8 $\ln C_e$ vs $\ln q_e$ Freundlich Isotherm

Plots were obtained between lnc_e and lnq_e for the three adsorbents and compared. The estimated coefficients of the Freundlich model (K_F and n) for GV dye adsorption onto soil and silver nanocomposites were listed in the table 1 below. The K_F value represents the degree of adsorption and n denotes the adsorption intensity. The value of n was higher than unity for all the adsorbents, indicating that GV ions were favorably adsorbed on soil and silver nanocomposites.

- **Temkin isotherm :**

The plot is drawn between lnc_e and q_e for the three adsorbents and the correlation parameters and coefficient are given in table 1.

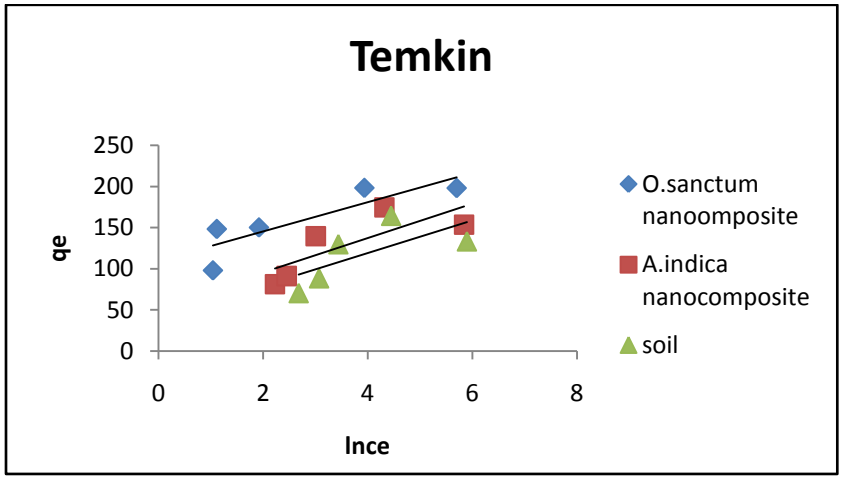

Figure 6.9 lnc_e vs q_e Temkin Isotherm

Table 1:

LANGMUIR PARAMETERS	**SOIL-AgNP (*O.sanctum*)**	**SOIL-AgNP (*A.indica*)**	**SOIL**
q_0 mg /g	200	166.67	142.857
K_L L/mg	1.6667	1.5	3.57
R^2	0.999	0.998	0.996
FREUNDLICH PARAMATERS			
K_F mg/g	9.79	9.66	13.17
n	6.25	6.54	13.89
R^2	0.858	0.863	0.796

TEMKIN PARAMETERS			
B J/mol	17.78	20.9	19.58
b	144.022	122.52	130.78
A L/mg	6.169	12.92	7.595
R^2	0.739	0.768	0.714

5.2.1.7 Thermodynamic studies:

To conclude whether the process is spontaneous in nature or not thermodynamic studies of an adsorption process is necessary. The figure 6.10 below shows the vant hoff plot for *O. sanctum* nanocomposite. Similar plots were drawn for the other two adsorbents (figure not shown). The following equations were used:

$$\Delta G^0 = -RT\ln K_C$$

$$\Delta G^0 = \Delta H^0 - T\Delta S^0$$

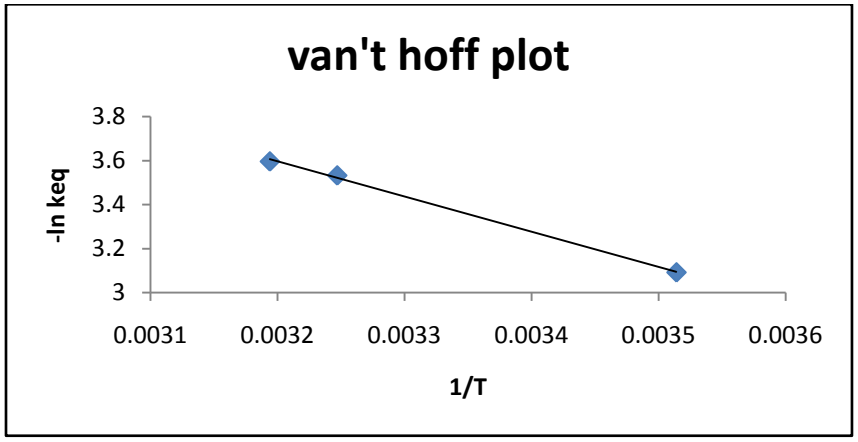

Figure 6.10 Vant hoff plot for *O.sanctum*

Table 2 shows the values of different thermodynamic parameters obtained. The negative value of ΔG^0 for all the temperatures, for the three adsorbents confirmed that the processes were spontaneous. Negative value of ΔH^0 implied that the adsorption processes were exothermic in nature. The positive value of ΔS^0 indicated the increase in randomness at the solid–liquid interface during adsorption. The calculated E_a value was less than 40 kJ mol^{-1} suggesting that the adsorption process of GV on nanocomposite followed physical adsorption.

TABLE 2:

PARAMETERS	ΔH^0 KJ mol^{-1}	ΔS^0 J mol^{-1} K^{-1}	ΔG^0 (25^0C) KJ mol^{-1}	ΔG^0 (30^0C) kJ mol^{-1}	ΔG^0 (35^0C) kJ mol^{-1}	ΔG^0 (40^0C) kJ mol^{-1}	ΔG^0 (45^0C) kJ mol^{-1}
Soil-AgNP (basil leaf)	-1.068	7.004	-6.92	-7.79	-9.04	-9.36	-10.24
Soil-AgNO (neem leaf)	-0.709	5.2	-6.41	-6.57	-7.32	-7.73	-8.40
Soil	-0.395	4.042	-6.29	-6.53	-7.08	-7.22	-7.67

5.2.1.8 Kinetic studies:

The Lagergren's pseudo-first-order and Ho–McKay's pseudo-second-order models (Ho and McKay, 1999) were applied to the experimental data for the three adsorbents shown in figure 6.11. The values of pseudo-first-order rate constants, k_1 (min^{-1}) and qe (g. mg^{-1}) were calculated for the three adsorbents from the slopes and intercepts of the graphs between $\log(q_e - q_t)$ versus t .The pseudo first order kinetics suggested that the rate of occupation of adsorption site is proportional to the number of unoccupied sites.

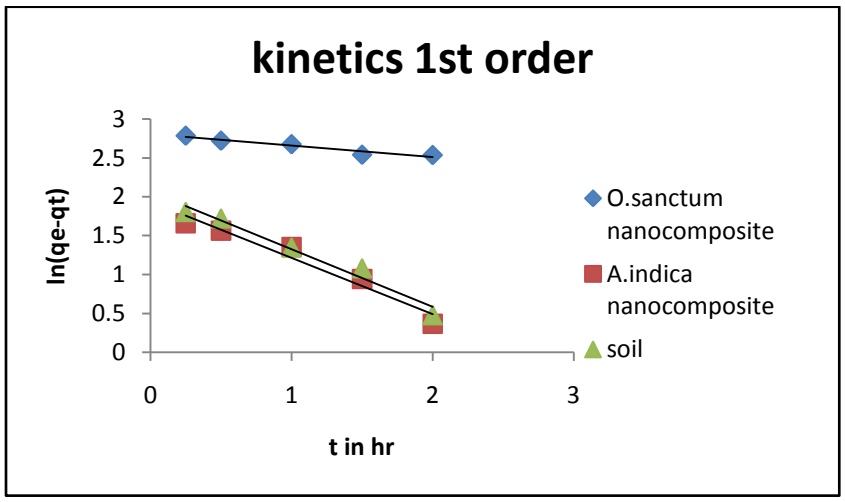

Figure 6.11 Kinetics 1^{st} order $\ln(q_e-q_t)$ vs t in hr

The plot between t/q_t versus t for the three adsorbents showed excellent fit to the pseudo-second-order equation. K_2 (g. mg^{-1} min^{-1}) value from second-order kinetics is quite same for all the three

adsorbents with R^2 value 0.999. From the above graphical representation and R^2 value obtained it is clearly observed that the experiment is following the pseudo-second order reaction.

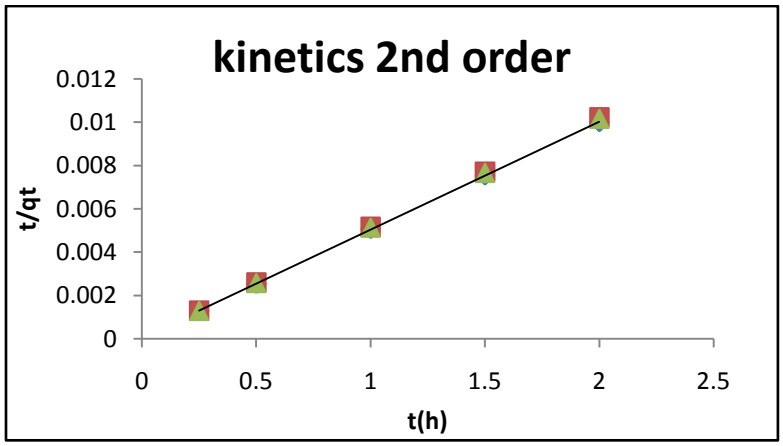

Figure 6.12 Kinetics 2nd order t/q_t vs t in hr

The values of the coefficient of Lagergren's pseudo-first-order and Ho–McKay's pseudo-second-order reactions are given in table no 3.

TABLE 3:

KINETICS 1ST ORDER COEFFICIENTS	**SOIL AgNP (*O.sanctum*)**	**SOIL-AgNP (*A.indica*)**	**SOIL**
K_1	0.148	0.722	0.738
lnq_e	3	1.932	2.063
R^2	0.932	0.952	0.97
KINETICS 2nd ORDER COEFFICIENTS			
q_e	0.005	0.005	0.005
K_2	0.002	0.002	0.002
R^2	0.999	0.999	0.999

5.2.1.9 Effect of mass of pore diffusion:

The intra particle diffusion is represented by the equation given below

$$q_t = K_p . t^{0.5} + C$$

The effect of intra particle pore diffusion of the adsorbate ions were determined by plotting a graph between q_t and $t^{0.5}$. Since the curve is linear hence we can deduct that the process is following intra particle diffusion which is assumed to be the rate limiting step.

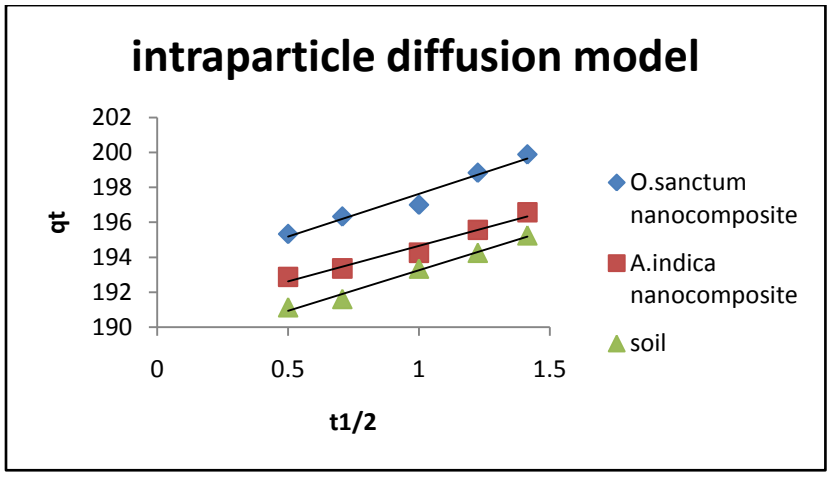

Figure 6.13 Intra particle diffusion q_t vs $t^{1/2}$

TABLE 4:

INTRA PARTICLE DIFFUSION PARAMETERS	**SOIL-AgNP (*O.sanctum*)**	**SOIL-AgNP (*A.indica*)**	**SOIL**
K_p	4.9	4.06	4.655
C	19.7	19.05	18.86

5.2.2 EXPERIMENT 2: Comparative study of the degradation of two dyes

In this experiment a comparative study for the removal of dyes is done between two dye containing solutions – Methylene Blue and Malachite Green of same concentration using Silver nanocomposites from the two leaf extracts (*O.sanctum* and *A.indica*) and soil. The experiment is performed to check which dye is getting adsorbed rapidly and efficiently in between the two dye solutions keeping all the regulating parameters (Temperature, pH, agitation speed etc) same. Now the effect of different parameters in the batch experiment are as follows.

5.2.2.1 Effect of mass of adsorbents:

Five conical flasks are taken and in them 100 ml solution of Methylene Blue dye of concentration 10ppm were taken and in them 25mg, 50mg, 75mg, 100 mg and 200 mg of nanocomposite adsorbent made of *O. sanctum* were added separately and placed in a shaker incubator at speed 120 and temperature 308K. The same process was carried out for nanocomposites made of *A. indica* and only soil adsorbents and percentage removal was obtained. The whole experiment was repeated with Malachite Green dye.

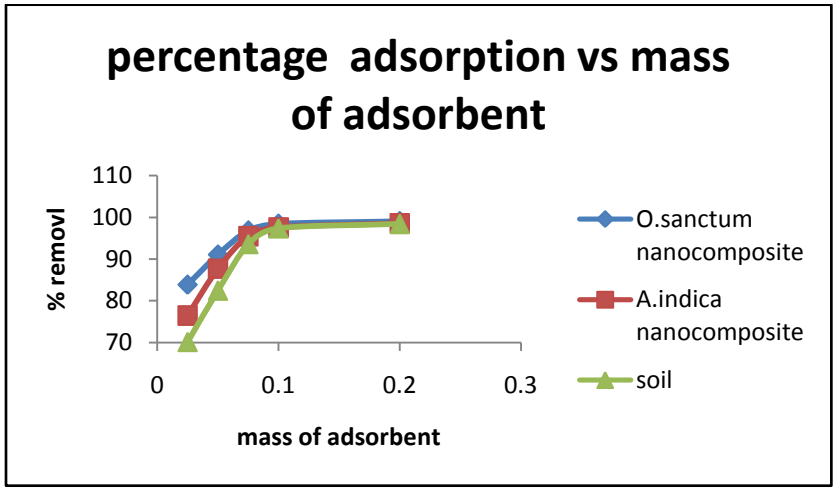

Figure 7.1 Effect of mass of adsorbent on Methylene blue dye

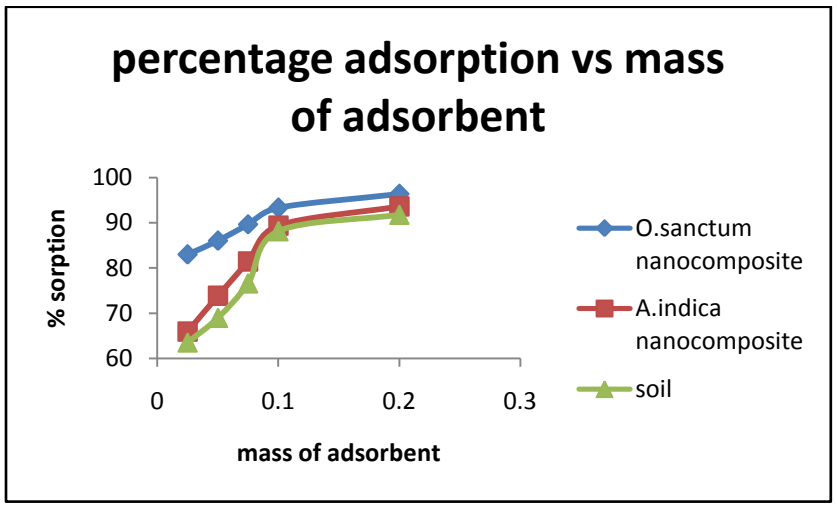

Figure 7.2 Effect of mass of adsorbent on Malachite green dye

It was observed from the two figures above that with the increase in the adsorbent dosage from 25mg to 200 mg there was a gradual increase in percentage removal for all the three adsorbents which may be due to increase in surface area and availability of more binding sites. It is observed that the percentage removal is higher in Methylene blue dye.

5.2.2.2 Effect of Temperature:

For both the dyes (Methylene Blue and Malachite Green) experiments were performed at the temperatures 298K, 303K, 308K, 313K and 318K respectively for all the three adsorbents at shaker speed 120 rpm and adsorbent dose 100 mg.

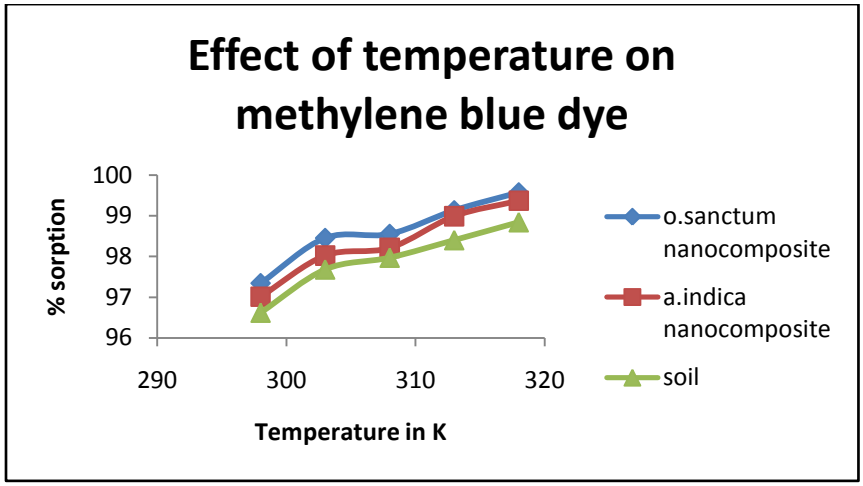

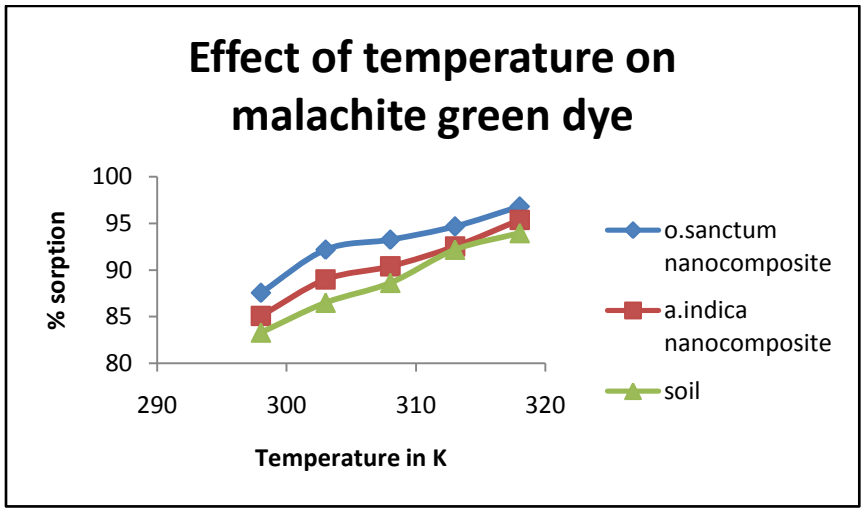

Figure 7.3 and 7.4 Effect of temperature on Methylene blue and Malachite green dyes respectively

In all the three adsorbents, for both the dyes with the increase in temperature there was an increase in the percentage removal shown in figures 7.3 and 7.4. Here also the percentage removal of Methylene Blue dye is higher compared to Malachite Green.

5.2.2.3 Effect of pH:

For both Methylene Blue and Malachite Green dye the pH stability of the three adsorbents were done in a range of pH 2, 4, 6, 8 and 10 having constant temperature 308K and shaker speed 120

rpm. UV- VIS spectrophotometer reading showed that maximum removal of dyes were obtained at pH 2 for both dyes from the solutions at maximum absorbance value 667 nm and 618 nm respectively.

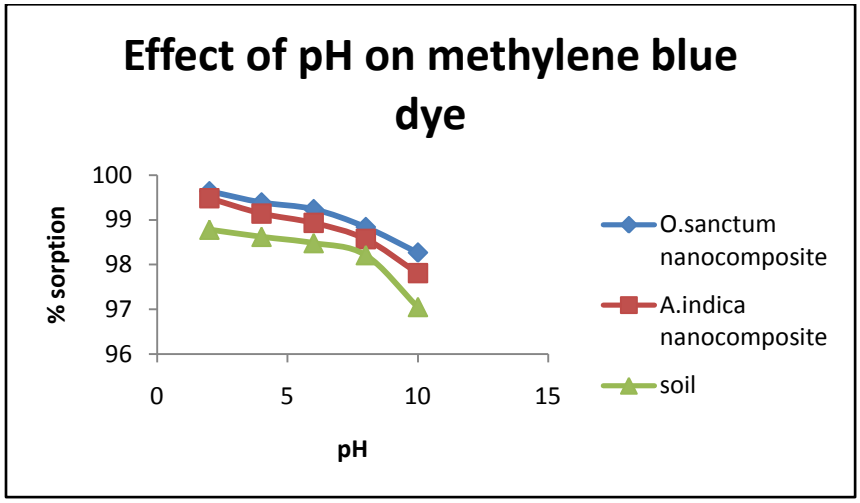

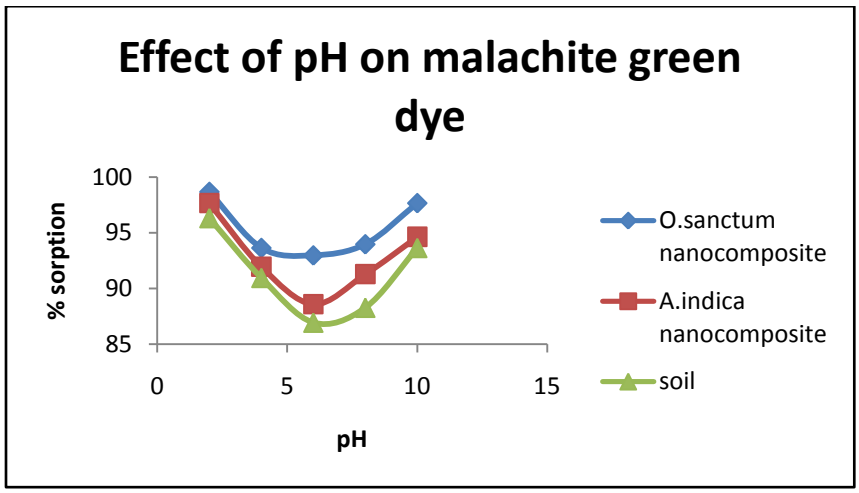

Figure 7.5 and 7.6 Effect of pH on Methylene blue and Malachite green dyes respectively

In the comparative study the maximum adsorption was showed by the soil-AgNP composite from *O.sanctum* leaf extract for Methylene Blue dye which was 99.6 %.

5.2.2.4 Effect of dye concentration:

The effect of the dye concentration for both the dyes at 2.5, 5, 10, 20, 25, 50 and 100 mg L^{-1} for three adsorbents at adsorbent dose 100mg, temperature 308K and pH 2 were shown in the figures 7.7 and 7.8. It was observed that in the first chart for methylene blue, the amount of dye adsorbed has decreased with increase in the dye concentration as shown in figure 7.7. It may be due to the

fact that as the amount of Methylene blue increases, the nanocomposite particles get saturated and looses its ability to adsorb more dye molecules.

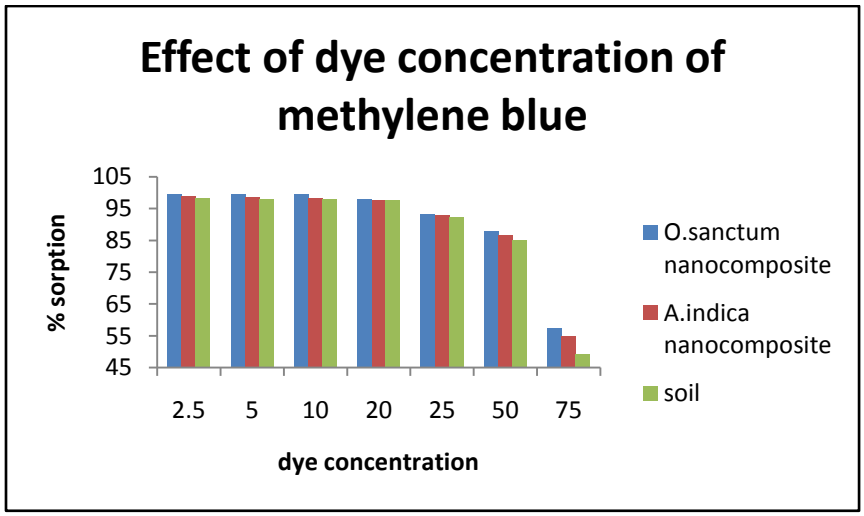

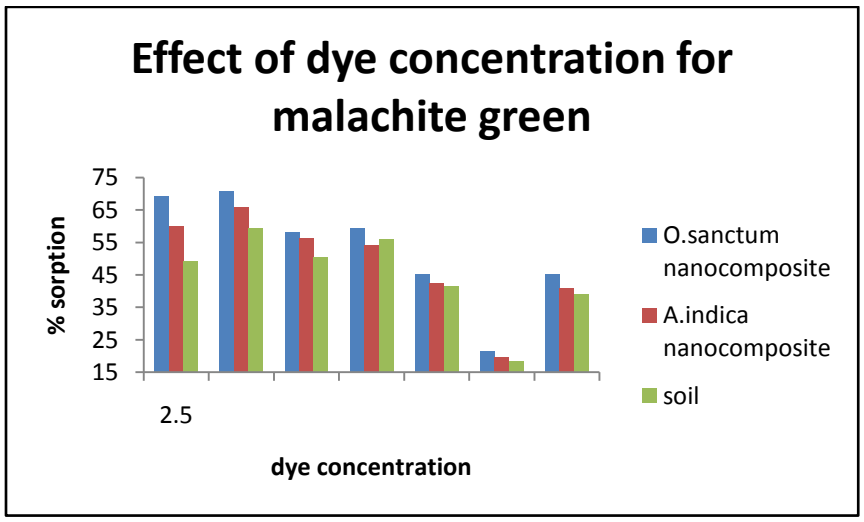

Figure 7.7 and 7.8 Effect of dye concentration on Methylene blue and Malachite green dyes respectively

In the second figure, 7.8 it was observed that with increase in dye concentration for all the three composites there was increase in percentage removal followed by a decrease and at the end it increases again.

5.2.2.5 Effect of contact time and agitation speed :

For both Methylene Blue and Malachite Green dyes the experiment of contact time was performed for times - 15mins, 30mins, 60mins,90mins and 120mins at pH 2, temperature 308K, adsorbent dose 100 mg and 120 rpm. The experiment was performed for soil, soil-AgNP for

O.sanctum and soil-AgNP for *A.indica*. It was observed in both the cases the percentage removal keeps on increasing as it reaches equilibrium there was no further change in the removal.

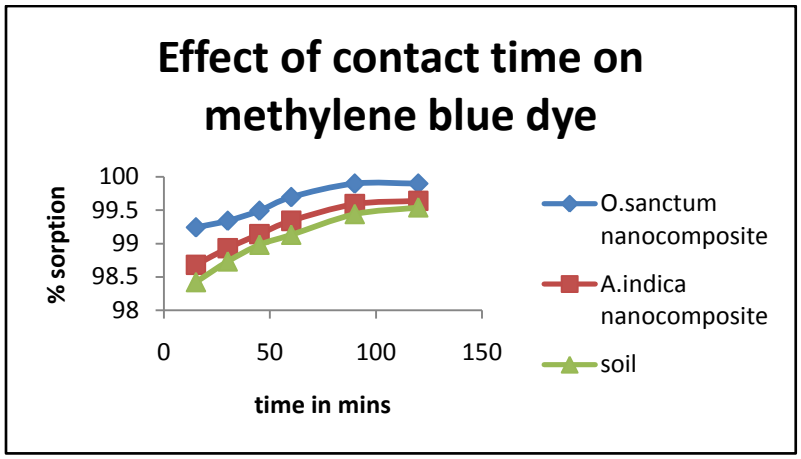

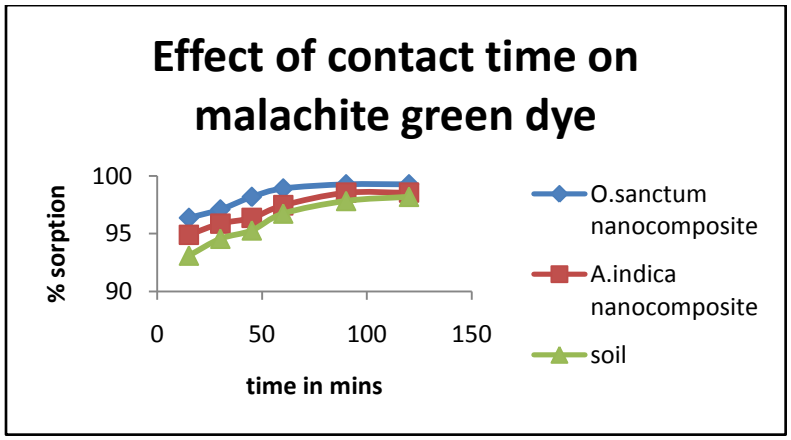

Figure 7.9 and 7.10 Effect of contact time on Methylene blue and Malachite green dyes respectively

It may be due to the fact that contact time increases the availability of active sites while further increase causes immobilization of the dyes molecules on the silver nanoparticles.

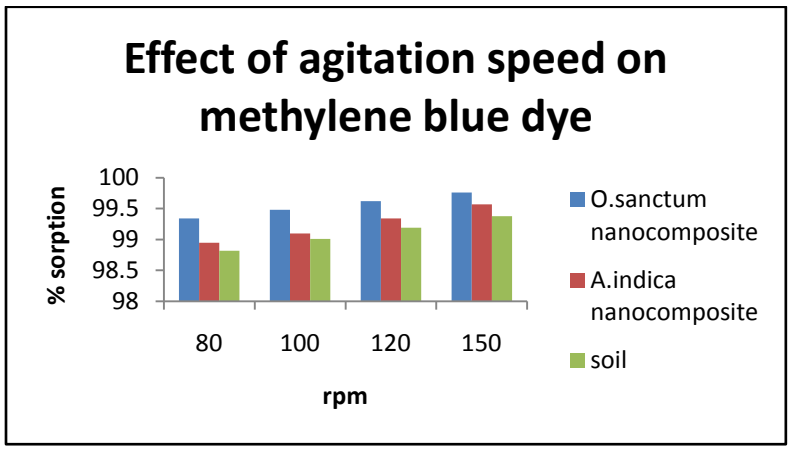

In case of the agitation speed experiment for both the dyes with the increase on rpm from 80 to 150 the percentage removal also increases shown in figure 7.11 and 7.12. This may be due to more agitation the dye molecules react more with the nanocomposites causing higher adsorption.

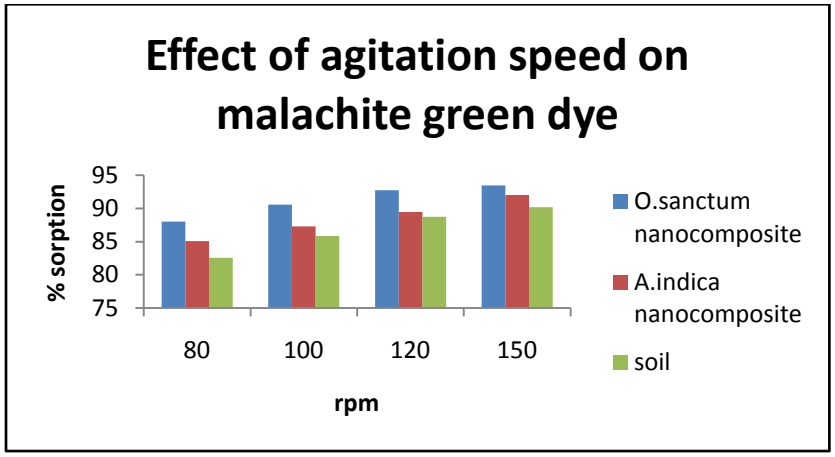

Figure 7.11 and 7.12 Effect of agitation speed on Methylene blue and Malachite green dyes respectively

5.2.2.6 Adsorption isotherms:

For both the Methylene Blue (Dye 1) and Malachite Green dye (Dye 2) the adsorption isotherm study is done since an adsorption isotherm represents the equilibrium relationship between the adsorbate adsorbed on the surface of adsorbent and concentration of adsorbate at constant temperature. Langmuir, Freundlich and Temkin model are fitted for the two dyes using all the three adsorbents.

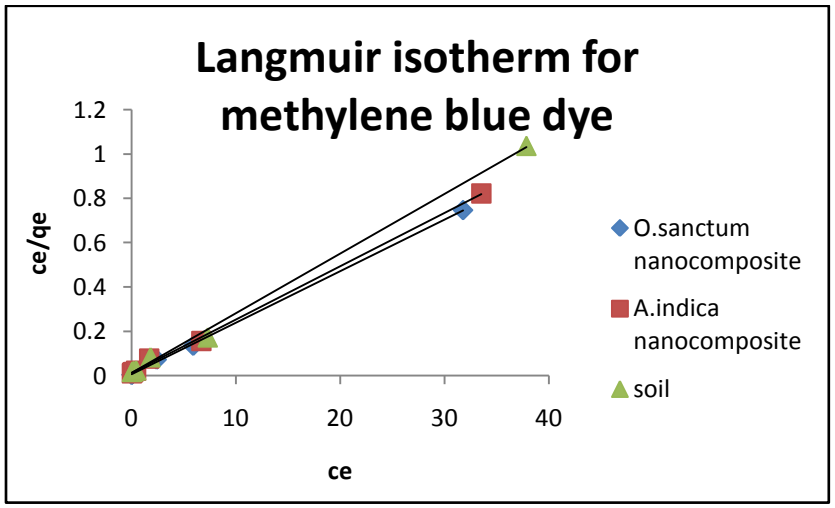

Figure 7.13 and 7.14 Langmuir isotherm for Methylene blue and Malachite green dyes respectively

Out of the three the Langmuir isotherm model is best fitted for both the dyes shown in the figure 7.13 nd 7.14. Langmuir isotherm is mainly suitable for a monolayer adsorption onto a surface

containing a finite number of identical sites. Hence we can deduct that monolayer adsorption of the dye is obtained in both the cases.

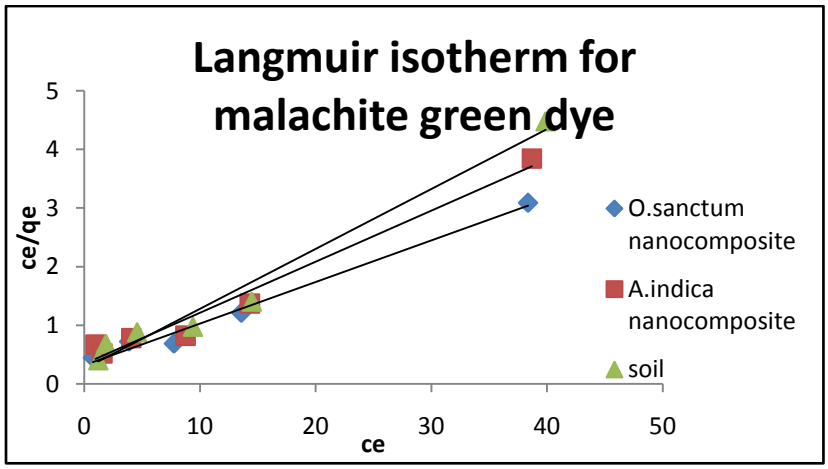

TABLE 5:

LANGMUIR PARAMETERS	**SOIL-AgNP (O.sanctum)**		**SOIL-AgNP (A.indica)**		**SOIL**	
	Dye 1	**Dye 2**	**Dye 1**	**Dye 2**	**Dye 1**	**Dye 2**
q_0 mg /g	43.48	14.085	41.667	11.494	38.46	10.53
K_L L/mg	3.833	0.223	1.846	0.257	2.1667	0.214
R^2	0.999	0.988	0.998	0.973	0.997	0.964
FREUNDLICH PARAMATERS						
K_F mg/g	18.32	2.349	16.17	1.465	14.59	1.931
n	2.89	1.603	2.53	1.427	2.51	1.558
R^2	0.907	0.895	0.89	0.851	0.847	0.871
TEMKIN PARAMETERS						
B J/mol	5.349	3.031	6.09	2.719	5.899	2.71
b	478.72	844.84	420.48	941.78	434.09	944.91
A L/mg	4.726	2.392	3.798	2.198	3.572	1.725
R^2	0.913	0.909	0.93	0.844	0.895	0.756

5.2.2.7 Thermodynamic studies:

To conclude whether the two processess are spontaneous in nature or not thermodynamic studies are necessary. Gibbs free energy change (ΔG^0), enthalpy (ΔH^0) and entropy (ΔS^0) were calculated for both the dyes using Vant Hoff plot to check the feasibility of the process and to validate the nature of the adsorption process. In the figures 7.15 and 7.16 below the Vant Hoff plots for Methylene Blue and Malachite Green dye are given using *O.sanctum* nanocomposite. Similar plots were drawn for the other two adsorbents (figure not shown).

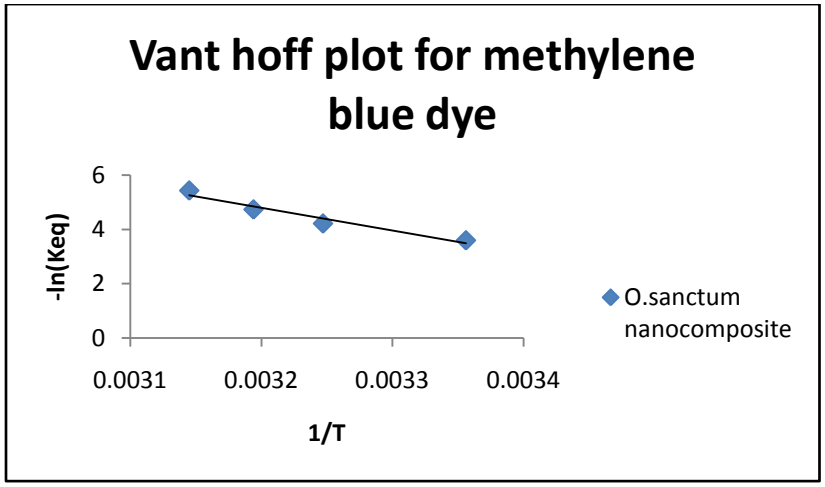

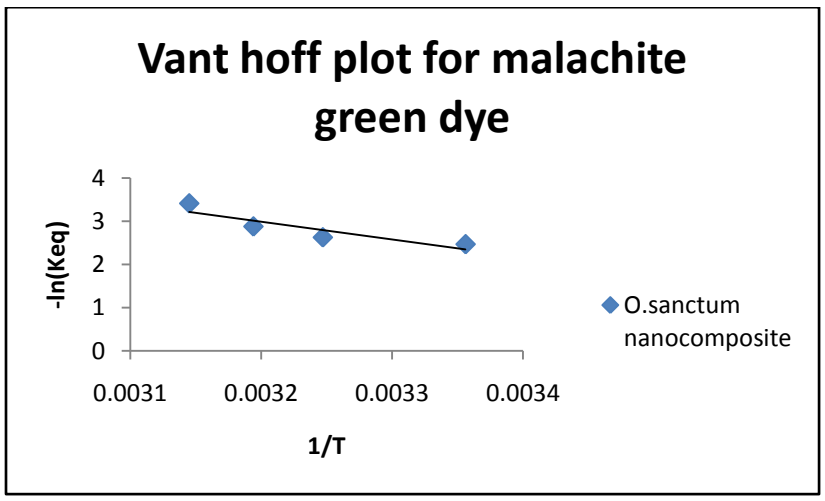

Figure 7.15 and 7.16 Vant hoff plot for Methylene blue and Malachite green dyes respectively

Table 6 shows the values of different thermodynamic parameters obtained. The study concluded that both the prcoess are spontaneous, exothermic in nature and has affinity towards the dye molecules. In the table 6 dye 1 and dye 2 represents Methylene Blue and Malachite Green respectively.

TABLE 6:

PARAMETERS		ΔH^0 KJ mol^{-1}	ΔS^0 J mol^{-1} K^{-1}	ΔG^0 (25^0C) KJ mol^{-1}	ΔG^0 (30^0C) kJ mol^{-1}	ΔG^0 (35^0C) kJ mol^{-1}	ΔG^0 (40^0C) kJ mol^{-1}	ΔG^0 (45^0C) kJ mol^{-1}
Soil-AgNP (basil leaf)	**Dye 1**	-8.39	31.63	-8.92	-10.46	-10.81	-12.33	-14.37
	Dye 2	-4.301	16.39	-4.85	-6.21	-6.72	-7.48	-9.01
Soil-AgNP (neem leaf)	**Dye 1**	-5.38	21.78	-8.62	-9.82	-10.26	-11.92	-13.38
	Dye 2	-4.11	15.76	-4.31	-5.05	-5.26	-6.55	-8.001
Soil	**Dye 1**	-3.18	14.33	-8.31	-9.43	-9.93	-10.73	-11.76
	Dye 2	-4.21	15.89	-3.98	-4.68	-5.25	-6.42	-7.25

5.2.2.8 Kinetics studies:

The study of adsorption kinetics describes the adsorbate uptake rate and predicts the residence time of dyes at the solid-liquid interface. For both the dyes the Lagergren's pseudo-first-order and Ho–McKay's pseudo-second-order models were applied to the experimental data using the three adsorbents. The values of pseudo-first-order rate constants, k_1 (min^{-1}) and qe (g. mg^{-1}) were calculated for the three adsorbents (values provide in table 7) from the slopes and intercepts of the graphs between $\log(q_e - q_t)$ versus t (graph not shown). On the contrary, the plot between t/q_t versus t for the three adsorbents showed excellent fit to the pseudo-second-order equation. K_2 (g. mg^{-1} min^{-1}) value from second-order kinetics is quite same for all the three adsorbents with R^2

value 0.999. It can thus be concluded that the reaction has followed a pseudo-second-order mechanism and not a pseudo-first-order mechanism.

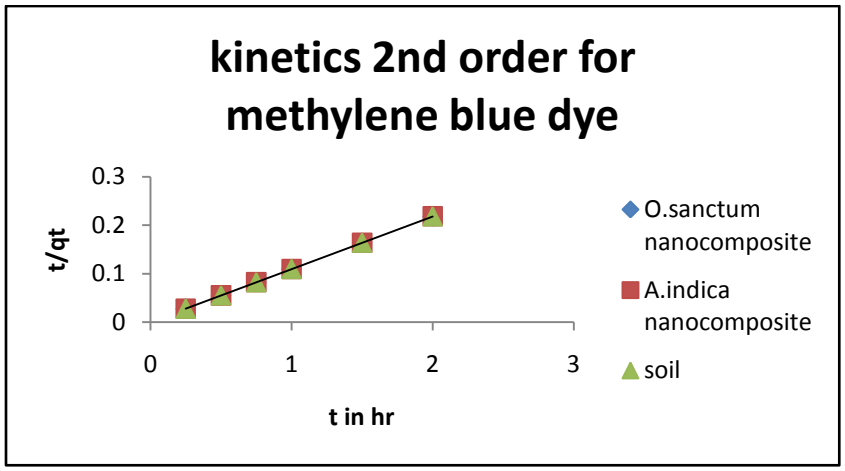

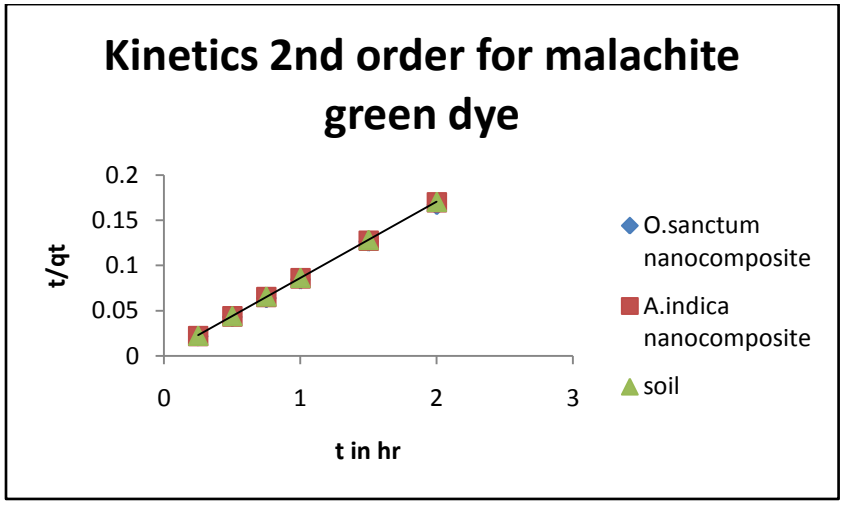

Figure 7.17 and 7.18 Kinetics 2nd order plot for Methylene blue and Malachite green dyes respectively

TABLE 7:

KINETICS 1ST ORDER COEFFICIENTS	**SOIL AgNP (*O.sanctum*)**		**SOIL-AgNP (*A.indica*)**		**SOIL**	
	Dye 1	**Dye 2**	**Dye 1**	**Dye 2**	**Dye 1**	**Dye 2**
K_1	0.001	0.163	0.001	0.129	0.001	0.14
lnq_e	3.546	0.915	3.547	0.852	3.548	0.739
R^2	0.905	0.929	0.92	0.915	0.931	0.946

KINETICS 2nd ORDER COEFFICIENTS	Dye 1	Dye 2	Dye 1	Dye 2	Dye 1	Dye 2
q_e	0.108	0.082	0.108	0.082	0.108	0.082
K_2	0.001	0.001	0.001	0.001	0.001	0.001
R^2	0.999	0.999	0.999	0.999	0.999	0.999

5.2.2.9 Effect of pore diffusion:

The effect of intra particle pore diffusion of the adsorbate ions were determined by plotting a graph between q_t and $t^{0.5}$ for both the dyes Methylene Blue (Dye 1) and Malachite Green (Dye 2).

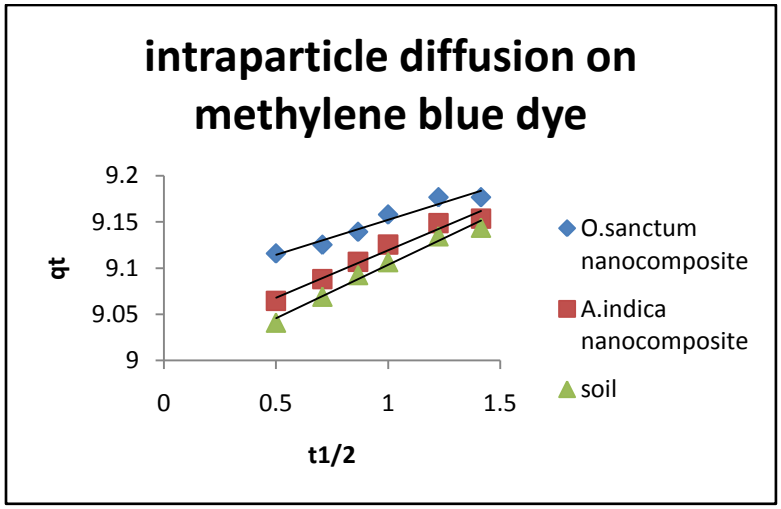

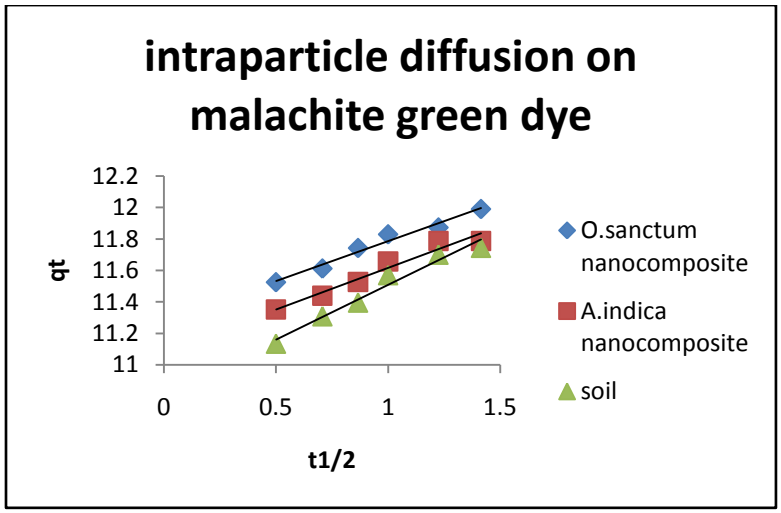

Figure 7.19 and 7.20 Intra particle diffusion on Methylene blue and Malachite green dyes respectively

Since the curve is linear in both cases, hence we can state that the process is following intra particle diffusion which is assumed to be the rate limiting step. Table 8 provides the value of the slopes and intercepts obtained from the three curves in each of the two graphs. The slope is denoted as the constant K_p and the intercept is denoted as C that determines the thickness of boundary layer.

TABLE 8:

INTRA PARTICLE DIFFUSION PARAMETERS	**SOIL-AgNP (*O.sanctum*)**		**SOIL-AgNP (*A.indica*)**		**SOIL**	
	Dye 1	**Dye 2**	**Dye 1**	**Dye 2**	**Dye 1**	**Dye 2**
K_p	0.075	0.506	0.102	0.53	0.115	0.696
C	9.076	11.28	9.016	11.08	8.988	10.81

5.2.3 EXPERIMENT 3: Study of a binary solution and its degradation

In this experiment, a binary solution is prepared using Methylene blue and Malachite green solution of concentration 10 ppm each in the ratio of 1:1, the resultant solution is then measured in a UV-VIS spectrophotometer where the maximum absorbance is obtained at 618 nm and 667 nm. Now this binary dye solution is treated with the three adsorbents (*O.sanctum* nanocomposite, *A.indica* nanocomposite and soil) under different conditions and percentage removal is obtained. The batch studies done using different parameters like adsorbent dose, temperature, pH, contact time, dye concentration, agitation peak and the study of isotherm, kinetics, thermodynamics are also done at two absorption peaks 618nm and 667nm and the result obtained are compared and various conclusions are drawn.

5.2.3.1 Effect of mass of adsorbents:

100ml of the binary solution containing Methylene blue and Malachite green dye in the ratio 1:1 is taken in five conical flasks and in them 25mg, 50mg, 75mg, 100 mg and 200 mg of nanocomposite adsorbent made of *O. sanctum* were added separately and placed in a shaker

incubator at temperature 308K and speed 120 rpm. The same process was carried out for nanocomposites made of *A. indica* and only soil adsorbents.

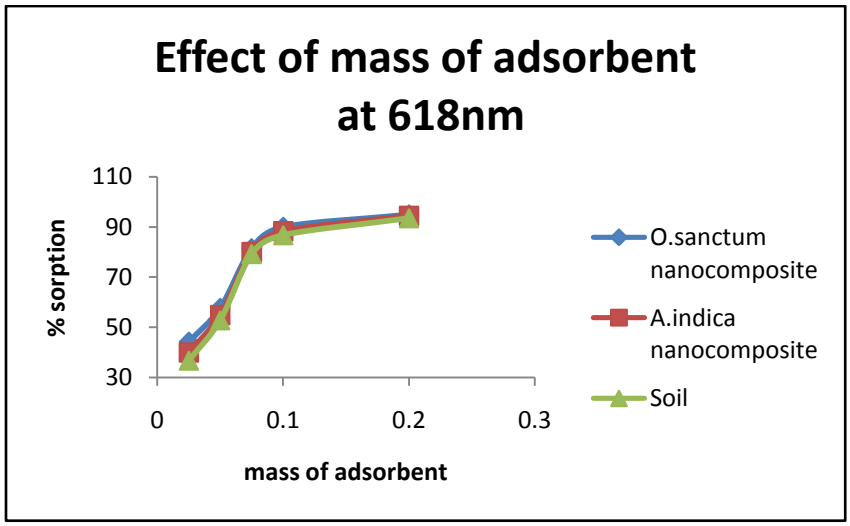

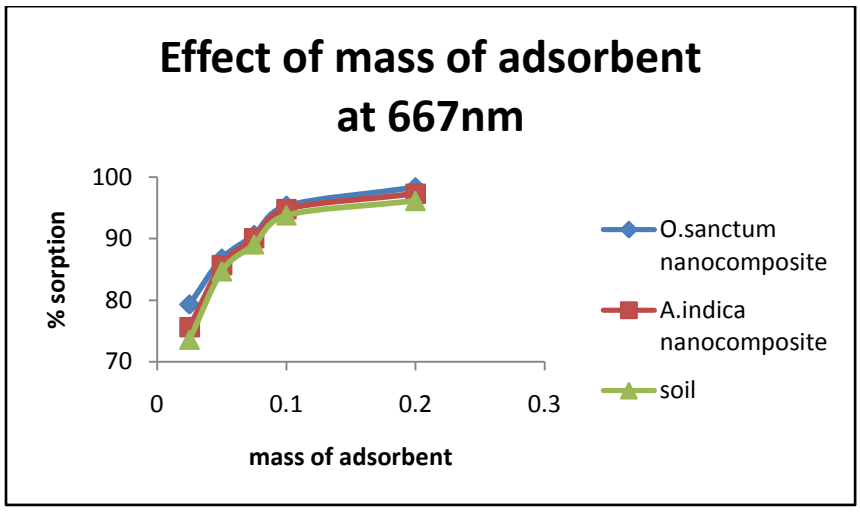

Figure 8.1 and 8.2 Percentage adsorption vs mass of adsorbent at 618nm and 667nm

It was observed in both the figures 8.1 and 8.2, with the increase in the adsorbent dosage from 25mg to 200 mg there was a gradual increase in percentage removal for all the three adsorbents. The reason of this behavior may be due to increased surface area of adsorption and availability of more binding sites.

5.2.3.2 Effect of Temperature:

The effect of temperature of the binary dye solution was obtained for the temperatures 298K, 303K, 308K, 313K and 318K respectively for all the three adsorbents at adsorbent dose 100 mg and shaker speed 120 rpm. In all the three adsorbents, with the increase in temperature there was

an increase in the percentage removal shown in the figures below. The increasing percentage removal may be due to presence of more binding sites for the dye molecules. The maximum percentage removal is obtained at 667 nm.

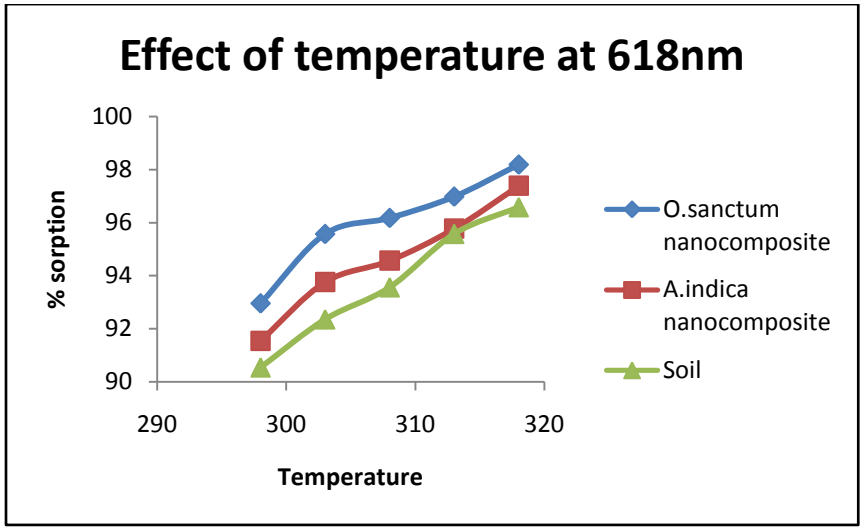

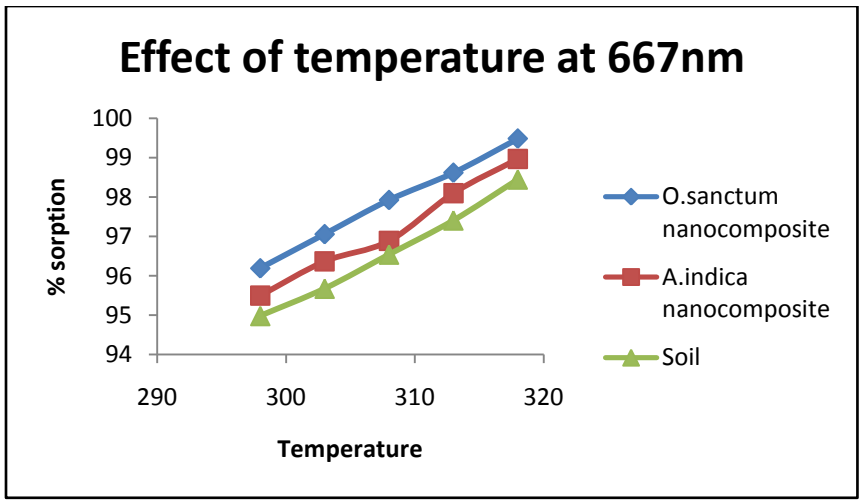

Figure 8.3 and 8.4 Percentage adsorption vs temperature at 618nm and 667nm

5.2.3.3 Effect of pH:

The effect of pH stability of the nanocomposites for the binary solution were done in a range of pH 2 to 10 at both 618nm and 667nm having constant adsorbent dose 100 mg, temperature 308K and shaker speed 120 rpm shown in the figures 8.5 and 8.6. In the comparative study the

maximum adsorption was showed by the soil-AgNP from *O.sanctum* which was 99.28 % at 667nm.

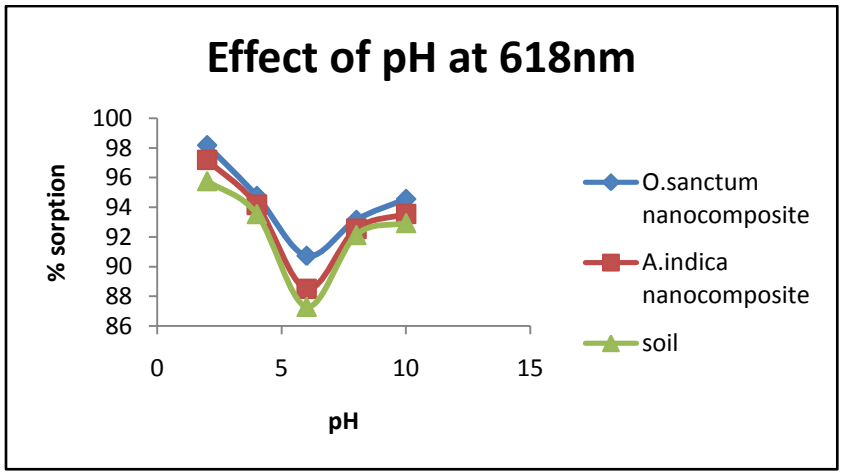

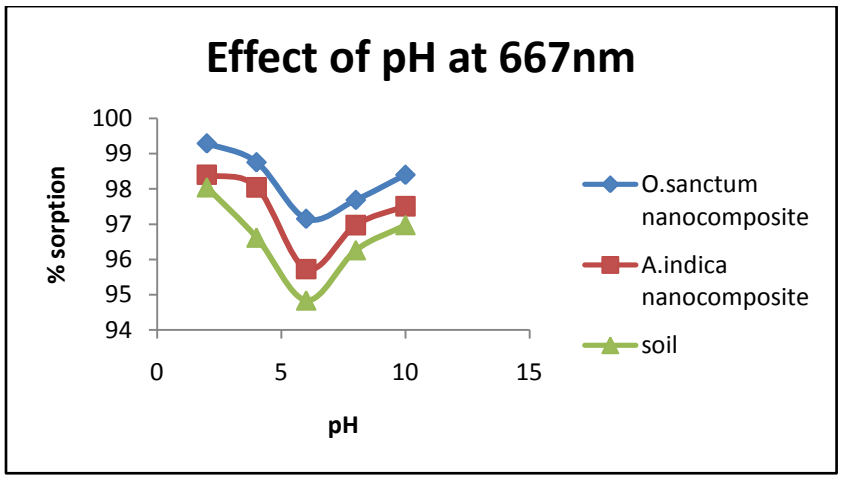

Figure 8.5 and 8.6 Percentage adsorption vs pH at 618nm and 667nm

5.2.3.4 Effect of dye concentration:

The effect of the dye concentration on the binary solution mixture in a range of 2.5 to 75 mg L^{-1} for three adsorbents at 308K and pH 2 were shown in the figures 8.7 and 8.8.

It was observed in both the curves at the beginning there is a slight increase followed by a gradual decrease with the increase in the dye concentration. This increasing behavior may result if there is an increase in the driving force from the concentration gradient.

As it reaches the equilibrium concentration, excess dyes remains in the solution causing aggregation and overlapping of the adsorption sites and decreases the percentage of adsorption.

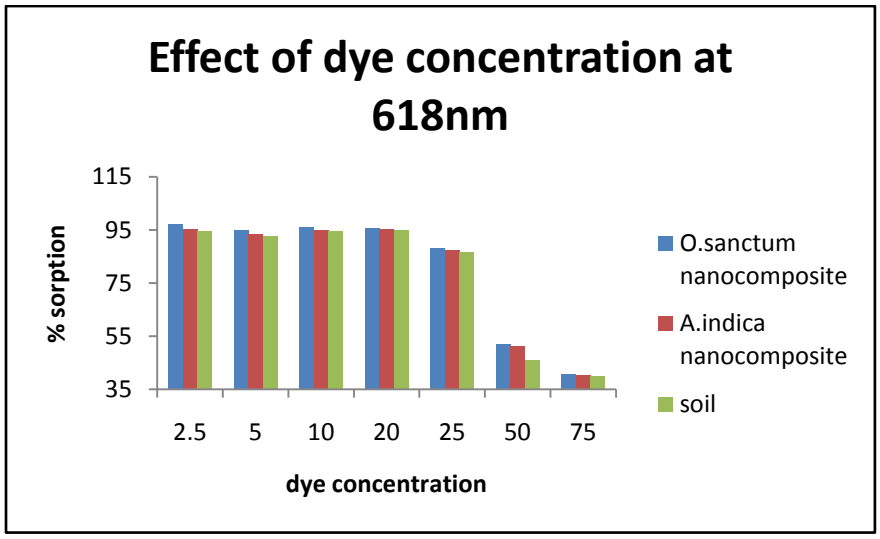

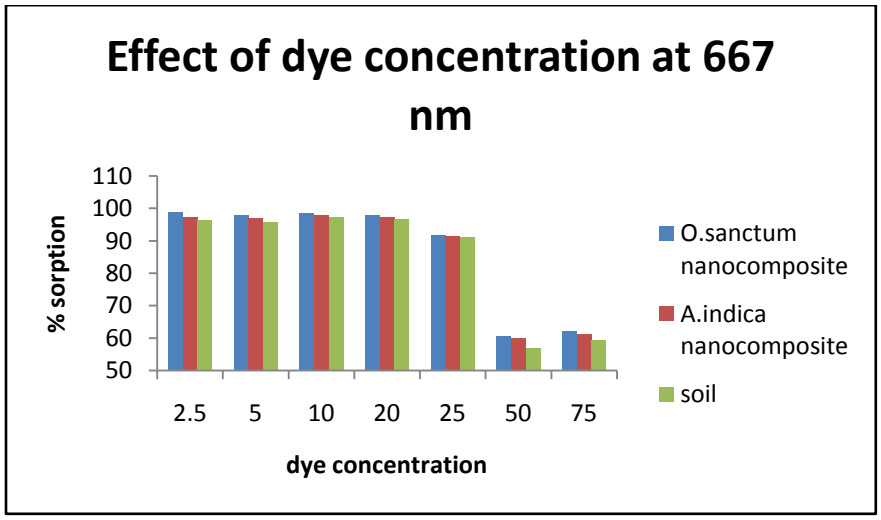

Figure 8.7 and 8.8 Percentage adsorption vs dye concentration at 618nm and 667nm

5.2.3.5 Effect of Contact time and agitation speed:

The experiment showing the effect of contact time was performed for time 15mins, 30mins, 45mins, 60mins, 90mins and 120mins for pH 2, temperature 308K and 120 rpm. The experiment was performed for the three adsorbents at both 618nm and 667 nm.

It was observed that the percentage removal keeps on increasing with increase in contact time. It may be due to the fact that contact time increases the availability of active sites that lead to rapid adsorption.

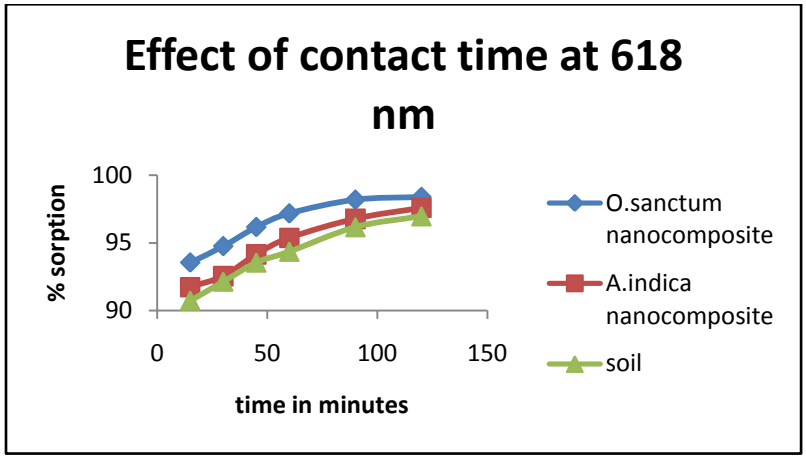

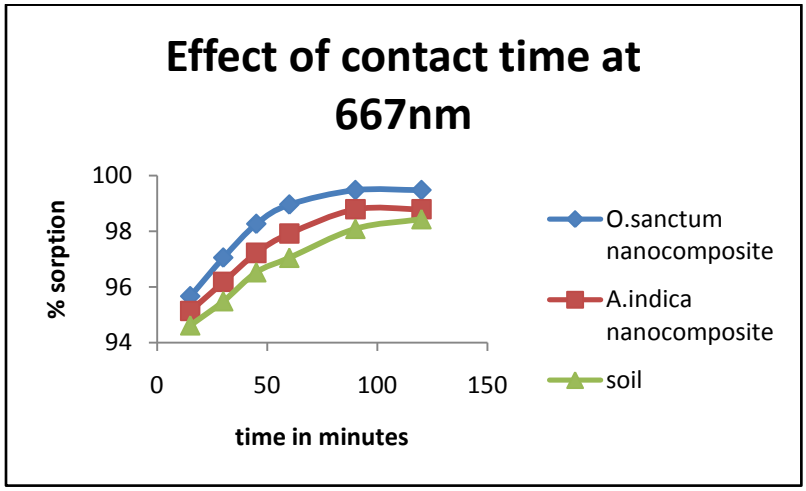

Figure 8.9 and 8.10 Percentage adsorption vs contact time at 618nm and 667nm

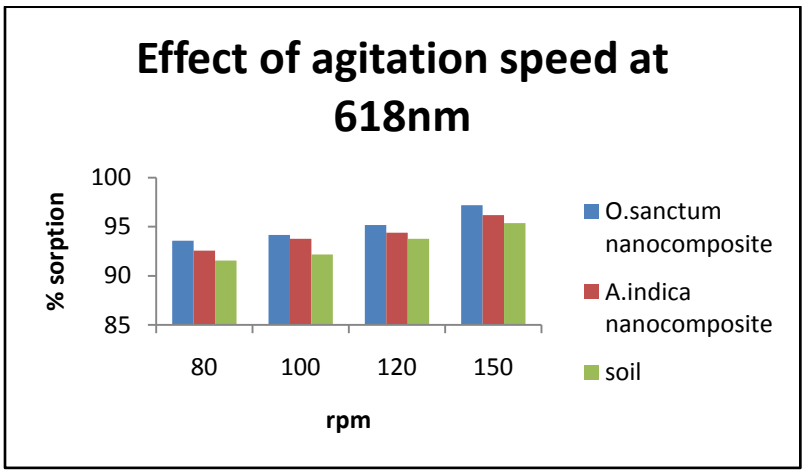

Figure 8.11 and 8.12 Percentage adsorption vs agitation speed at 618nm and 667nm

In the effect of agitation speed experiment, the adsorbent dose, temperature, pH and dye concentration are kept constant. It is obtained that with the increase of rpm from 80 to 150 the percentage removal increased for the three adsorbents at both 618 and 667nm, shown in the figures 8.11 and 8.12.

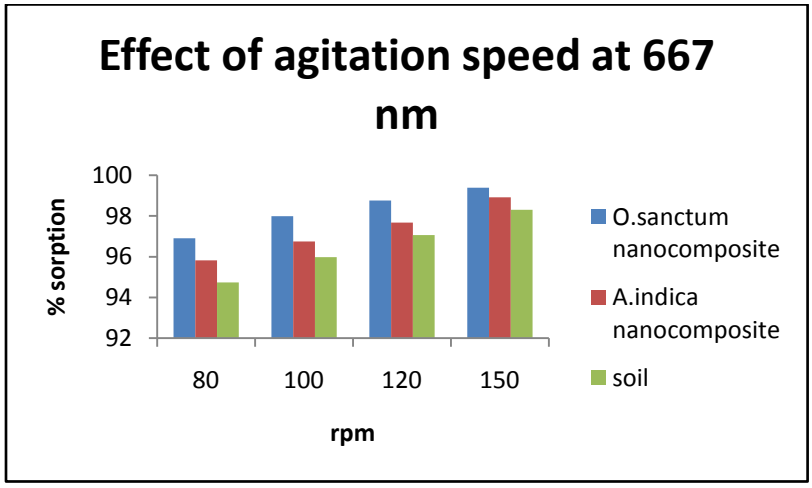

5.2.3.6 Adsorption isotherms:

To find out the relationship between the adsorbate adsorbed on the surface of adsorbent and concentration of adsorbate at constant temperature three isotherms were plotted at 618 and 667 nm – Langmuir, Freundlich and Temkin. In Langmuir isotherm plot the experimental data c_e/q_e were plotted against c_e for the three nanocomposites at temperature 308K shown in the figures 8.13 and 8.14 below.

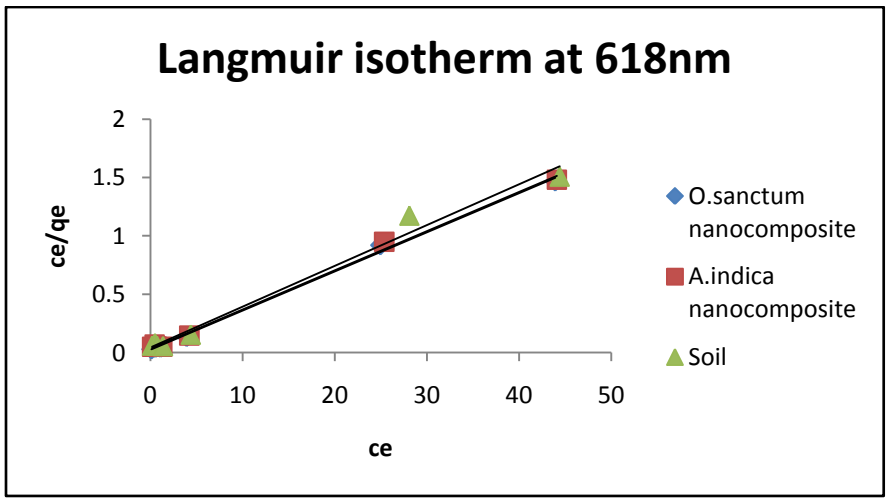

Figure 8.13 and 8.14 Langmuir isotherm of binary solution at 618nm and 667nm

In Freundlich and Temkin isotherm plots were obtained for the three adsorbents(figure not shown) Out of the three isotherm model the Langmuir model is best fitted which indicates the surface of silver nanoparticles and soil had accommodated a monolayer of adsorbate without any interaction between adsorbed species. Values obtained are provided in table 9.

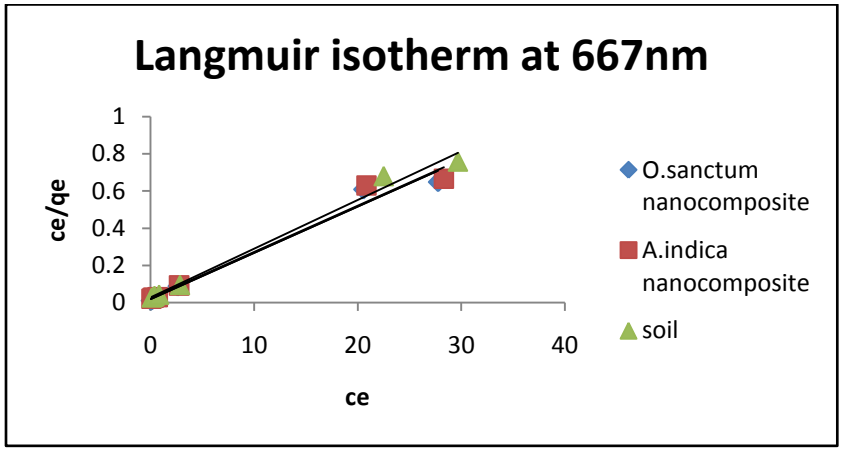

TABLE 9:

LANGMUIR PARAMETERS	**SOIL-AgNP (O.sanctum)**		**SOIL-AgNP (A.indica)**		**SOIL**	
	618nm	**667nm**	**618nm**	**667nm**	**618nm**	**667nm**
q_0 mg /g	30.303	41.67	30.303	41.67	28.57	38.46
K_L L/mg	1.375	1.412	0.943	1.043	0.833	0.963
R^2	0.997	0.989	0.995	0.978	0.995	0.899
FREUNDLICH PARAMATERS						
K_F mg/g	20.49	18.84	17.17	16.79	15.50	15.36
n	1.203	2.959	1.427	2.71	1.558	2.688
R^2	0.97	0.658	0.981	0.6	0.975	0.553
TEMKIN PARAMETERS						
B J/mol	4.933	4.874	5.254	5.345	4.686	5.181
b	519.09	525.38	487.38	479.09	546.46	494.25
A L/mg	3.598	4.676	3.114	3.955	3.293	3.773
R^2	0.634	0.706	0.616	0.664	0.52	0.588

5.2.3.7 Thermodynamic studies:

To determine whether the process is spontaneous in nature or not thermodynamic studies of an adsorption process is done at both 618 nm and 667 nm. In the figures below the Vant hoff plot between $-\ln K_{eq}$ and 1/T is drawn for the *O.sanctum* nanocomposite at both 618nm and 667 nm.

Parameters like Gibbs free energy change (ΔG^0), enthalpy change (ΔH^0) and entropy change (ΔS^0) were also calculated using the Vant Hoff plot to confirm the nature of the adsorption process. Similar plots were drawn for the other two adsorbents (figure not shown) and different values obtained from them are listed in table 10.

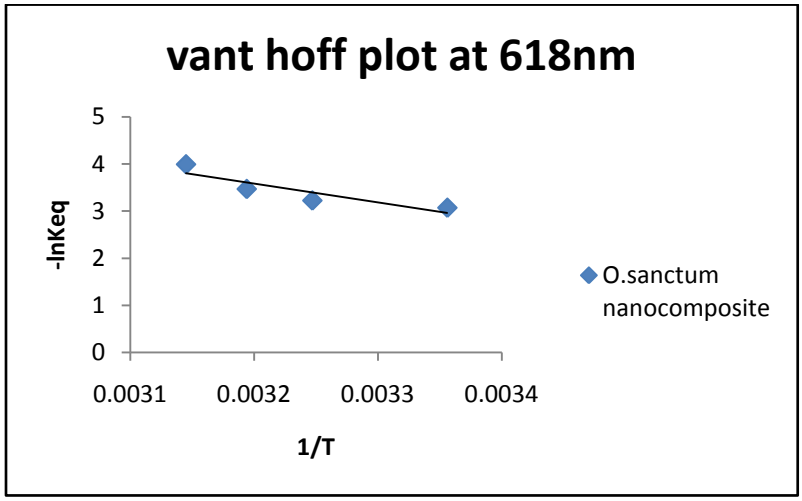

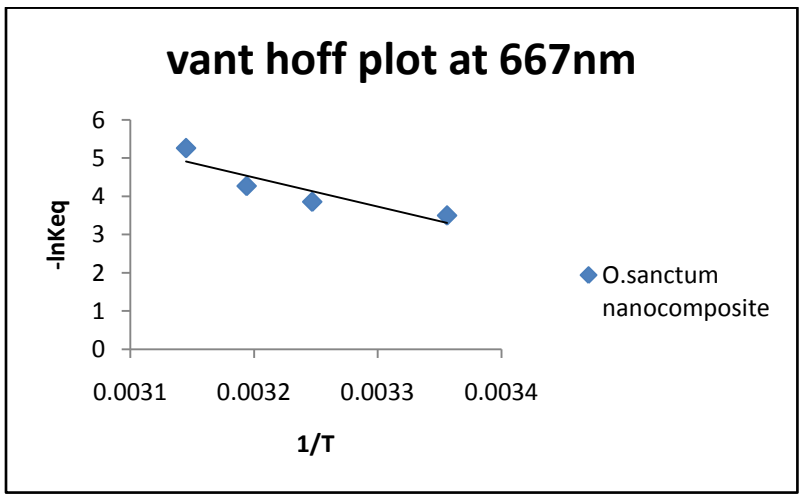

Figure 8.15 and 8.16 Vant hoff plot of binary solution at 617nm and 667nm

From the figure the values of different parameters are obtained from which we can deduce that the process is spontaneous, exothermic in nature and has an affinity towards the dye molecule.

Table 10 shows the values of different thermodynamic parameters obtained.

5.2.3.8 Kinetic studies:

The pseudo-first-order curve is plotted (figure not shown) and values of pseudo-first-order rate constants, k_1 (min^{-1}) and log q_e (g. mg^{-1}) were calculated for the three adsorbents from the slopes and intercepts of the graphs between log (q_e - q_t) versus t (values provided in table 11). On the other hand, the plot between t/q_t versus t for the three adsorbents showed excellent fit to the pseudo-second-order equation. K_2 (g. mg^{-1} min^{-1}) value from second-order kinetics is quite same for all the three adsorbents with R^2 value 0.999. It can thus be concluded that the reaction has followed a pseudo-second-order mechanism and not a pseudo-first-order mechanism. The values of parameters are provided in table 11.

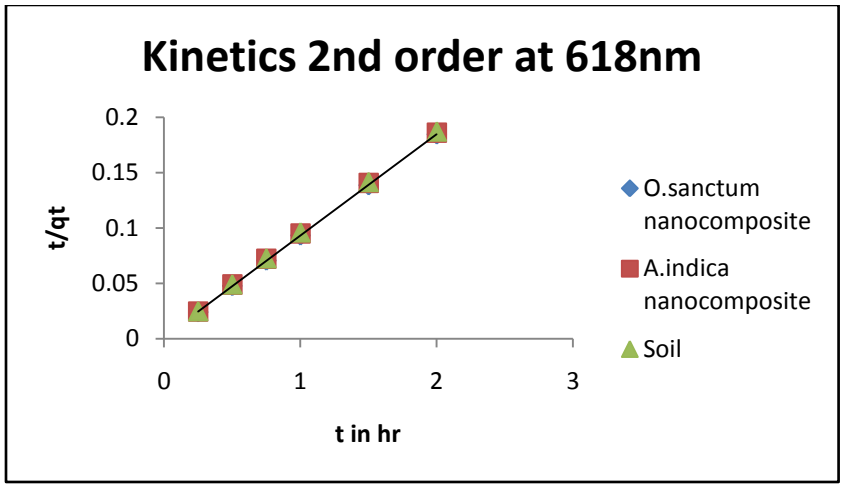

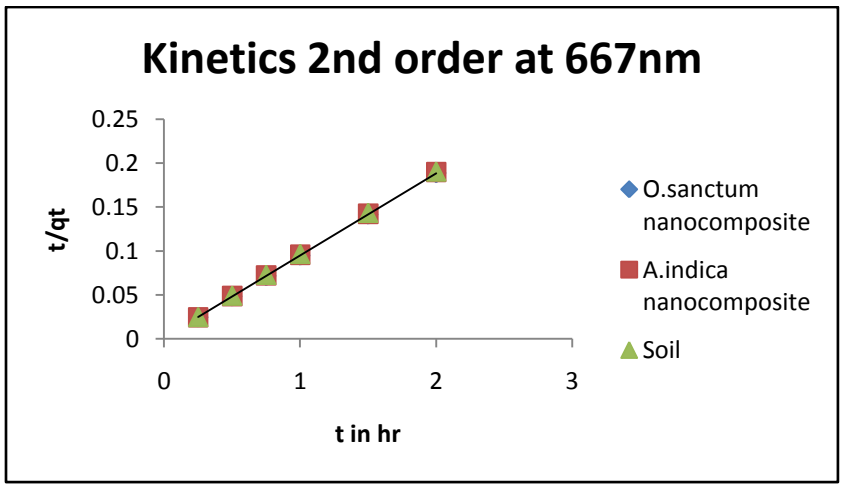

Figure 8.17 and 8.18 Kinetics 2nd order of binary solution at 618nm and 667nm

TABLE 10:

PARAMETERS		ΔH^0 KJ mol^{-1}	ΔS^0 J mol^{-1} K^{-1}	ΔG^0 (25^0C) KJ mol^{-1}	ΔG^0 (30^0C) kJ mol^{-1}	ΔG^0 (35^0C) kJ mol^{-1}	ΔG^0 (40^0C) kJ mol^{-1}	ΔG^0 (45^0C) kJ mol^{-1}
Soil-AgNP (basil leaf)	**618nm**	-3.39	16.35	-6.39	-7.74	-8.26	-9.03	-10.56
	667nm	-7.61	28.85	-8	-8.81	-9.87	-11.10	-13.87
Soil-AgNP (neem leaf)	**618nm**	-3.97	15.91	-5.90	-6.29	-7.32	-8.12	-9.56
	667nm	-5.76	22.44	-7.57	-8.26	-8.80	-10.26	-12.05
Soil	**618nm**	-4.02	15.91	-5.59	-6.28	-6.85	-7.99	-8.83
	667nm	-4.65	18.6	-7.29	-7.79	-8.54	-9.43	-10.96

TABLE 11:

KINETICS 1ST ORDER COEFFICIENTS	**SOIL AgNP (*O.sanctum*)**		**SOIL-AgNP (*A.indica*)**		**SOIL**	
	618nm	**667nm**	**618nm**	**667nm**	**618nm**	**667nm**
K_1	0.305	0.22	0.381	0.22	0.392	0.233
lnq_e	18.63	21.42	18.6	21.19	18.51	19.59
R^2	0.879	0.778	0.95	0.861	0.957	0.93

KINETICS 2nd ORDER COEFFICIENTS	618nm	667nm	618nm	667nm	618nm	667nm
K_2	0.002	0.001	0.002	0.001	0.002	0.001
q_e	0.092	0.094	0.092	0.094	0.092	0.094
R^2	0.999	0.999	0.999	0.999	0.999	0.999

5.2.3.9 Effect of pore diffusion:

The effect of intra particle pore diffusion of the adsorbate ions were determined by plotting a graph between q_t and $t^{0.5}$ for the binary dye solution at both 618nm and 667nm.

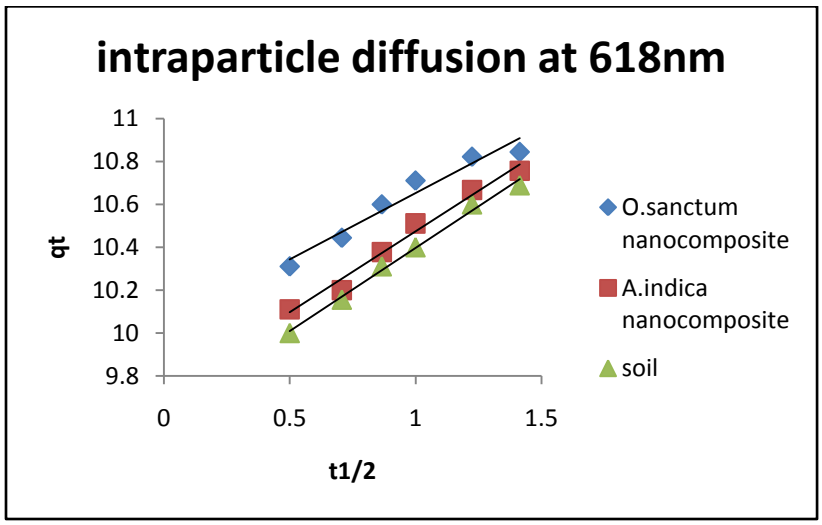

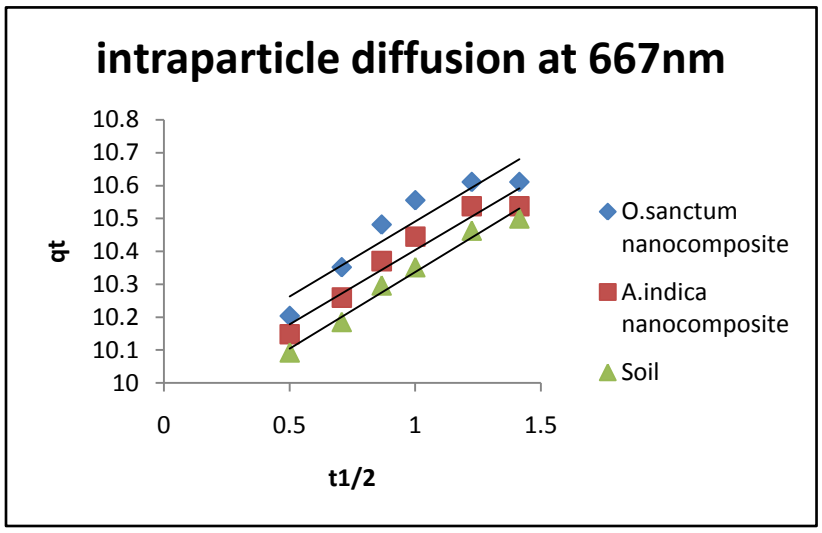

Figure 8.19 and 8.20 Intra particle diffusion of binary solution at 618nm and 667nm

Since the curve is linear in both cases, hence we can state that the process is following intra particle diffusion which is assumed to be the rate limiting step. Table 12 provides the value of the slopes and intercepts obtained from the three curves in each of the two graphs.

TABLE 12:

INTRA PARTICLE DIFFUSION PARAMETERS	**SOIL-AgNP (*O.sanctum*)**		**SOIL-AgNP (*A.indica*)**		**SOIL**	
	618nm	**667nm**	**618nm**	**667nm**	**618nm**	**667nm**
K_p	0.618	0.455	0.754	0.451	0.776	0.466
C	10.03	10.03	9.718	9.953	9.619	9.871

5.2.4 EXPERIMENT 4: Comparative study for the removal of two binary solutions of different ratios.

In the experiment 4, two binary solutions were prepared using Methylene blue (MB) and Malachite green (MG) dye solution in the ratio 7:3 and 3:7 respectively. It was done to check that with the change in the ratio of the dye solutions whether there was any change in the percentage removal or not. Now this two binary mixtures were prepared separately and then they were treated with three adsorbents, silver nanocomposite made of basil leaf extract, silver nanocomposite made of neem leaf extract and soil (same adsorbent used before) and various batch experiments were performed varying parameters like adsorbent dose, temperature, pH, dye concentration etc. Isotherm, Kinetics and Thermodynamic studies were also done and compared. Here also spectrophotometer reading of the dye solution showed maximum absorption at 618nm and 667nm so the entire study is done for both the dye solutions at 618nm and 667nm.

5.2.4.1 Effect of mass of adsorbents:

Two binary solutions were prepared using Methylene blue (MB) and Malachite green (MG) of 10ppm each in the ratio 7:3 (Solution 1) and 3:7 (solution 2) respectively. Then five conical flasks were taken for each solutions and in them 100 ml of first solution was added along with

25mg, 50mg, 75mg, 100 mg and 200 mg of nanocomposite adsorbent made of *O. sanctum.* After certain time they were taken out centrifuged and measured in a spectrophotometer. Then they were placed in a shaker incubator at temperature 308K and speed 120 rpm. Similarly experiments were performed using *A.indica* nanocomposite and soil as adsorbent.

It was observed from the four graphs obtained that with the increase in the adsorbent dosage from 25mg to 200 mg there was a gradual increase in percentage removal for all the three adsorbents. The reason of this behavior may be due to increased surface area of adsorption and availability of more binding sites.

5.2.4.2 Effect of Temperature:

For both the binary solutions of Methylene blue (MB) and Malachite green (MG) in the ratio 7:3 and 3:7, the effect of temperature was obtained for the temperatures 298K, 303K, 308K, 313K and 318K respectively for all the three adsorbents at adsorbent dose 100 mg and shaker speed 120 rpm. In all the three adsorbents, for both the solutions with the increase in temperature there was an increase in the percentage removal shown in the figures.

The increasing temperature may be explained by the increased attraction of binding sites with the dye molecules at higher temperature or an increase in motion of the dye molecules which may result in rapid adsorption.

5.2.4.3 Effect of pH:

For both the first binary solutions of Methylene blue (MB) and Malachite green (MG) in the ratio 7:3 and 3:7, the effect of pH on the nanocomposites were done in a range of pH 2 to 10 having constant temperature 308K, adsorbent dose 100 mg and shaker speed 120 rpm.

UV- VIS spectrophotometer reading showed that for both the solutions maximum removal of dyes were obtained at pH 2 for all the three adsorbents from the solutions at both the λ_{max} value 618 nm and 667nm.

In the comparative study the maximum adsorption was showed by the soil-AgNP from *O.sanctum* which was 98.65 % at 667nm in the first binary solution (MB:MG = 7:3). The four graphs obtained are given below.

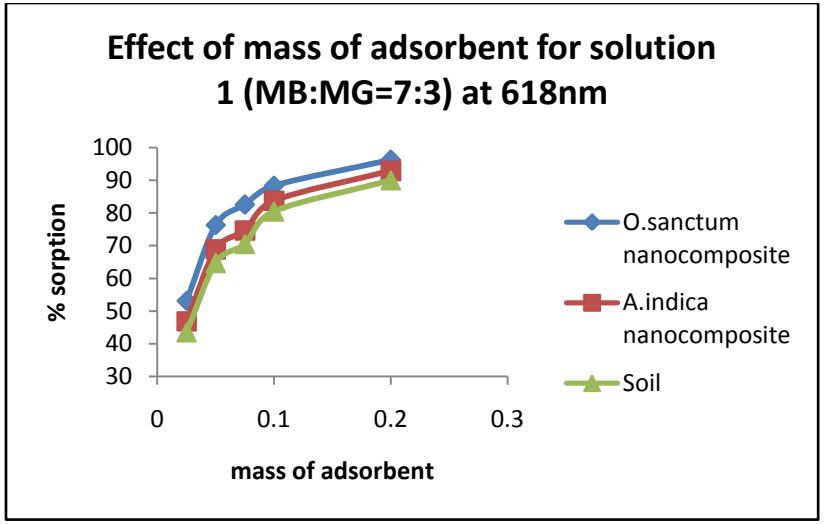

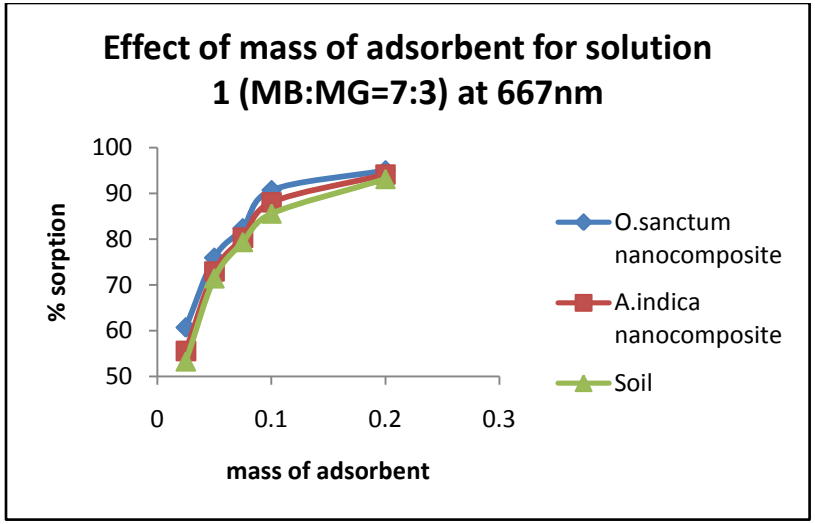

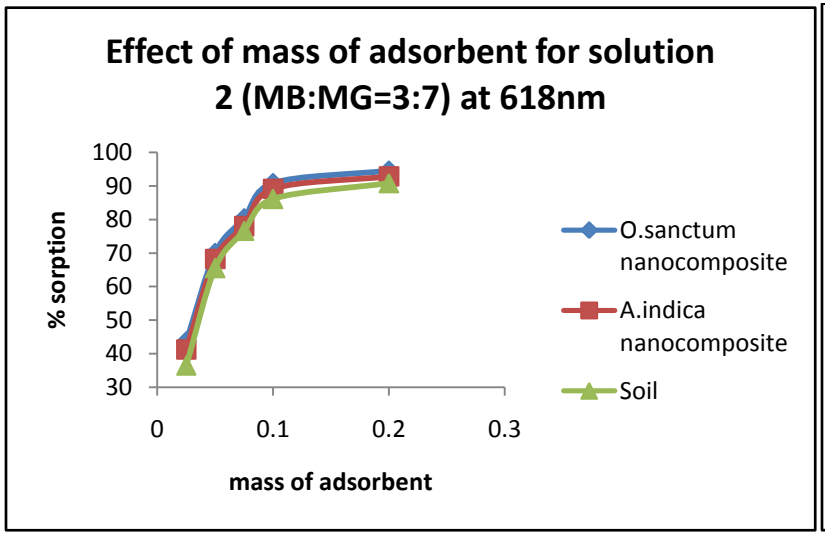

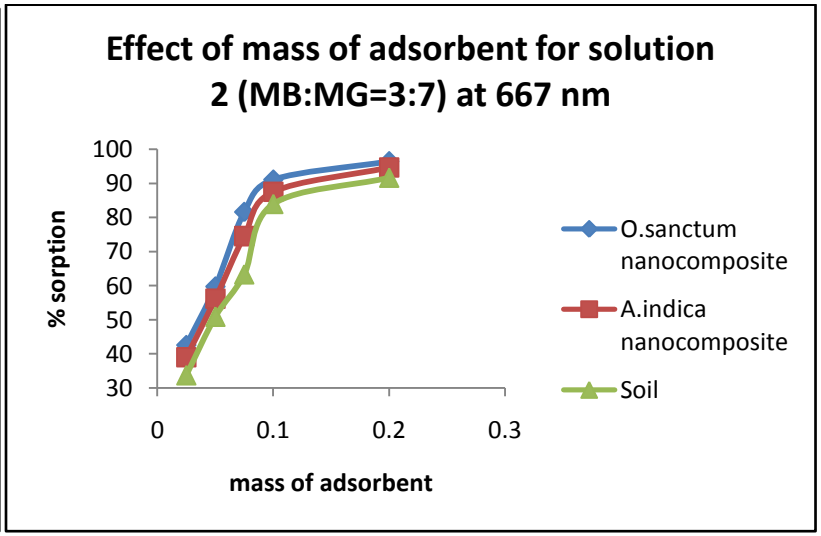

Figure 9.1, 9.2, 9.3 and 9.4 shows the effect of mass of adsorbent for both binary solutions

5.2.4.4 Effect of dye concentration:

The effect of the dye concentration in a range of 2.5 to 75 mg L^{-1} for three adsorbents at 308K and pH 2 were shown for both the binary solutions at 618nm and 667nm.

It was observed in the first solution (MB:MG=7:3) that until a certain point, the amount of dye adsorbed increased with increase in the dye concentration as shown in the figures at both 618 and 667nm , after which there was a gradual decrease. This increasing behavior may result if there is an increase in the driving force from the concentration gradient. Above the equilibrium concentration, the adsorption site in AgNP composites were saturated as a result excess dyes remains in the solution and decreases the percentage of adsorption.

In the second binary solution (MB:MG=3:7) there is a gradual decrease of the Percentage removal with the increase in the dye concentration at both 618nm and 667nm that may be due to decrease in the driving force from the concentration gradient resulting poor accumulation of the dye ions near the active sites of the nanocomposites.

5.2.4.5 Effect of contact time and agitation speed:

The experiment of contact time was performed for time - 15mins, 30mins, 45 mins, 60mins, 90mins and 120mins for pH 2, temperature 308K and 120 rpm. The experiment was performed for both the binary solutions using soil, silver nanocomposite from *O.sanctum* and silver nanocomposite from *A.indica*. It was observed that the percentage removal keeps on increasing with increase in contact time for both the solutions at 618nm and 667nm. It may be due to the fact that contact time increases the availability of active sites leading to more adsorption.

Similar trend is obtained for the effect of agitaton speed experiment. With the increase of rpm from 80 to 150 the percentage removal increased in both the solutions at 618 nm and 667 nm shown in the figures.

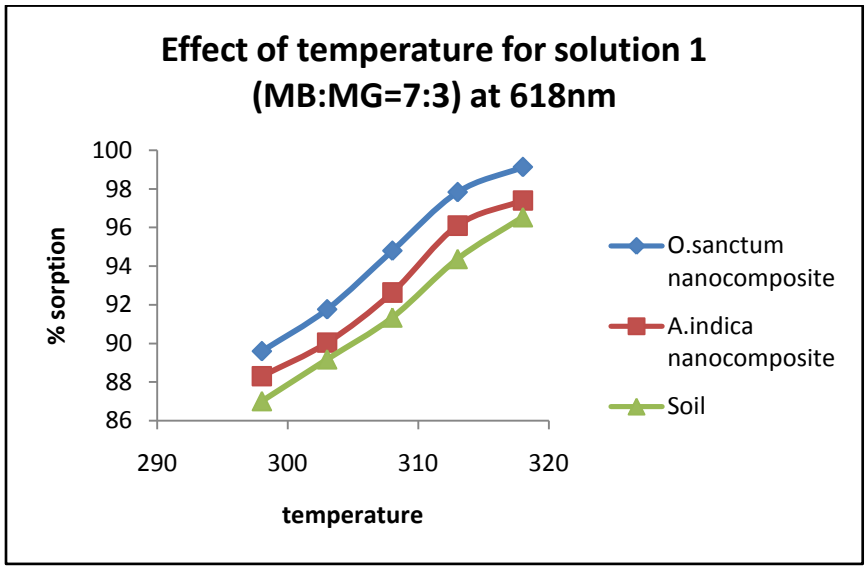

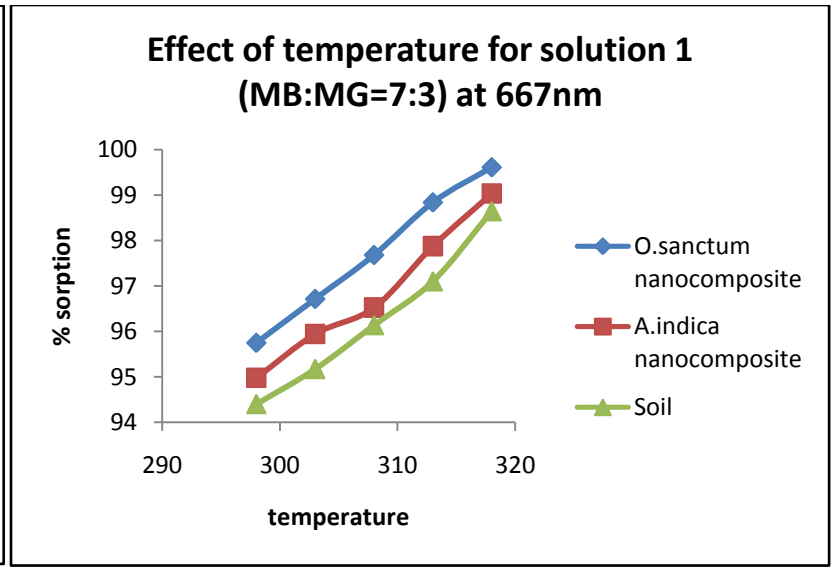

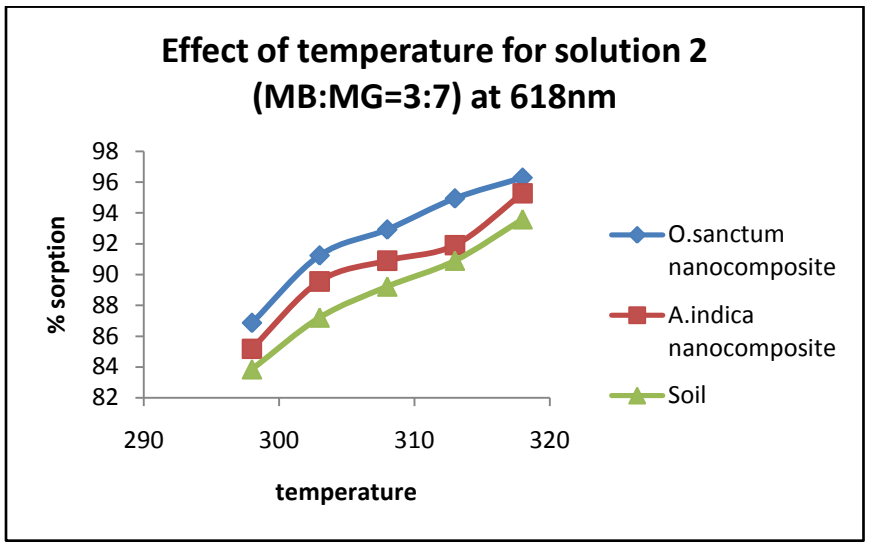

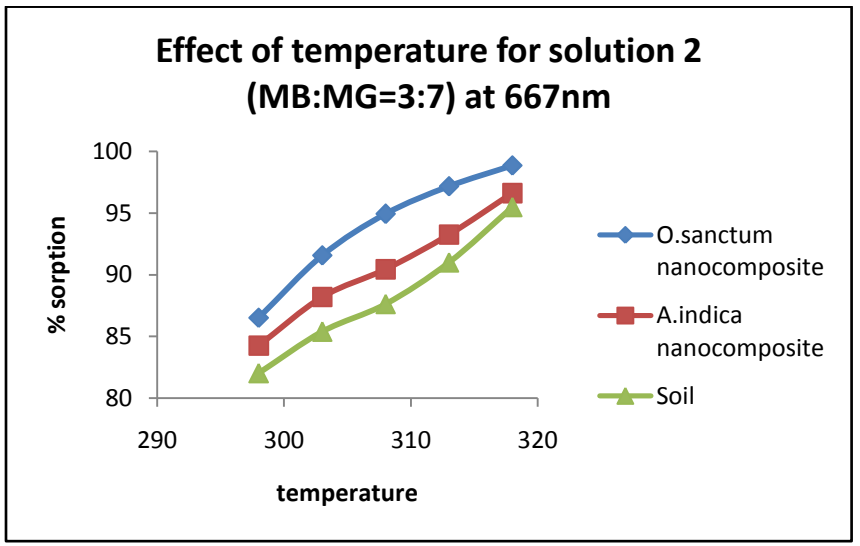

Figure 9.5, 9.6, 9.7 and 9.8 shows the effect of temperature for both binary solutions

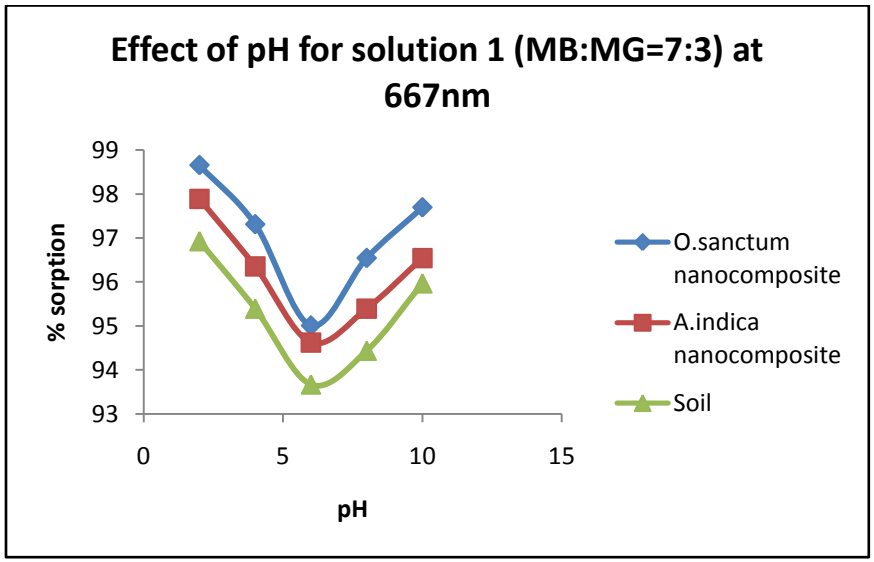

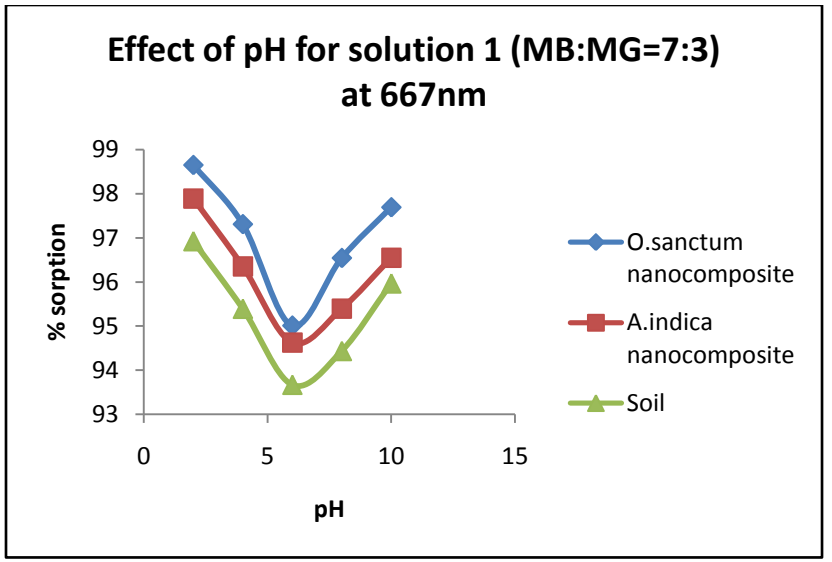

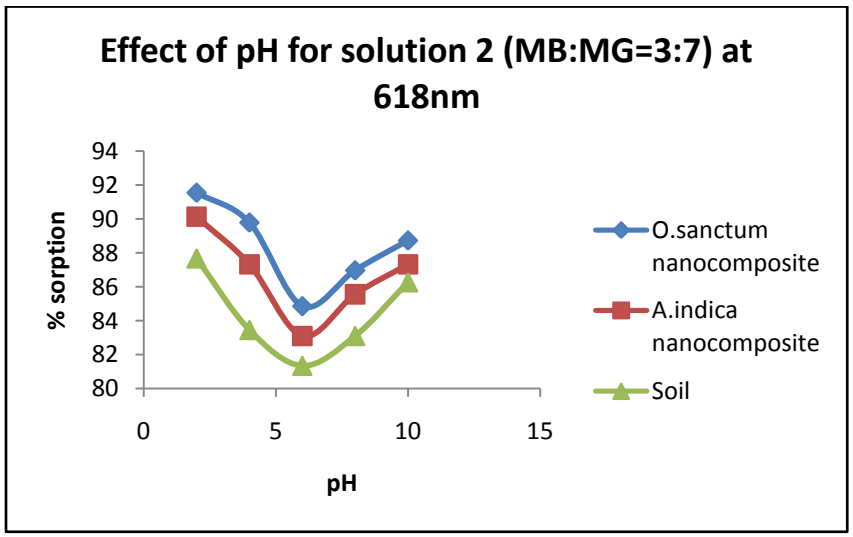

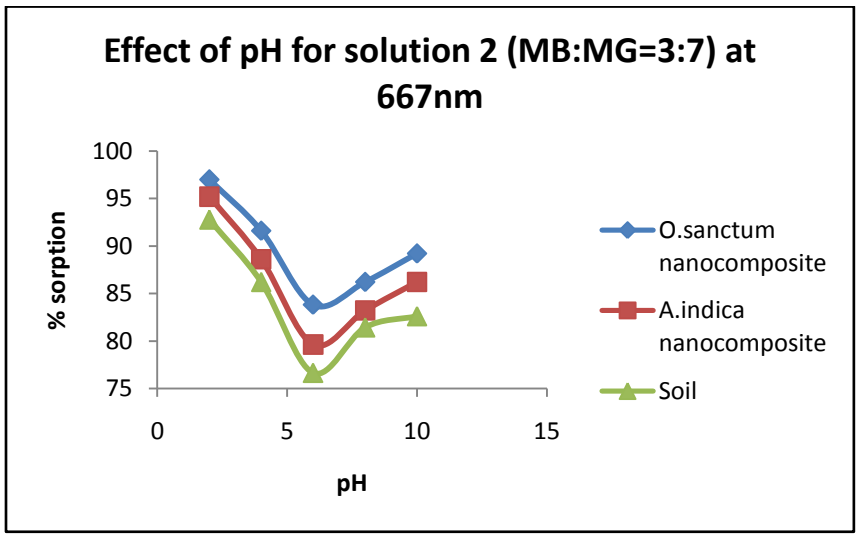

Figure 9.9, 9.10, 9.11 and 9.12 shows the effect of pH for both binary solutions

5.2.4.6 Adsorption isotherms:

For the two binary solutions of different ratios, to find out the relationship between the adsorbate adsorbed on the surface of adsorbent and concentration of adsorbate at constant temperature three isotherms were plotted at 618 and 667 nm – Langmuir, Freundlich and Temkin. In Langmuir isotherm plot the experimental data c_e/q_e were plotted against c_e for the two binary solutions using three composites at temperature 308K shown in the figures below. The coefficients and parameters obtained are also listed in table 13. In Freundlich isotherm, plots were obtained between $\ln c_e$ and $\ln q_e$ for the three adsorbents at both 618nm and 667nm and in Temkin isotherm the plots were drawn between $\ln c_e$ and q_e for the three adsorbents(figure not shown) and the correlation parameters and coefficient were listed in table 13.

5.2.4.7 Thermodynamic studies:

To determine whether the process is spontaneous in nature or not, thermodynamic studies of the two binary solutions, solution 1 (Methylene Blue:Malachite Green = 7:3) and solution 2 (Methylene Blue : Malachite Green = 3:7) is done at both 618 nm and 667 nm. In the figures below the Vant hoff plot between $-\ln K_{eq}$ and 1/T is drawn for the *O.sanctum* nanocomposite at both 618nm and 667 nm. Parameters like Gibbs free energy change (ΔG^0), enthalpy change (ΔH^0) and entropy change (ΔS^0) were also calculated using the Vant Hoff plot to confirm the nature of the adsorption process. Similar plots were drawn for the other two adsorbents (figure not shown) and different values obtained from them are listed in table 14.

5.2.4.8 Kinetic studies and study of pore diffusion:

The Lagergren's pseudo-first-order and Ho–McKay's pseudo-second-order models were applied to the experimental data for the two binary solutions of different ratios using three adsorbents at both 618nm and 667nm. The plot between t/q_t versus t for the three adsorbents showed excellent fit to the pseudo-second-order equation. K_2 (g. mg^{-1} min^{-1}) value from second-order kinetics is quite same for all the three adsorbents with R^2 value 0.999. It can thus be concluded that the reaction has followed a pseudo-second-order mechanism and not a pseudo-first-order mechanism. The values of parameters are provided in table 15.

The pore diffusion experiment shows linear graphs in all the cases suggesting the rate limiting step in all the cases.

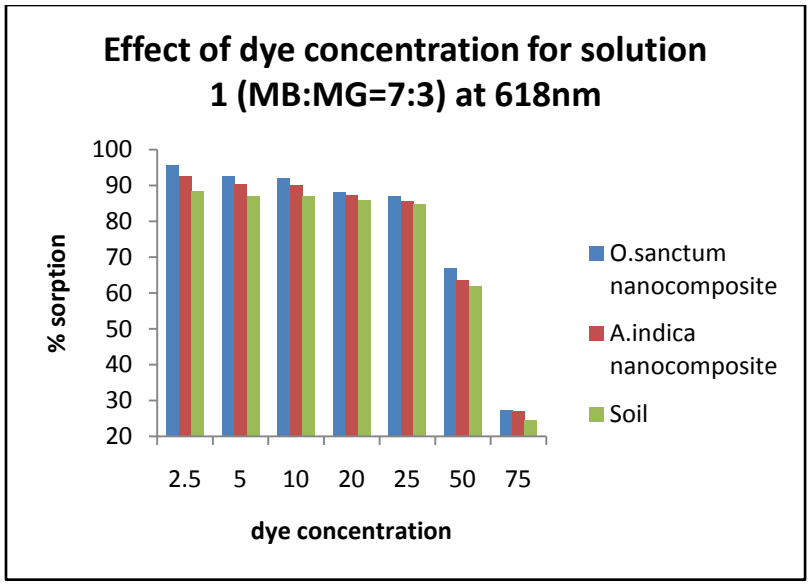

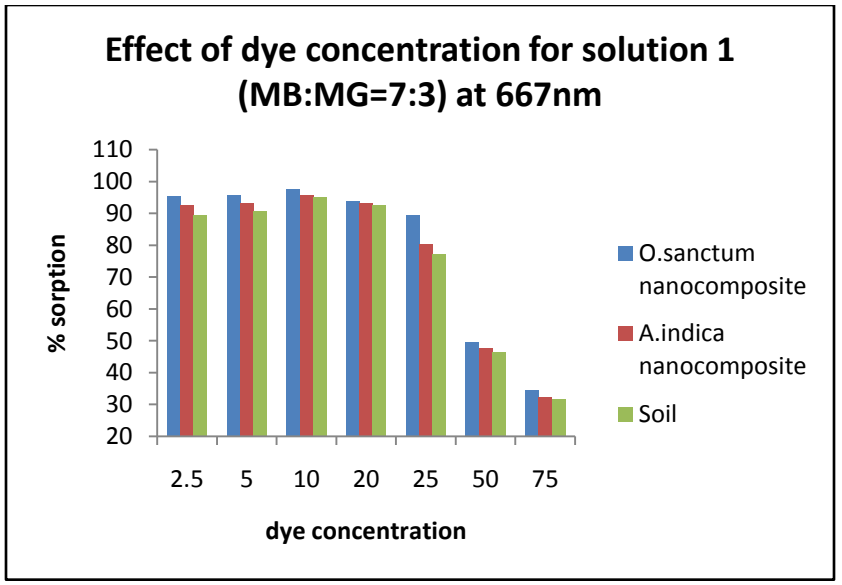

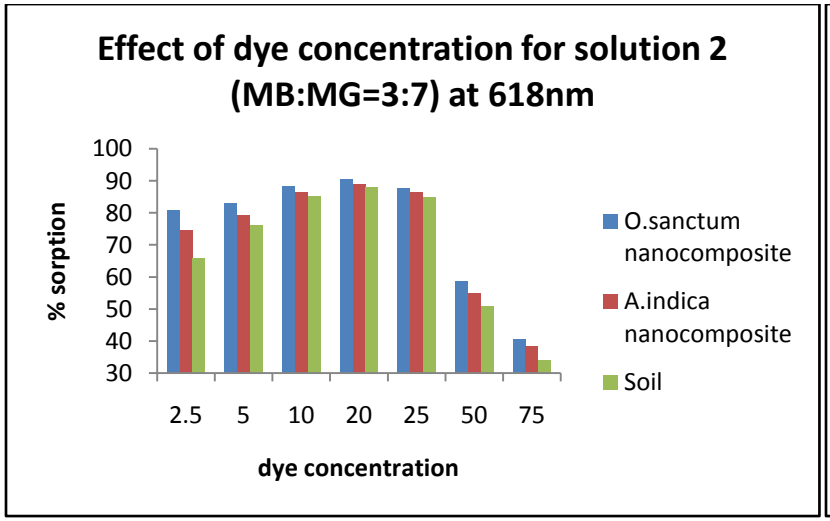

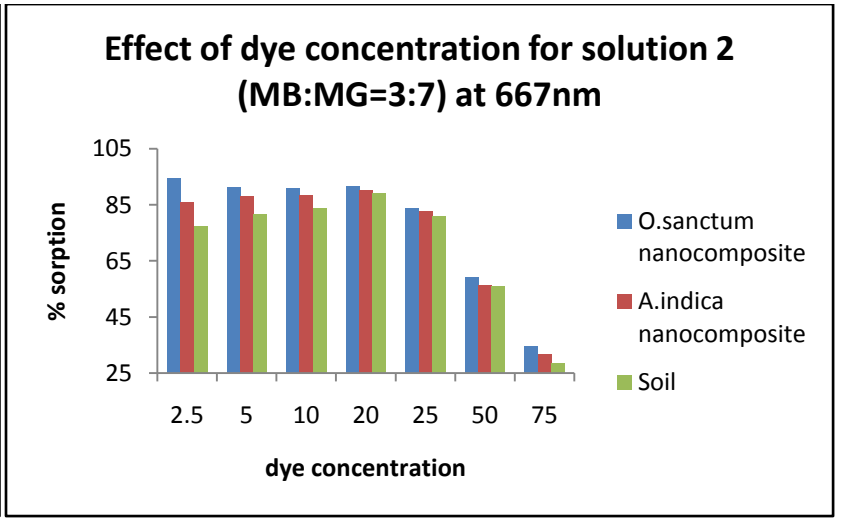

Figure 9.13, 9.14, 9.15 and 9.16 shows the effect of dye concentration for both binary solutions

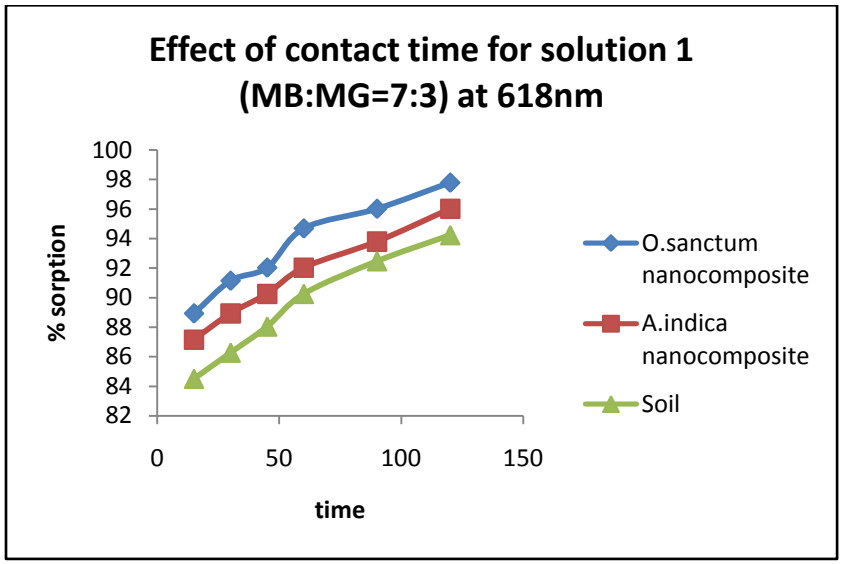

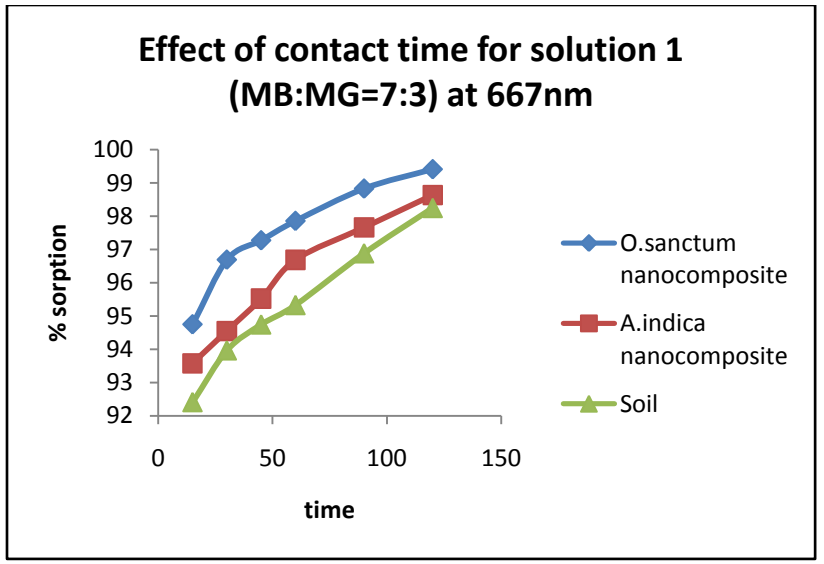

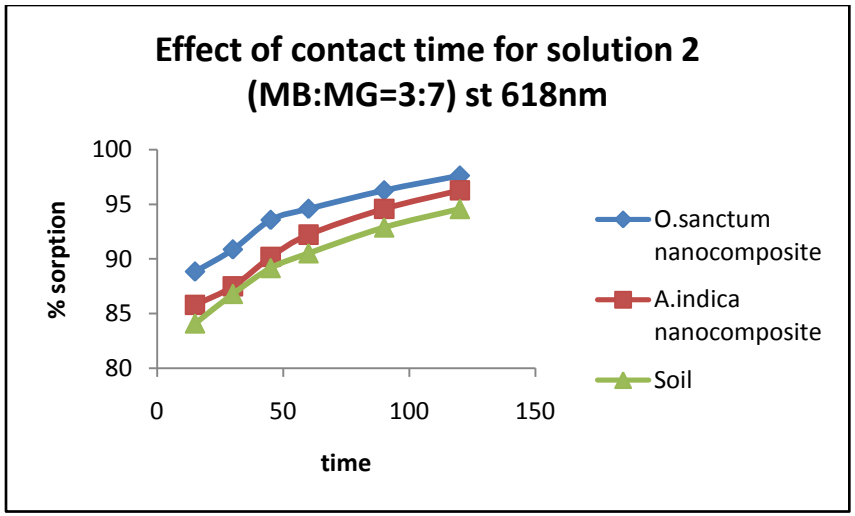

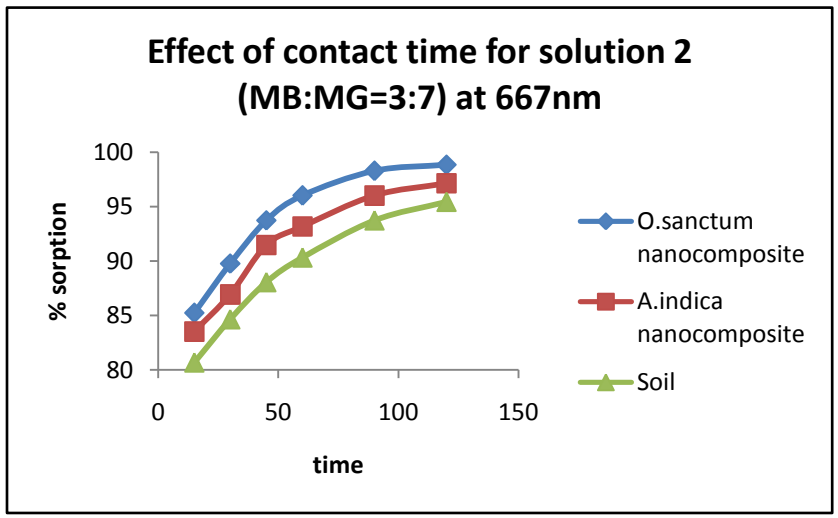

Figure 9.17, 9.18, 9.19 and 9.20 shows the effect of contact time for both binary solutions

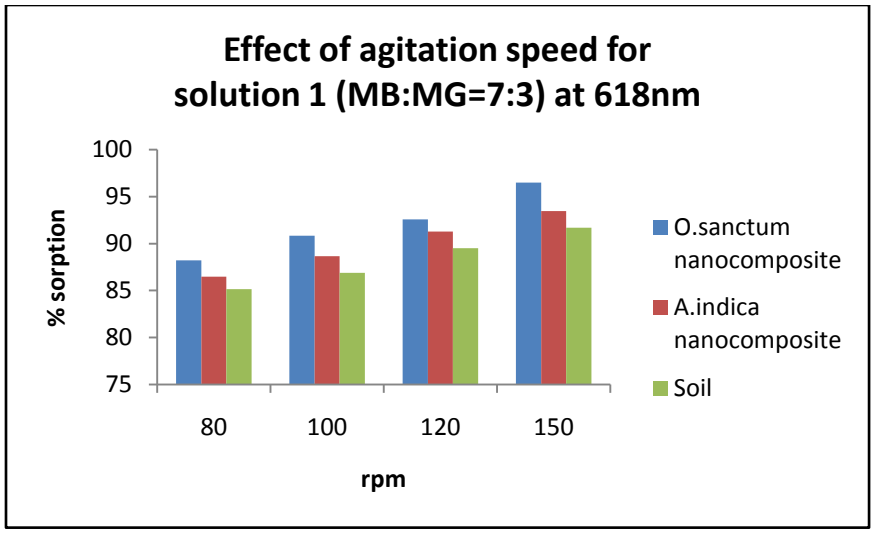

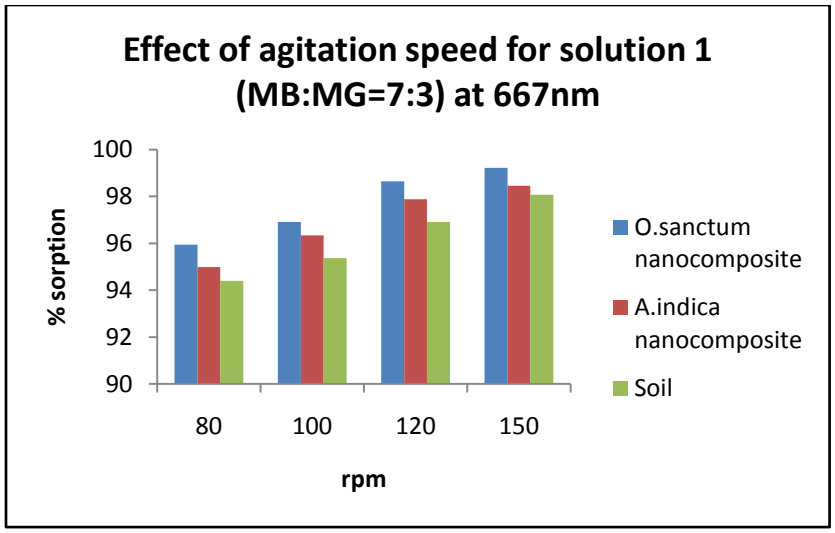

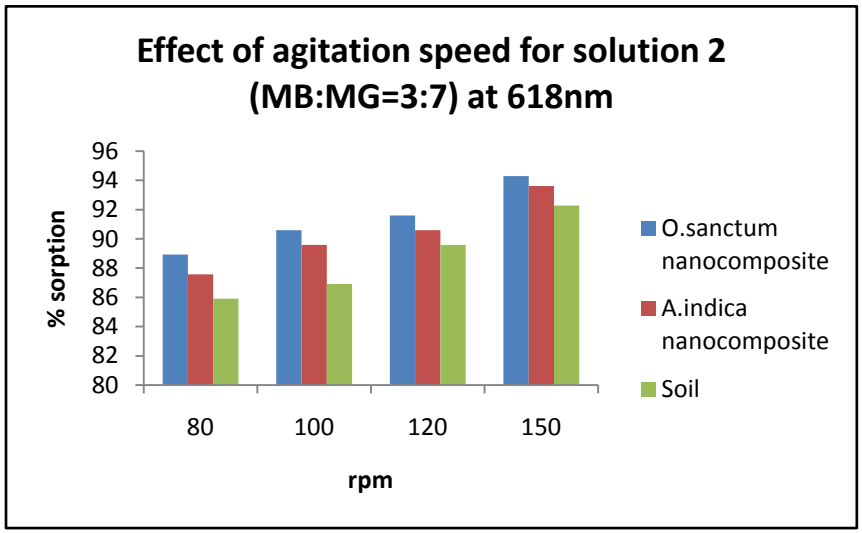

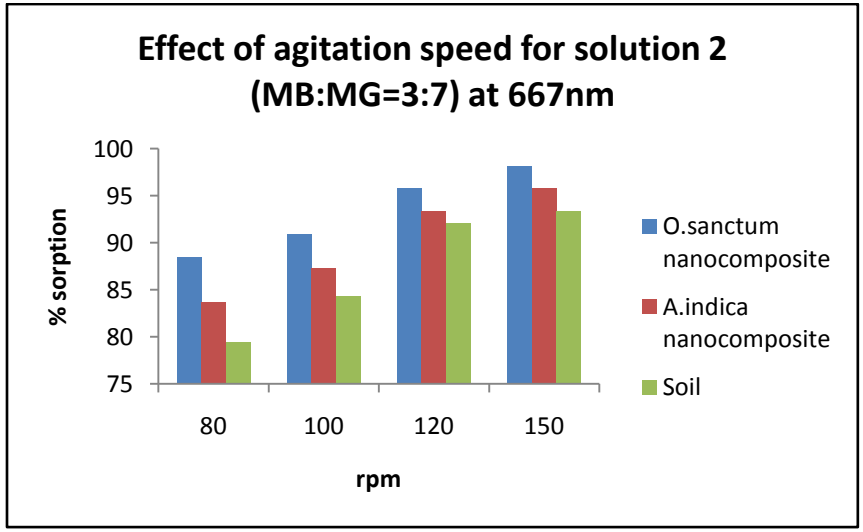

Figure 9.21, 9.22, 9.23 and 9.24 shows the effect of contact time for both binary solutions

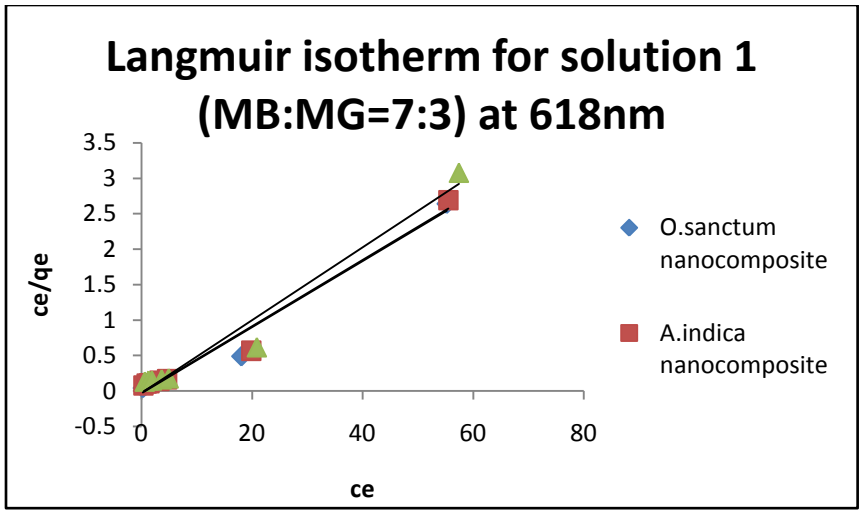

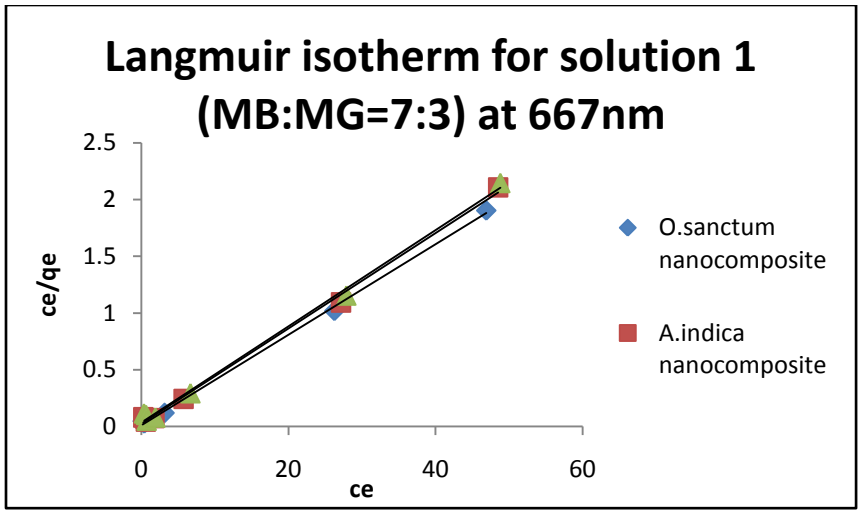

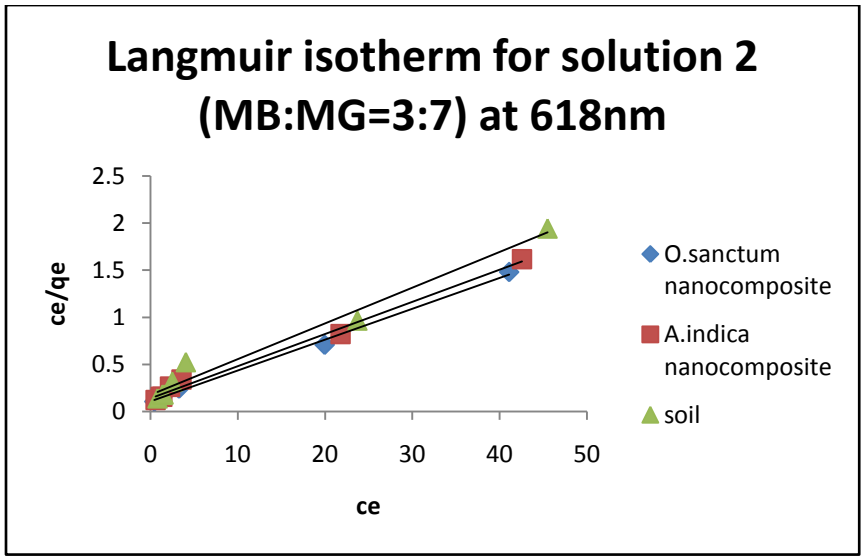

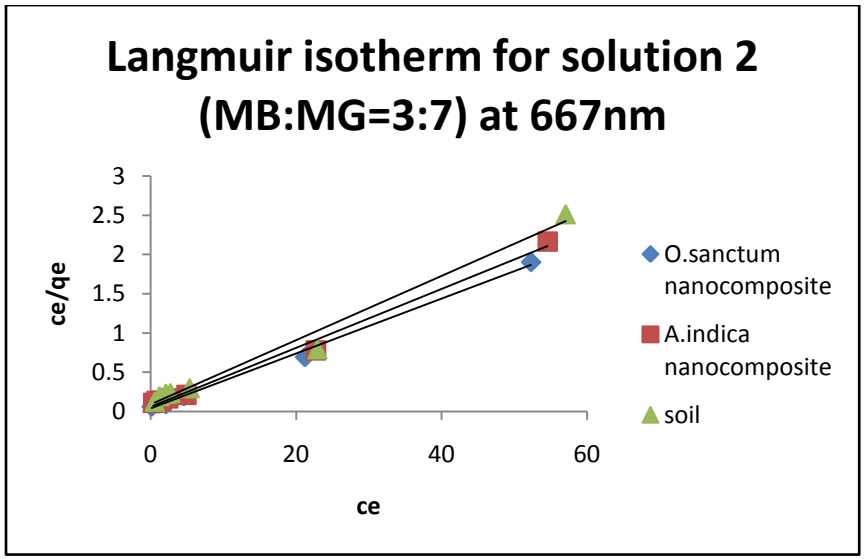

Figure 9.25, 9.26, 9.27 and 9.28 shows the Langmuir isotherm for both binary solutions

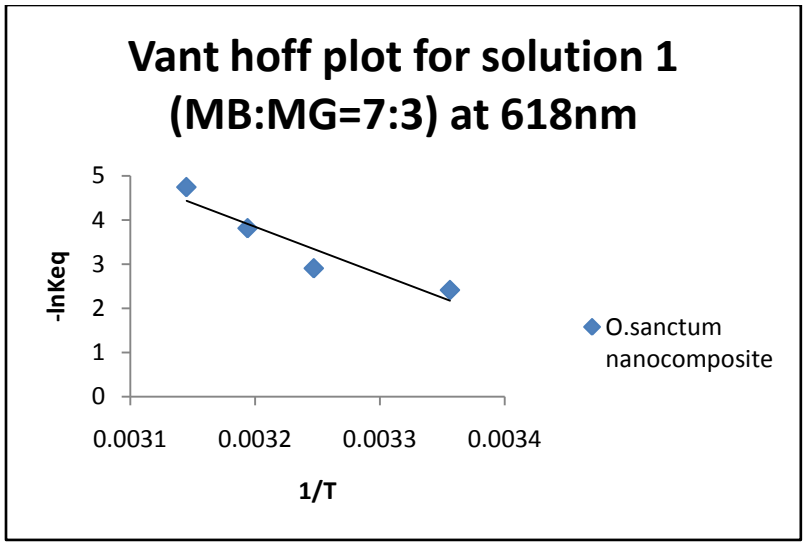

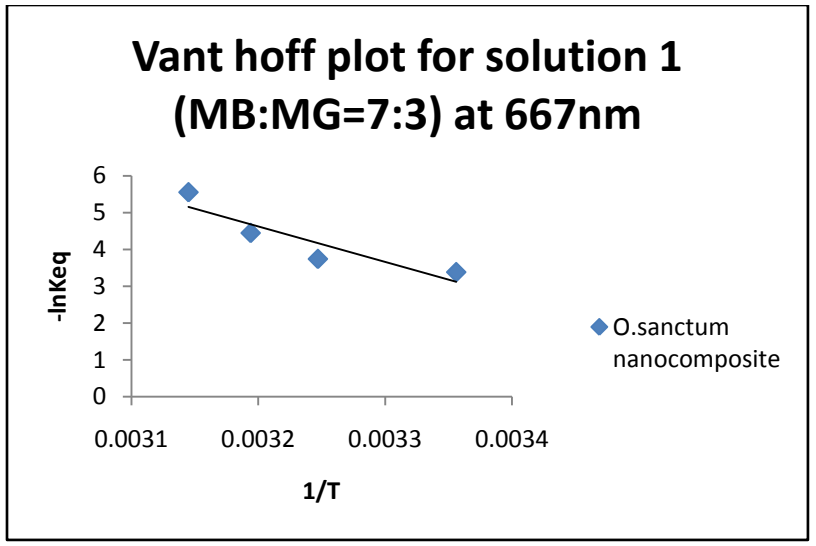

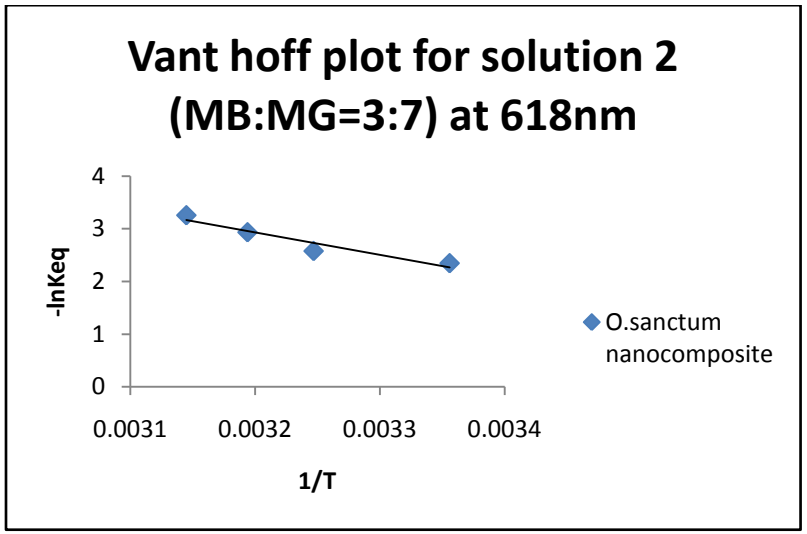

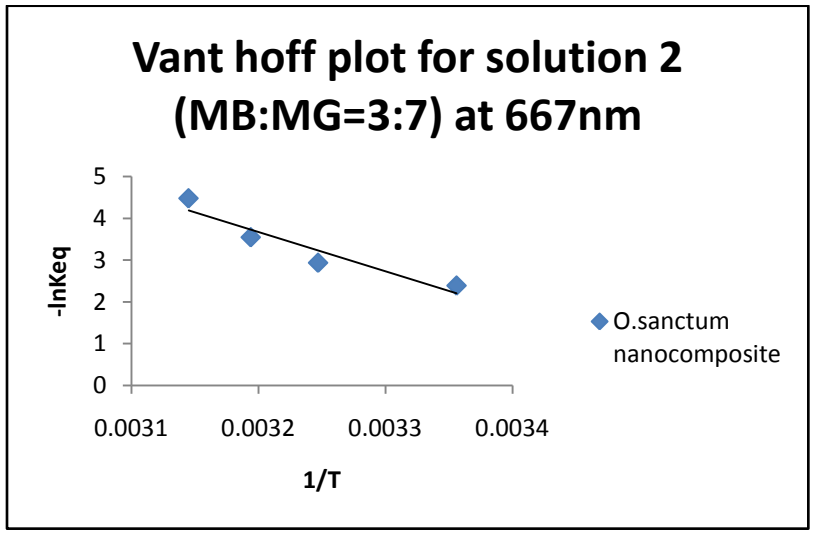

Figure 9.29, 9.30, 9.31 and 9.32 shows the Vant Hoff plot for both binary solutions

TABLE 13:

LANGMUIR PARAMETERS FOR SOLUTION 1	**SOIL-AgNP (O.sanctum)**		**SOIL-AgNP (A.indica)**		**SOIL**	
	618nm	**667nm**	**618nm**	**667nm**	**618nm**	**667nm**
q_0 mg /g	31.25	29.41	29.41	27.03	27.03	25
K_L L/mg	0.296	0.89	0.245	0.61	0.21	0.44
R^2	0.996	0.995	0.991	0.992	0.975	0.984
FREUNDLICH PARAMATERS FOR SOLUTION 1						
K_F mg/g	5.83	1.39	4.22	1.043	2.89	0.84
n	0.742	9.89	0.66	7.04	0.49	4.31
R^2	0.954	0.96	0.95	0.94	0.913	0.928
TEMKIN PARAMETERS FOR SPLUTION 1						
B J/mol	7.56	5.014	7.382	5.201	7.098	5.24
b	338.72	510.71	346.89	492.35	360.77	488.31
A L/mg	3.27	12.84	2.75	7.5	2.39	5.22
R^2	0.862	0.865	0.818	0.797	0.767	0.694
LANGMUIR PARAMETERS FOR SOLUTION 2	**SOIL-AgNP (O.sanctum)**		**SOIL-AgNP (A.indica)**		**SOIL**	
	618nm	**667nm**	**618nm**	**667nm**	**618nm**	**667nm**
q_0 mg /g	41.67	25.64	40	23.81	41.67	23.81
K_L L/mg	0.462	3.25	0.368	1.91	0.25	1.14
R^2	0.997	0.998	0.996	0.997	0.983	0.996

FREUNDLICH PARAMATERS FOR SOLUTION 2	**618nm**	**667nm**	**618nm**	**667nm**	**618nm**	**667nm**
K_F mg/g	11.57	15.96	9.78	11.49	7.99	9.77
n	2.09	1.55	1.91	1.62	1.712	1.57
R^2	0.949	0.84	0.911	0.755	0.878	0.694
TEMKIN PARAMETERS FOR SOLUTION 2						
B J/mol	7.818	4.622	8.341	4.698	9.095	4.727
b	327.54	554.03	307.002	545.06	281.55	541.72
A L/mg	6.26	33.14	4.04	18.43	2.601	13.804
R^2	0.965	0.847	0.963	0.738	0.943	0.691

TABLE 14:

PARAMETERS FOR SOLUTION 1		ΔH^0 KJ mol^{-1}	ΔS^0 J mol^{-1} K^{-1}	ΔG^0 (25^0C) KJ mol^{-1}	ΔG^0 (30^0C) kJ mol^{-1}	ΔG^0 (35^0C) kJ mol^{-1}	ΔG^0 (40^0C) kJ mol^{-1}	ΔG^0 (45^0C) kJ mol^{-1}
Soil-AgNP (basil leaf)	**618nm**	-10.71	38.12	-5.34	-6.08	-7.44	-9.92	-12.53
	667nm	-9.62	35.41	-7.72	-8.52	-9.58	-11.57	-14.68
Soil-AgNP (neem)	**618nm**	-6.78	24.82	-5.01	-5.55	-6.48	-8.34	-9.58

Soil-AgNP (neem leaf)	**667nm**	-6.45	24.62	-7.28	-7.97	-8.51	-9.97	-12.24
Soil	**618nm**	-5.57	20.69	-4.71	-5.31	-6.03	-7.34	-8.79
	667nm	-5.61	21.65	-6.99	-7.51	-8.23	-9.14	-11.34
PARAMETERS FOR SOLUTION 2		ΔH^0 KJ mol^{-1}	ΔS^0 J mol^{-1} K^{-1}	ΔG^0 (25^0C) KJ mol^{-1}	ΔG^0 (30^0C) kJ mol^{-1}	ΔG^0 (35^0C) kJ mol^{-1}	ΔG^0 (40^0C) kJ mol^{-1}	ΔG^0 (45^0C) kJ mol^{-1}
Soil-AgNP (basil leaf)	**618nm**	-4.26	16.54	-4.68	-5.90	-6.59	-7.64	-8.61
	667nm	-9.41	33.76	-4.61	-6.02	-7.51	-9.22	-11.84
Soil-AgNP (neem leaf)	**618nm**	-3.56	13.99	-4.33	-5.42	-5.89	-6.33	-7.95
	667nm	-5.88	21.58	-4.16	-5.07	-5.76	-6.84	-8.87
Soil	**618nm**	-3.37	13.16	-4.08	-4.83	-5.41	-5.99	-7.09
	667nm	-5.59	20.36	-3.76	-4.49	-5.02	-6.02	-8.08

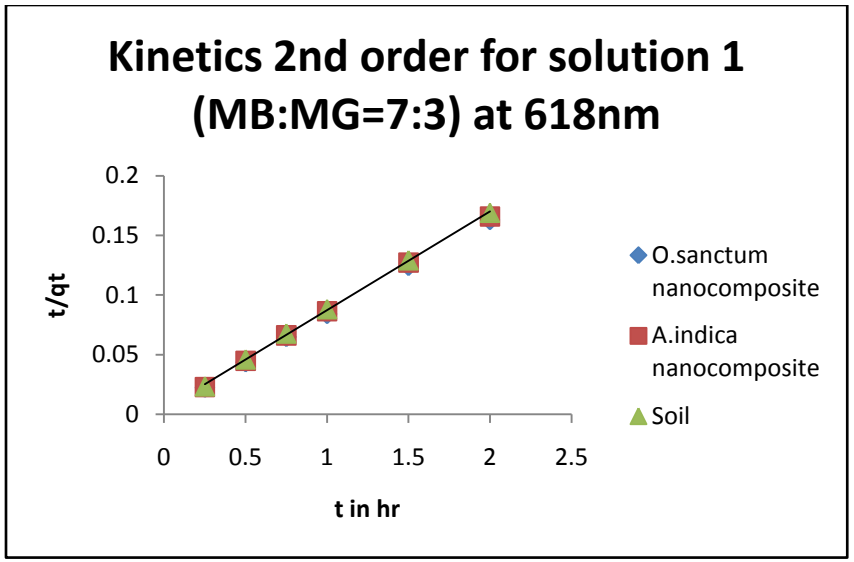

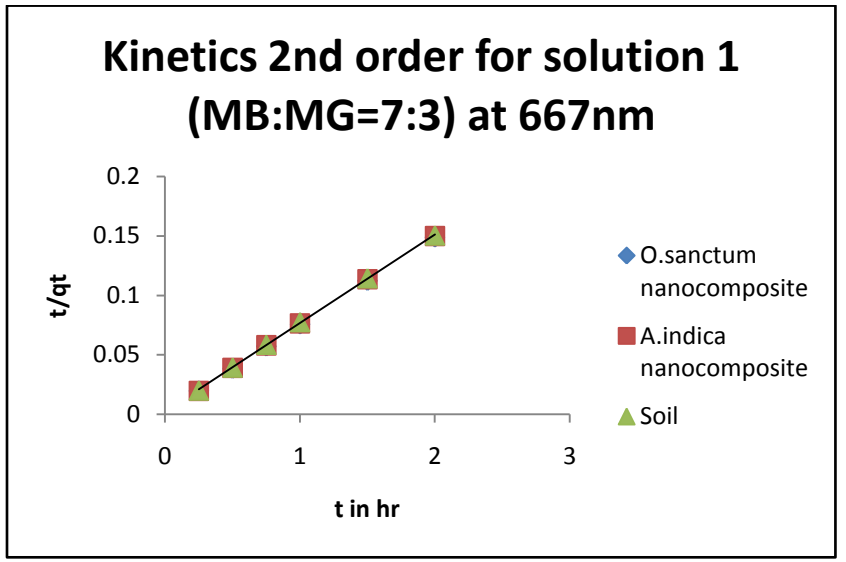

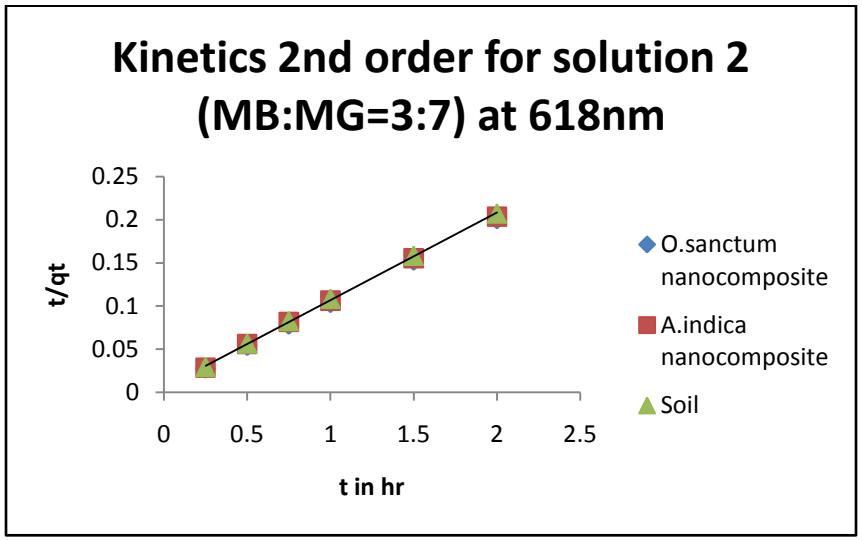

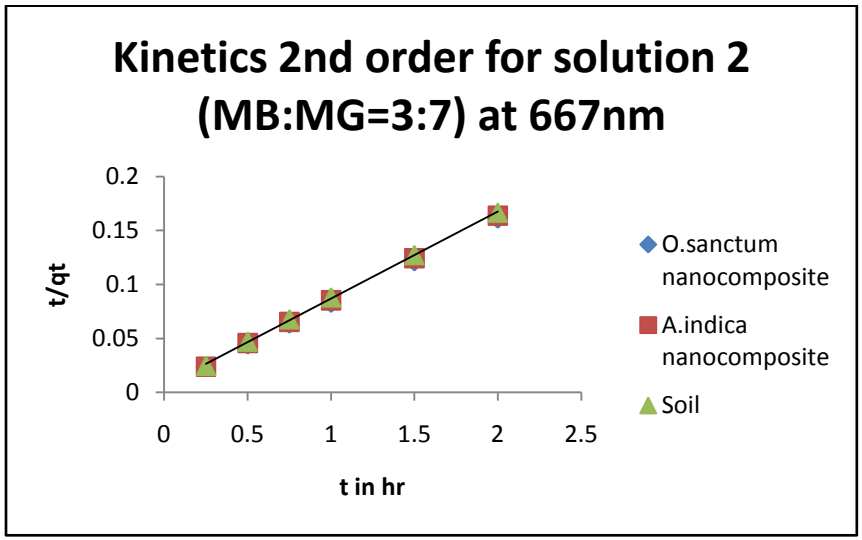

Figure 9.33, 9.34, 9.35 and 9.36 shows the Kinetics 2nd order plot for both binary solutions

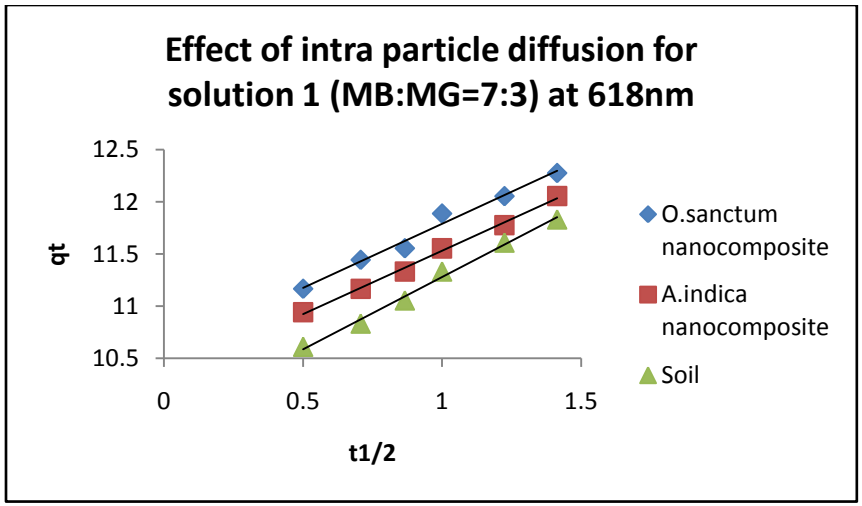

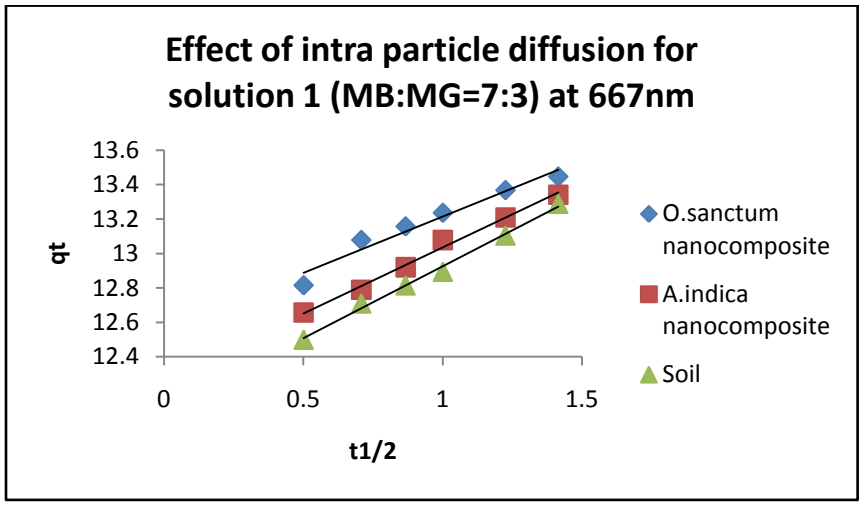

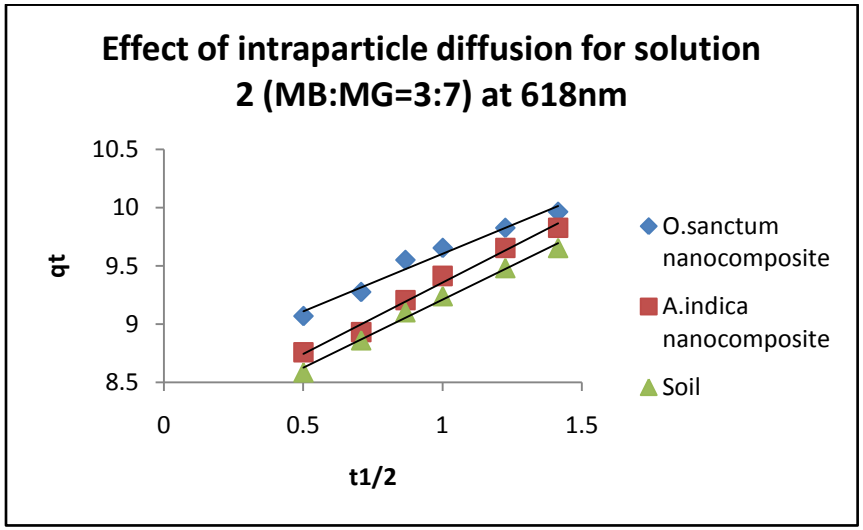

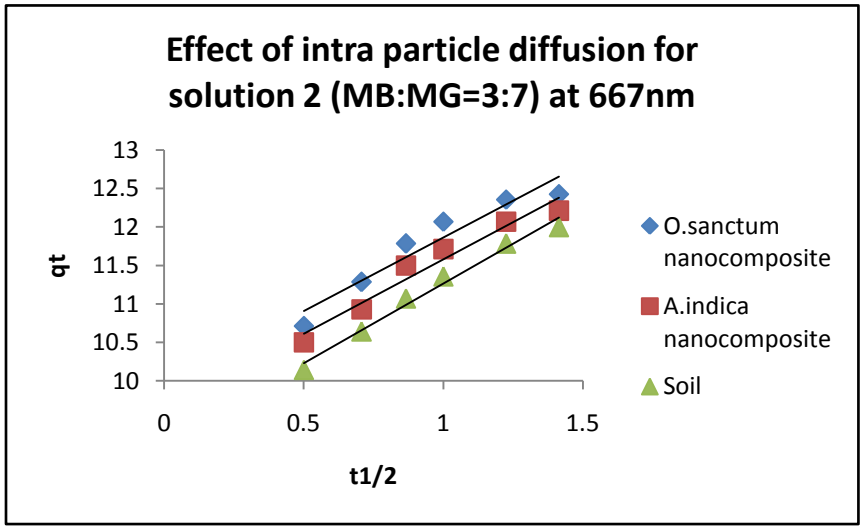

Figure 9.37, 9.38, 9.39 and 9.40 shows the intra particle diffusion plot for both binary solutions

TABLE 15:

KINETICS 1ST ORDER COEFFICIENTS FOR SOLUTION 1	**SOIL AgNP (*O.sanctum*)**		**SOIL-AgNP (*A.indica*)**		**SOIL**	
	618nm	**667nm**	**618nm**	**667nm**	**618nm**	**667nm**
K_1	0.62	0.325	0.62	0.39	0.705	0.427
lnq_e	25.61	12.9	24.02	12.23	23.37	11.67
R^2	0.952	0.886	0.984	0.964	0.972	0.98
KINETICS 2nd ORDER COEFFICIENTS FOR SOLUTION 1	**618nm**	**667nm**	**618nm**	**667nm**	**618nm**	**667nm**
q_e	0.082	0.074	0.082	0.074	0.082	0.074
K_2	0.004	0.002	0.004	0.002	0.004	0.002
R^2	0.999	0.999	0.999	0.999	0.999	0.999
KINETICS 1ST ORDER COEFFICIENTS FOR SOLUTION 2	**SOIL AgNP (*O.sanctum*)**		**SOIL-AgNP (*A.indica*)**		**SOIL**	
	618nm	**667nm**	**618nm**	**667nm**	**618nm**	**667nm**
K_1	0.494	0.932	0.62	0.958	0.588	1.033
lnq_e	19.21	19.79	17.8	18.61	15.98	18.79
R^2	0.918	0.833	0.957	0.883	0.946	0.928
KINETICS 2nd ORDER COEFFICIENTS FOR SOLUTION 2	**618nm**	**667nm**	**618nm**	**667nm**	**618nm**	**667nm**
q_e	0.101	0.08	0.101	0.08	0.101	0.08
K_2	0.005	0.006	0.005	0.006	0.005	0.006
R^2	0.999	0.999	0.999	0.999	0.999	0.999

TABLE 16:

INTRA PARTICLE DIFFUSION PARAMETERS FOR SOLUTION 1	**SOIL-AgNP (*O.sanctum*)**		**SOIL-AgNP (*A.indica*)**		**SOIL**	
	618nm	**667nm**	**618nm**	**667nm**	**618nm**	**667nm**
K_p	1.226	0.656	1.214	0.769	1.387	0.856
C	10.56	12.55	10.31	12.26	9.89	12.08
INTRA PARTICLE DIFFUSION PARAMETERS FOR SOLUTION 2	**SOIL-AgNP (*O.sanctum*)**		**SOIL-AgNP (*A.indica*)**		**SOIL**	
	618nm	**667nm**	**618nm**	**667nm**	**618nm**	**667nm**
K_p	0.991	1.91	1.226	1.936	1.17	2.068
C	8.613	9.955	8.131	9.644	8.04	9.197

5.2.5 EXPERIMENT 5: Model experiment.

The effluents from the industries are not always dumped in the water sources. Sometimes they are dumped in the ground in isolated locations and barren lands by creating big landfills. These landfills can cause serious hazard since they pollute the ground water below. This method of dumping paints, dye solutions or any kind of chemicals, heavy metal containing substances are illegal and band throughout the world.

5.2.5.1 Experimenal setup:

These dumped chemicals have detrimental impact on humans as well as environment in different ways. They can easily leach into the water sources or affect the ground water, they can contaminate and poison the soil and they also pollute the air. So to check whether the nanocomposite made of *O.sanctum* is eligible for removal of the dye effluents in such cases a

model experiment is done. In the model experiment a column is prepared using polyacrylic sheet with a semipermeable membrane in between as shown in the figure 10.1. Now in the total height of 19 cm, the bottom 4 cm is nanocomposite and the above 12 cm is dye solution of concentration 20ppm and pH 2, since optimum pH obtained is 2 from the previous batch experiments. The whole setup was kept at room temperature. Now the experiment was performed for 15 days. Each day the dye containing solution was added at the top and adsorbed solution was taken out of the bottom and the optical density was measured in a spectro photometer and a graph is plotted between time (in days) and the percentage removal. Similar experiment is performed using only soil as adsorbent and Methylene Blue dye solution. The figure of the set up is given

Figure 10.1 The column used in the model experiment

In the result in both the cases we can see that at the beginning the percentage removal is less which gradually increases upto a certain point and then decreases. It may be due to the fact that

at the beginning the dye molecules react with active sites of the adsorbent causing rapid adsorption as a result the increasing tendency. But after some time, the active sites get occupied and the adsorption process slows down and excess dye molecules are released in the bottom thus decreasing the percentage removal.

Graph of percentage removal vs time:

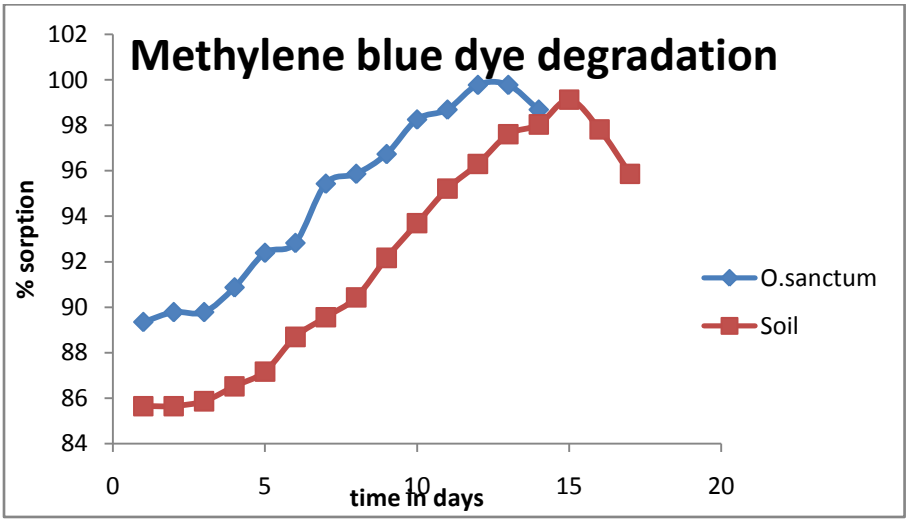

Figure 10.2 The percentage removal vs time graph for the model experiment

5.2.6 FUTURE SCOPES OF THE PROJECT:

In this project few batch experiments were performed, showing the effectiveness of the nano adsorbent formed. The further studies that can be performed are

- A continuous process can be done using the three adsorbents for the degradation of dyes and the results can be tallied or compared.
- The silver nanocomposite can be synthesized using various plant leaves, fruits, barks, seeds and peel extract. In this experiment only two leaf extracts were used. Further comparative studies can be performed using different plant part extracts.
- In case of Binary solution of dyes derivative spectrophotometry can be used for further analysis.
- In case of the model experiment to prevent the ground water contamination a more specific method can be used by creating an artificial land fill and performing the experiment for a longer period of time.

CONCLUSION

6.0 CONCLUSION

Thus from the characterization of the three adsorbents done and the comparative studies from the Batch experiments following conclusions were drawn.

The following conclusions were made based on the results of the study:

Silver nanoparticles were obtained from the leaf extracts of basil (*O.sanctum*) and neem (*A.indica*) which was observed by the color change from pale green to Dark reddish brown when the leaf extracts were added to the silver nitrate solution. Further the UV-VIS Spectroscopic result showed the maximum adsorption peak at 422 and 435nm respectively. It is also considered that the flavonoids, terpenoids, phenolic group and protein structures present in the leaf extracts are responsible for the reduction of the silver nitrate salt and release of silver ions.

TEM and SEM studies revealed the morphology, shape and size of the silver nanopaticles formed which is spherical with size around 38nm. FTIR studies revealed the presence of alkane, amide, free alcohol, phenol, disulfide, chloride, hydrogen bond, carboxyl group and alkene present in the sample. XRD studies showed the presence of crystalline silver of size 32 to 38 nm along with quartz, feldspar, mica, amphibole, kaolinite and calcite due to the presence of soil in the composite.

In the batch experiments, all the comparative studies were favored at high temperature and lower pH with a little adsorbent dosage. The solution pH controls the electrostatic interactions, which can have a profound effect on the adsorption process. In the first experiment the percentage dye removal was highest for adsorbent made of basil plant with the removal of dye around 99.4 % .In the second experiment better adsorption is observed in the Methylene Blue Dye. Similarly in Binary mixtures also the best adsorption is observed at 667nm. To the experimental equilibrium data in all the experiments the Langmuir isotherm model provided best fit which indicates a monolayer adsorption on the surface and also they followed the Ho and McKay's second order kinetics.

Thus it can be concluded from the study that silver nanocomposite from different sources can be considered as an ecofriendly, simple, cost effective and less energy consuming process for removal of hazardous dyes from the aqueous solutions.

REFERENCES

7.0 REFERENCES:

1. A. Babuponnusami, K. Muthukumar, A review on Fenton and improvements to the Fenton process for wastewater treatment, Journal of Environmental Chemical Engineering 2 (2014) 557–572.
2. A. Baghizadeh, S. Ranjbar, V.K. Gupta, M. Asif, S. Pourseyedi, M.J. Karimi, R. Mohammadinejad, Green synthesis of silver nanoparticles using seed extract of *Calendula officinalis* in liquid phase, Journal of Molecular Liquids 207 (2015) 159–163.
3. A. Saeed, M. Sharif, M. Iqbal, Application potential of grapefruit peel as dye sorbent: kinetics, equilibrium and mechanism of crystal violet adsorption. J Hazard Mater (2010) 179:564–572.
4. Are you and your family eating toxic food dyes?, Mercola.com (2011)
5. B. Kumar, K. Smita, L. Cumbal, A. Debut, Green synthesis of silver nanoparticles using Andean Blackberry fruit extract, Saudi Journal of Biological Sciences (2015).
6. B. Yahyaei, S. Azizian, Rapid adsorption of binary dye pollutants onto the nanostructred mesoporous alumina, Journal of Molecular Liquids 199 (2014) 88–95.
7. B. Sadhegi, F. Gholamhoseinpoor, A study on the stability and green synthesis of silver using *Ziziphora tenuior*(Zt) extract at room temperature, SpectrochimicaActa Part A : Molecular and Biomolecular spectroscopy 134 (2015) 310-315.
8. C. Wan, J. Li, Cellulose aerogels functionalized with poly pyrrole and silver nanoparticles: In-situ synthesis, characterization and antibacterial activity, Carbohydrate Polymers 146 (2016) 362–367.
9. C.J. Pandian, R. Palanivel, S. Dhananasekaran, Green synthesis of nickel nanoparticles using *Ocimum sactum* and their application in dye and pollutant adsorption, Chinese journal of Chemical engineering 23(2015) 1307-1315.
10. D.A. Kumar, V. Palanichamy, S.M. Roopan, Green synthesis of silver nanoparticles using *Alternanthera dentata* leaf extract at room temperature and

their antimicrobial property, Spectrochimica Acta Part A : Molecular and Biomolecular spectroscopy 127 (2014) 168-171.

11. Dyes, General Survey by Gerald Booth (2000), Ullmann's encyclopedia of industrial chemistry
12. E.M. Evangelin Femila, R. Srimathi, D. Charumathi, Removal of Malachite Green using Silver nanoparticles via adsorption and chemical degradation, International journal of pharmacy and pharmaceutical science.
13. G.M. Raghavendra, J. Jung, D. Kim, J. Seo, Step-reduced synthesis of starch-silver nanoparticles, International Journal of Biological Macromolecules 86 (2016) 126–128.
14. G.M. Sulaiman, A.B. Mohammad , Green synthesis, antimicrobial and cytotoxic eefects of silver nanoparticles using *Eucalyptus chapmaniana* leave extract. Asian Pac J Trop Biomed (2013) 3(1):58-63.
15. P. Gharbani, M. Khosravi, S.M. Tabatabaii, K. Zare, S.I. Dastmalch and A. Mehrizad (2010) Degradation of trace aqueous 4-chloro-2-nitrophenol occurring in pharmaceutical industrial wastewater by ozone Int. J. Environ. Sci. Tech., 7 (2), 377- 384.
16. H. Hou, R. Zhou, P. Wu, L. Wu, Removal of Congo Red from aqueous solution with hydroxyapatite/chitosan composite, Chemical Engineering Journal 211-212 (2012) 336-342.
17. H. Mazaheri, M. Ghaedi, A. Asfaram, S. Hajati, Performance of CuS nanoparticle loaded on activated carbon in the adsorption of methylene blue and bromophenol blue dyes in binary aqueous solutions: Using ultrasound power and optimization by central composite design, Journal of Molecular Liquids 219 (2016) 667–676.
18. H. Padalia, P. Moteriya, S. Chanda, Green synthesis of silver nanoparticles
19. H.M.F. Freundlich (1906) Over the adsorption in solution. J PhysChem 57:385–471.
20. H.M.M. Ibrahim, Green synthesis and characterization of silver nanoparticles using banana peel extract and their antimicrobial activity against representative

microorganisms, Journal of Radiation Research and Applied Sciences 8 (2015) 265-275.

21. I. Langmuir (1916) The constitution and fundamental properties of solids and liquids. J Am ChemSoc 38:2221–2295.

22. Impact of Dye industries on the Environment, Slideshare.in (2014)

23. K. Natarajan, S. Selvary, R.V. Murty, Microbial production of silver nanoparticles. Dig J Nanomater Bios (2010) 5:135–140.

24. Living in colors: the potential dangers of Artificial Dyes, Rachel Hennessey, Forbes.com

25. M. Ali, B. Kim, K.D. Belfield, D. Norman, M. Brennan, G.S. Ali, Green synthesis and characterization of silver nanoparticles using *Artemisia absinthium* aqueous extract — A comprehensive study, Materials Science and Engineering C 58 (2016) 359–365.

26. M. Atarod, M. Nasrollahzadeh, S.M. Sajadi, Euphorbia heterophylla leaf extract mediated green synthesis of Ag/TiO_2 nanocomposite and investigation of its excellent catalytic activity for reduction of variety of dyes in water, Journal of Colloid and Interface Science 462 (2016) 272–279.

27. M. Ghaedi, M. Yousefinejad, M. Safarpoor, H.Z. Khafri, M.K. Purkait, *Rosmarinus officinalis* leaf extract mediated green synthesis of silver nanoparticles and investigation of its antimicrobial properties, Journal of Industrial and Engineering Chemistry 31 (2015) 167–172.

28. M. K. Satapathy, P. Das, Optimization of crystal violet dye removal using novel soil-silver nanocomposite as nanoadsorbent using response surface methodology, Journal of Environmental Chemical Engineering 2 (2014) 708–714.

29. M. Zargar, K. Shameli, G.R. Najafi, F. Farahani, Plant mediated green biosynthesis of silver nanoparticles using *Vitex negundo* L. extract, Journal of Industrial and Engineering Chemistry 20 (2014) 4169–4175.

30. M.A. Hossain, M. Kumita, Y. Michigami, S. Mori, Kinetics of Cr (VI), adsorption on used black tea leaves, J.Chem. Eng .Jpn 38 (6) (2005) 402-406.

31. M.B. Gholivand, Y. Yamini, M. Dayeni, S. Seidi, E. Tahmasebi, Absorptive removal of alizarin red-S and alizarin yellow CG from aqueous solutions using polypyrrole - coated magnetic nanoparticles, Journal of Environment and Chemical Engineering 3 (2015) 529-540.
32. M.J. Ahmed G. Murtazaa, A. Mehmooda, T.M. Bhatti, Green synthesis of silver nanoparticles using leaves extract of *Skimmia laureola*: Characterization and antibacterial activity, Materials Letters153(2015)10–13.
33. M.K. Satapathy, P. Banerjee, Plant-mediated synthesis of silver-nanocomposite as a novel azodye adsorbent, ApplNanosci, 5 (1) (2013) 1-9.
34. M.M.D. Jiminez, V.H. Montoya, M.P.E. Gonzalez, Performance of mango seed adsorbents in the adsorption of anthraquinone and azo acid dyes in single and binary aqueous solutions, Bioresource Technology 100 (2009) 6199–6206.
35. Methylene Blue, The American Society of Health-System Pharmacists (2016).
36. N.M. Mahmoodi, R. Salehi, M. Arami, Binary system dye removal from colored textile wastewater using activated carbon: Kinetic and isotherm studies, Desalination 272 (2011) 187–195.
37. P. Jolly, K. Manas, Dhananjay K. Deshmukh, Removal of methyl orange by activated carbon modified by silver nanoparticles, Appl. Water Sci, 3(2013) 367-374.
38. P. Velmurugan, S. Shivakumar, S.Y. Chae, J.S. Ho, Y.P. In, S.J. Min, H.S. Chul, Synthesis and characterization comparison of peanut shell extract silver nanoparticles with commercial silver nanoparticles and their antifungal activity, Journal of Industrial and Engineering Chemistry 31 (2015) 51–54.
39. P. Velusamy, J. Das, R. Pachaiappan, B. Vaseeharan, K. Pandian, Greener approach for synthesis of antibacterial silver nanoparticles using aqueous solution of neem gum (*Azadirachta indica* L.), Industrial Crops and Products 66 (2015) 103–109.
40. P. Kumar, M. Govindraju, S. Senthamilselvi, K. Premkumar, Photocatalytic degradation of methyl orange dye using silver (Ag) nanoparticles synthesized from *Ulvalactuca*, Colloids and Surfaces B: Biointerfaces 103 (2013) 658-661.
41. Problems caused by textile dyes, Textile learner.blogspot.in

42. Q. Sun, X. Kai, J. Li, M. Zheng, Z. Chen, C.P. Yu, Green synthesis of silver nanoparticles using tea leaf extract and evaluation of their stability and antibacterial property, Colloids and surfaces A: Physicochemical and Engineering aspects 444 (2014) 226-231.
43. R. Ahmad, Studies on adsorption of crystal violet dye from aqueous solution onto *Coniferous pinus* bark powder (CPBP). J Hazard Mater (2009) 171:767–773.
44. R. Amooaghaie, M.R. Saeri, M. Azizi, Synthesis, characterization and biocompatibility of silver nanoparticles synthesized from *Nigella sativa* leaf extract in comparison with chemical silver nanoparticles, Ecotoxicology and Environmental Safety 120 (2015) 400–408.
45. R. Zhou, M.P. Srinivasan, Photocatalysis in a packed bed: Degradation of organic dyes by immobilized silver nanoparticles, Journal of Environmental Chemical Engineering 3 (2015) 609-616.
46. R. Mariselvam, A.J.A. Ranjitsingh, A.U.R. Nanthini, K. Kalirajan, C. Padmalatha, P.M. Selvakumar, Green synthesis of silver nanoparticles from the extract of inflorescence of *Cocos nucifera* for enhanced antibacterial activity, Spectrochimica Acta Part A : Molecular and Biomolecular spectroscopy 129 (2014) 537-541.
47. S. Joseph, B. Mathew, Microwave-assisted green synthesis of silver nanoparticles and the study on catalytic activity in the degradation of dyes, Journal of Molecular Liquids 204 (2015) 184–191.
48. S. Patra, S. Mukherjee, AK. Barui, A. Ganguli, B. Sridhar,CR.Patra,Green Synthesis, Characterzation of gold and silver nanoparticles and their potential application for cancer therapeutics, Material Science and Engineering C 53 (2015) 298-309.
49. S. Prabhu, E.K. Poulose, Silver nanoparticles: mechanism of antimicrobial action, synthesis, medical applications, and toxicity effects. Int Nano Lett (2012) 2:32–42.
50. S. Pugazhendhi, E. Kirubha, P.K. Palanisamy, R. Gopalakrishnan, Synthesis and characterization of silver nanoparticles from *Alpinia calcarata* by Green

approach and its applications in bactericidal and nonlinear optics, Applied Surface Science 357 (2015) 1801–1808.

51. S. Saha, D. Chattopadhyay, K. Acharya, Preparation of silver nanoparticles by bioreduction using *Nigrospora oryzae* culture filtrate and its antimicrobial activity. Dig J Nanometer Bios 2011;6:1519-28.
52. S. Senthilkumaar, P. Kalaamani, C.V. Subburaam, Liquid phase adsorption of crystal violet onto activated carbons derived from male flowers of coconut. J Hazard Mater (2006) 136:800–808.
53. S. Srivastava, R. Sinha, D. Roy (2004), "Toxicological effects of malachite green", Aquatic Toxicology 66 (3): 319–29.
54. S.M. Pourmortazavi, M. Taghdiri, V. Makari, M.R. Nasrabadi, Procedure optimization for green synthesis of silver nanoparticles by aqueous extract of *Eucalyptus oleosa*, Spectrochimica Acta Part A : Molecular and Biomolecular spectroscopy 136 (2015) 1249-1254.
55. S. Shivamani, B.L. Grace, Removal of Dyes from Wastewater using Adsorption -A Review, IJBST (2009), 2(4):47-51.
56. T.S. Anirudhan, M. Ramachandran, Adsorptive removal of basic dyes from aqueous solutions by surfactant modified bentonite clay (organoclay): Kinetic and competitive adsorption isotherm, Process Safety and Environmental Protection 95 (2015) 215–225.
57. Transport processes and unit operations, Christie Geankoplis, 3rd edition
58. Triarylmethane and diarylmethane dyes, Gessner and Mayer (2000), Ullmann's encyclopedia of industrial chemistry
59. U.A. Guler, M. Ersan, E. Tuncel, F. Dugensi, Mono and simultaneous removal of crystal violet and safranin dyes from aqueous solutions by HDTMA-modified *Spirulina sp.,* Process Safety and Environmental Protection 99 (2016) 194–206.
60. Unit operations of Chemical Engineering, Mcabe and Smith, 6th edition.
61. V.A. Kumar, Y. Nakajima, T. Uchida, T. Hanajiri, T. Maekawa, Synthesis of nanoparticles composed of silver and silver chloride for plasmonic photocatalyst

using an extract from the needles of *Pinus densiflora*, Malterial Letters 176 (2016) 169-172.

62. V. Dhand, L. Soumya, S. Bharadwaj, S. Chakra, D. Bhatt, B. Sreedhar, Green synthesis of silver nanoparticles using *Coffea Arabica* seed extract and its antibacterial activities, Material Science and Engineering C 58 (2016) 36-53.
63. V. Kathiravan, S. Ravi, S. Ashokkumar, S. Velmurugan, K. Elumalai, C.P. Khatiwada, Green synthesis of silver nanoparticles using *Croton sparsiflorus morong* leaf extract and their antibacterial and antifungal activities, Spectrochimica Acta Part A : Molecular and Biomolecular spectroscopy 139 (2015) 200-205.
64. X.S. Wang, X. Liu, L. Wen, Y. Zhou, Z. Li, Comparison of basic dye crystal violet from aqueous solution by low-cost biosorbents, Sep Sci Technol(2008) 43:3712–3731.
65. Y.S. Ho, G. McKay (1999) Pseudo-second-order model for sorption processes. Proc Biochem 34:451–465.

APPENDIX I

LIST OF TABLES: **Page No**

APPENDIX II

LIST OF FIGURES: